WAX DEPOSITION FROM KEROSENE ONTO COOLED SURFACES

By

Michael Abraha Ghedamu

B.A.Sc., Addis Ababa University, 1989

A THESIS SUBMITTED IN PARTIAL FULFILLMENT OF

THE REQUIREMENTS FOR THE DEGREE OF

MASTER OF APPLIED SCIENCE

IN

THE FACULTY OF GRADUATE STUDIES

CHEMICAL ENGINEERING

We accept this thesis as conforming

to the standard

THE UNIVERSITY OF BRITISH COLUMBIA

May 1995

In presenting this thesis in partial fulfilment of the requirements for an advanced degree at the University of British Columbia, I agree that the Library shall make it freely available for reference and study. I further agree that permission for extensive copying of this thesis for scholarly purposes may be granted by the head of my department or by his or her representatives. It is understood that copying or publication of this thesis for financial gain shall not be allowed without my written permission.

Department of Chemical Engineering

The University of British Columbia
Vancouver, Canada

Date May 30, 95

DE-6 (2/88)

Abstract

Wax fouling is a major problem in some oil refineries. The main objective of this project was to test different surfaces with the aim of eliminating or at least reducing wax deposits in heat exchangers. Wax is separated in oil refineries by cooling the wax-laden petroleum stream in chillers and then scraping off the deposited wax mechanically from the surfaces of the heat exchangers (chillers). The solid wax is separated from the liquid petroleum stream by means of filters.

An experimental test rig was set up to study ways of eliminating or reducing wax deposits by changing some of the operating conditions as well as the surface type of the heat transfer area. A double pipe heat exchanger 0.72 m long with inner tube (ID=9.96 mm, OD=12.45 mm) and outer pipe (ID=25.4 mm) was used. The solution tested was wax dissolved in kerosene, which flowed through the annular section while the cooling water flowed countercurrently in the inner tube. The effects of flow velocity of wax-kerosene, of bulk temperature, of wax-kerosene concentration and of heat transfer surface type have been studied. Two types of wax were used: refined wax and slack wax. The surfaces used were: uncoated stainless steel, sand-blasted stainless steel, chrome-plated stainless steel, n-C18 silane-coated chrome-plated stainless steel, Heresite Si 57 E coated stainless steel (shiny), Heresite P-400/L-66 coated stainless steel (dull) and n-C18 silane coated stainless steel.

The cloud point for each wax-kerosene concentration investigated (5, 10, 15 and 20 wt. % wax) was measured using ASTM procedures. The rheology of wax-kerosene was also investigated to determine if the mixtures were Newtonian or non-Newtonian. All mixtures were found to be Newtonian. The mixture viscosity was determined at temperatures from the cloud point upwards at each concentration.

A Kern-Seaton (1959) equation was used to determine R_f^* and θ_c from the resistance vs. time experimental data. The wax deposit showed a decrease in R_f^* with increasing Re, with increasing T_b and with decreasing concentration. Similar results were found by Bott and Gudmundsson (1977b). From the plots of R_f^* vs. Re, the hierarchy in increasing R_f^* was found to be: Heresite-coated stainless steel (dull and shiny) < n-C18 silane coated stainless steel < n-C18 silane-coated chrome-plated stainless steel < chrome-plated stainless steel < uncoated stainless steel < sand-blasted stainless steel. A similar hierarchy with four of the seven tubes was shown with respect to R_f^* vs. T_b. That plastics show a lower wax deposit compared to metal surfaces has been shown by previous investigations.

After some deposition had occurred, the removal of wax chunks from the surface and occasional bare patches were visually observed on all tubes except the two Heresite-coated tubes and the sand-blasted stainless steel. The phenomenon of deposit sliding was observed on the chrome-plated stainless steel, where the sliding velocity was recorded.

The concentration and bulk temperature of a petroleum stream may be fixed by refinery conditions. However, a lower wax deposit on heat transfer surfaces can be obtained by using a smooth surface material which has a low affinity for wax, and high flow velocity or turbulence.

Table of Contents

List of Tables

List of Figures

Acknowledgments

I would like to express my sincere gratitude to Professors A. P. Watkinson and N. Epstein for their guidance and suggestions which played a very important role in the completion of this study. My thanks also go to Dr. Tom Broadhurst and the Imperial Oil Limited staff, and to Heresite Protective Coatings Inc., for their valuable advice and service.

Thanks are also due to the staff of the Department of Chemical Engineering Workshop, Office and Stores for their invaluable assistance.

Chapter 1

1. Introduction

Petroleum waxes are broadly defined as waxes which naturally occur in the various fractions of crude petroleum. Some crudes contain little or no wax, whereas others are so waxy that they are semisolid at room temperature.

There are three main types of petroleum waxes: paraffin waxes, microcrystalline waxes, and petrolatum. Paraffin waxes are mainly composed of straight-chain molecules with a small number of branched chains and crystallize in large, well formed, distinct crystals of plate and needle types. Typically paraffin waxes contain 18-56 carbon atoms. Microcrystalline waxes have molecules of 40-50 carbon atoms and crystals formed are small and indistinct. This type of wax contains more branched hydrocarbons compared to paraffin. Petrolatum contains both solid and liquid hydrocarbons.

Wax is recovered as a product from some refineries. The separation of wax from a paraffin distillate is made possible by the fact that the solubility of wax in the distillate decreases with decreasing temperature. The petroleum stream is first chilled in heat exchangers to a low temperature to solidify the wax, which is then removed from the heat transfer surface by scraping. The chilling may be accompanied by incremental dilution as in the DILCHILL process where a petroleum stream is diluted by a solvent such as propane, which is a good solvent for oil but a poor one for wax, and then chilled.

The scraped wax is recovered usually by a vacuum type filter. As a further means

of reducing the oil content a fresh solvent is used to wash the filter cake on the vacuum drum. Scraped surfaces provide good heat transfer but a non-optimum environment for the crystallization of wax. This is because the wax which is deposited on the cold chiller wall, and subsequently scraped off, has poor filtration performance. Therefore, industrial research has been targeted at ways to crystallize the wax and recover it in an easily filterable form.

The objective of this research was to investigate the factors which control the accumulation of wax from petroleum streams on heat exchange surfaces. The effects on the buildup of the wax layer, of flow velocity, bulk temperature, and concentration of wax in solvent kerosene were therefore studied. Experiments were done using different tube surfaces to determine the effect on wax attachment and removal. The rheology of wax in kerosene was investigated to aid in interpretation of the deposition results.

Chapter 2

2. Literature Survey

The desired precipitation of wax for recovery as a product in oil refineries was described in Chapter 1. In the oil industry, the formation of any predominantly organic matter in oil well tubing, surface flowlines and other production equipment (Hunt, 1962) is referred as paraffin deposition. This undesired precipitation gives rise to operating problems in oil production and pipeline systems. The deposits consist mainly of n-paraffins with smaller amounts of branched and cyclic paraffins and aromatics (Jorda, 1966).

Paraffins in oil show normal solubility-temperature behavior, i.e. solubility decreases as temperature is lowered. Heat treatment has therefore been found beneficial in the improvement of pumping of certain waxy crude oils. The temperature at which wax crystals first appear in cooling a solution is defined as the cloud point. Standard empirical tests (Standard Test Methods, ASTM D2500-91 and IP 219/93) have been devised to determine this temperature.

The crystalline nature of paraffins has been investigated by a number of workers (Holder and Winkler, 1965). Modification of the wax crystal structure by additives during deposition or gelling can improve the flow properties (Brod et al., 1971).

Wax deposition as a fouling problem

Fouling can be defined as the accumulation of undesired solid material at a phase

interface (Epstein, 1983). The five primary categories of fouling are crystallization, particulate, chemical reaction, corrosion, and biological fouling.

In the oil industry, fouling is taken to mean the formation of any undesirable deposit on heat exchanger surfaces which increases resistance to heat transmission or flow. The deposition of wax on cooled surface is therefore a fouling problem.

Epstein (1983) has discussed the sequential events which occur in most fouling systems as initiation, transport of foulant to the surface (mass transfer), attachment (adhesion), removal (spalling, sloughing off) and aging.

The effect of fouling in terms of thermal resistance on heat transfer equipment is expressed in the fundamental equation for the overall heat transfer coefficient U at the outside of the surfaces as:

$$\frac{1}{U} = R_{fo} + \frac{1}{h_o} + R_w + \frac{A_o}{A_i} R_{fi} + \frac{A_o}{A_i} \frac{1}{h_i} \qquad (1)$$

Here R_{fo} and R_{fi} refer to the thermal resistance of the fouling deposit on the outside and inside of the surface, respectively. While the fouling resistance can be described by a time function starting at zero and proceeding asymptotically, a constant value of the fouling resistance is generally used for design. This value is then interpreted as the thermal resistance to be reached in some "reasonable" time interval after which the equipment is cleaned. However, the fact that at time zero, the equipment is clean and, therefore, may operate under drastically different conditions than just before cleaning, is rarely examined. Allocation of exaggerated R_f values does not guarantee longer operating

time. On the contrary, in many cases it can contribute to more rapid deterioration of the overall heat transfer coefficient.

The fouling resistance at any time can be calculated as

$$R_f = \frac{1}{U} - \frac{1}{U_o} \tag{2}$$

where U_o is the overall heat transfer coefficient at time zero. R_f can also be written as

$$R_f \approx \frac{x}{k_d} = \frac{m}{\rho k_d} \tag{3}$$

for a small thickness x with respect to diameter.

Many researchers have studied fouling problems based on measurement of R_f, x, *or* m. Work pertinent to this project is summarized below.

The effect of operational variables

While many other effects may be present in a specific fouling process, the following process variables appear to be most important (Taborek et al., 1972).

1. Flow velocity- Moderate to very strong effects on most fouling processes, because of the influence on deposition and removal rates.

2. Surface temperature -Affects most fouling processes; particularly, crystallization and chemical reaction fouling because of strong influence on rates.

3. Fluid bulk temperature- Affects reaction and crystallization rates, and solubility of fouling species.

Effects of surface material and structure

1. Material- Possible catalytic effect on reaction; corrosion can affect adhesion.

2. Surface- Roughness, size and density of cavities will affect crystalline nucleation, sedimentation and adhesion of deposits. Both surface material and structure have their greatest influence in fouling initiation rather than for the continued fouling process.

The fouling resistance versus time curves generally follow one of the four types of behavior–linear, falling rate, asymptotic, or saw-tooth. Hunt (1962), and Patton and Jessen (1970) found that paraffin deposition increased asymptotically with time.

Kern-Seaton Equation

Kern and Seaton (1959) derived an equation for asymptotic fouling, which can be used for fitting of the data for fouling of wax in kerosene.

Deposition of wax can be considered to involve two steps–transport of paraffin molecules to the cooled surface, and integration of the molecules into the deposit structure. Removal of wax deposits can also occur due to the effects of shear on the wax structure. The net rate of deposit accumulation is the difference between deposition and removal rates.

Deposition

The component must be transported from the bulk of the fluid, where its

concentration is C_b, to the heat transfer surface where its concentration in the adjacent fluid is C_s. Assuming turbulent flow,

$$\dot{m}_d = k_t(C_b - C_s) \tag{4}$$

where k_t is a turbulent mass transport coefficient. The surface integration step is then given by

$$\dot{m}_d = k_r C_s^n \tag{4a}$$

where k_r is the surface integration constant and n the order of the integration step.

Removal

Removal of the deposit may or may not begin right after deposition has started. That it does so is an assumption implicit in the removal model originally proposed by Kern and Seaton, and further developed by Taborek et al. (1972).

$$\dot{m}_r = \frac{Bm\tau_s}{\psi} \tag{5}$$

This equation states that removal rate increases linearly with deposit thickness and hence with m, and with the shear stress τ_s. The fact that removal increases with increasing layer thickness suggests that the shear strength of the deposit is decreasing, or other mechanisms which reduce the stability of the layer are taking place. Although the continuous coexistence of removal with deposition (especially particulate deposition) is more readily rationalized in turbulent than in laminar flow, the fouling rate at any time according to this assumption is given by

$$\frac{dm}{d\theta} = \dot{m}_d - \dot{m}_r = \dot{m}_d - \frac{Bm\tau_s}{\psi} \tag{6}$$

Integration of Eq. (6) from the initial conditions $\theta = 0, m = 0$ on the assumption that the only variables in Eq. (6) during the course of fouling are θ and m yields the well-known Kern-Seaton equation represented in Fig. 1.

$$m = m^*(1 - e^{\frac{-\theta}{\theta_c}}) \tag{7}$$

where m* is the asymptotic mass per unit surface area and the time constant is given by

$$\theta_c = \frac{m}{\dot{m}_r} = \frac{m^*}{\dot{m}_d} = \frac{\psi}{B\tau_s} \tag{8}$$

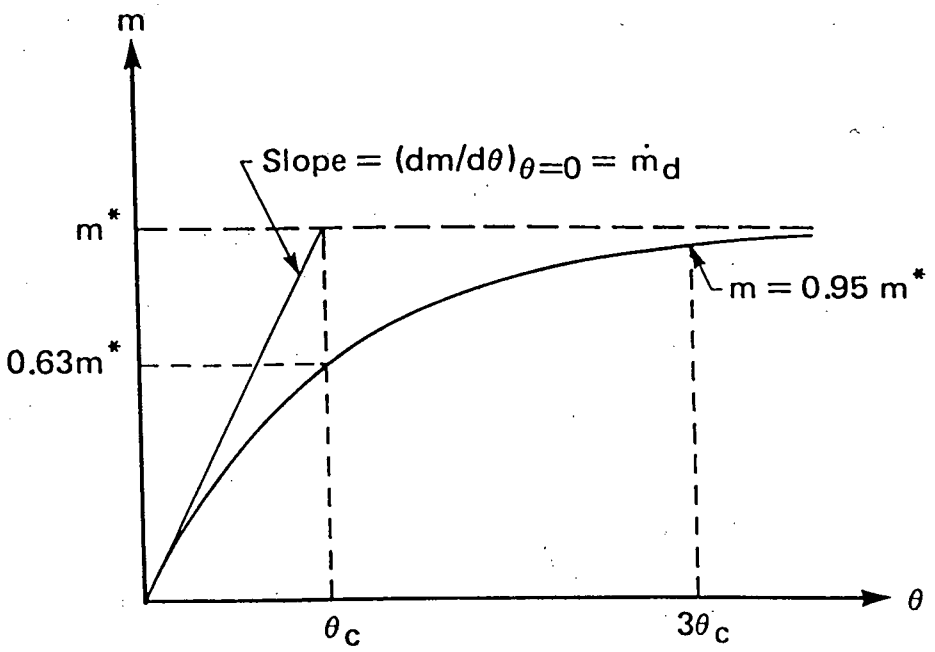

Fig. 1. Plot of Eq. (7), after Kern and Seaton (1959).

Since deposit removal is desirable to obviate the need for scraping the surface in wax chillers, some discussion of deposit strength and removal processes is appropriate.

From Eq. (8) it is seen that θ_c can be interpreted as the average residence time of an element of fouling deposit on the heat transfer surface, as well as the time it would take to accumulate the asymptotic fouling deposit m^* if the fouling proceeded linearly at the initial deposition rate $\dot{m}_d$. By putting $\theta = \theta_c$ in Eq.(7), m works out to be 0.632m*, so that θ_c is also the actual time required to achieve 63.2% of the asymptotic fouling resistance. θ_c can also be interpreted as one-third the actual time required to achieve 95% of the asymptotic fouling resistance. It is generally recommended that θ for an experimental run be at least equal to $3\theta_c$ in order to determine a reliable value of R_f^*. Since $m^* = \dot{m}_d \theta_c$ and $\theta_c \propto 1/\tau_s \propto 1/u_*^2$ in turbulent flow, it follows that even if $\dot{m}_d$ is directly proportional to u_*, as would be the case under conditions of turbulent mass transfer control at high values of Sc, m* and hence R_f^* would still decrease as the velocity increases. This generalization has commonly been found in practice , at least when deposit removal occurs (Gudmundsson, 1981). Only if deposit strength ψ is also directly proportional to u_*, as inferred by Gudmundsson (1977) from the inverse proportionality of θ_c with fluid velocity for wax deposits solidifying from hydrocarbon streams, might this generalization falter. The evidence for a velocity dependence of ψ is still tenuous.

Nevertheless, deposit removal has been observed to occur simultaneously with deposition (Epstein, 1981) in certain instances, and for those cases θ_c can reasonably be represented by Eq.(8). According to Cleaver and Yates (1976), it is not simple viscous shear that lifts (or is capable of lifting) particles from the deposit back to the mainstream, but the periodic bursts that are randomly distributed over less that 0.5% of the surface at any instant. They referred to these bursts as miniature tornadoes, and that this

characterization is not a metaphor has been vindicated by experiments (Dinkelacker, 1979) which showed that there is a measurable wall suction associated with the turbulent bursting.

For a given deposit and fluid, a minimum friction velocity u_* is required before the turbulent bursts can become effective in removing some of the deposit. By reference to Eq. (8), it is reasonable to generalize the criterion to be fulfilled by any deposit as

$$\theta_c < (\theta_c)_{crit} \tag{9}$$

or, since $\theta_c \propto (\psi / \tau_s) \propto (\psi / u_*^2)$,

$$\frac{u_*^2}{\psi} > \left(\frac{u_*^2}{\psi}\right)_{crit} \tag{10}$$

where the subscript "crit" denotes some critical value for a given fluid. Note that the numerator in Eq. (10) represents hydrodynamic forces tending to disrupt the deposit while the denominator represents the adhesive or cohesive strength of the deposit, depending on which is weaker.

Taborek et al. (1972) have explained the deposit strength in a different way. The removal potential is given by

$$\phi_r = \frac{C\tau_s}{R_b} \tag{11}$$

where R_b is deposit bond resistance. This may be considered the adhesive strength of the deposit per unit area at the plane of the weakest adhesion. The following speculations are made based on limited observation.

1. R_b increases with uniformity of the deposit structure (highest for pure crystals and

polymers, lowest for discrete particles).

2. R_b may decrease with deposit thickness due to increasing number of planes of potential weakness. This may be expressed mathematically as

$$R_b = \psi\left(\frac{1}{x}\right)^m \tag{12}$$

where ψ is a function of the deposit structure and m is a constant to be determined experimentally.

3. R_b is a function of the original surface characteristics only if the deposit-surface interface adhesion is weaker than deposit internal cohesion. This accounts for the fact that specially prepared smooth surfaces retard fouling in some instances and not in others.

Eq. (7) can be differentiated to find the initial rate of fouling, i.e.

$$\left.\frac{dm}{d\theta}\right|_{t=0} = \frac{m^*}{\theta_c} \tag{13}$$

Models of wax deposition

Fredensland et al. (1988) have developed a new theory for precipitation of wax from hydrocarbon solutions based on the theory of multicomponent polymer solutions. The wax appearance points were determined and agree in most cases within ± 4 K with the measured ones.

Majid et al. (1990) used the equilibrium model developed by Erbar (1973) to predict deposition. The model is developed by using material balances and equilibrium values of components of an oil containing wax. It assumes that none of the wax which

diffuses to the wall and deposits is removed by shear forces. Calculations done on a crude oil pipeline have shown that wax deposition goes through a maximum with flowrates. The wax-equilibrium model requires a very detailed oil analysis as input data, however.

Svendsen (1993) has developed a mathematical model for the prediction of wax deposition in both open and closed pipeline systems, using a combination of analytical and numerical methods. The model includes phase equilibria, phase transition and fluid dynamics. It is known that wax deposition occurs if there is a negative radial temperature gradient present in the flow and if the wall temperature is below the cloud point. The cloud point is sometimes referred to as the precipitation temperature of the particular oil, or the wax appearance point (WAP). The amount of deposition depends on the oil composition. The model is consistent with these experimental observations. If the liquid/solid phase transition expressed by the change in moles of liquid with temperature, $\partial L/\partial T$, is small at the wall temperature, then the model predicts that wax deposition can be considerably reduced even when the wall temperature is below the WAP. If, in addition, the coefficient of thermal expansion, α_i, is sufficiently large, some components may separate and move in opposite radial directions at temperatures below the WAP. Thus the wax would move to the bulk fluid from the wall region. No comparison of the theoretical results to experimental data was given.

Experimental studies of wax deposition

Jessen and Howell (1958) studied the effect of flowrate on paraffin wax deposition in steel and plastic coated steel pipe. Microcrystalline wax at concentrations of about 2.3 to 8.4 g/L in kerosene solutions and several crude oils were circulated at bulk temperatures from 29 ^{o}C to 42^{o}C, which were below the cloud point. In laminar flow, the deposition increased with flowrate, reaching a maximum prior to transition to turbulent

flow, and then decreased with increasing flowrate. In laminar flow, the positive effect of flowrate was explained in terms of more particles being carried by the moving stream, providing a greater opportunity for deposition on the pipe surface. At high velocities viscous drag exerted by the stream tended to remove the accumulation. Where drag becomes equal to or exceeds the shear stresses within the deposited wax, a removal mechanism is provided. Paraffin deposited at high flowrates was observed to be considerably harder than paraffin deposited at lower flowrates. The increase in both viscous drag and shearing stresses on the paraffin deposit at high flowrates was considered to account for the gradual decrease in deposition at high flowrates. Experiments were not done to determine the effects of T_b and concentration.

The effect of flowrate on paraffin deposition was studied by Toronov (1969) using a 5 % solution of technical paraffin in kerosene. The apparatus consisted of a room temperature reservoir from which the solution flowed to an experimental chamber. The paraffin deposited on the outside of a jacketed tube cooled from the inside with water 10°C below ambient. Neither the melting point of the wax used nor the solution cloud point were given. The thickness of the paraffin deposit was measured after 2 minutes by a camera fitted with a microscope. The results showed that the deposit thickness decreases with increasing velocity and that the deposit hardness, as expressed by the velocity required to remove it from the tube wall, increases with velocity. Toronov explained that as the flowrate increases only those wax crystals and crystal clusters capable of firm attachment to the surface, and having good cohesion between themselves, will not be removed from the deposit.

Patton and Casad (1970) studied paraffin deposition on a cold surface inserted into

a well stirred wax solution maintained above its cloud point temperature. They found that the amount deposited increased asymptotically with time. The initial rate of deposition and the asymptotic deposit amount both decreased with increased stirring. Water was circulated at 29°C through the annulus of the test cell to maintain the solution temperature 3 °C above its cloud point. The deposits which formed on the cold probes tended to slide off smooth surfaces and flake off roughened surfaces. But roughness seemed to have no effect with a high molecular weight wax. Plastic coatings on the surface showed a decrease in wax deposit which was solely attributed to reduction in heat transfer. Deposit weight decreased with increasing stirring rate, and increased as the temperature differential between the solution cloud point and the probe face temperature increased. This work is discussed further below under the effects of surface properties.

Bott and Gudmundsson (1977b) reported that Armenski et al. (1971), in a study analyzing reduction in pipe diameter due to paraffin deposition, observed slight removal of deposits following their establishment. During the cooling of waxy kerosene in simulated heat exchanger tubes, a fluctuating deposit thickness was observed.

Eaton and Weeter (1976), using a rotating disc apparatus, showed that deposition was low at extreme velocities and much higher at intermediate values. In their work, the fluid velocity was accurately maintained by varying the disk rotational speed, and the paraffin deposition determined by weighing. The bulk temperature of the oil was varied from 4 to 30° C .The wax deposition reached a maximum at around 17 °C. The rotational speed of the disk was varied from 0 to 2500 rpm to simulate different flow rates. The paper states that the wax deposit rate increases from 0 to a peak value at 1000 rpm and decreases thereafter up to 2500 rpm, but does not indicate whether the rpm range

is for laminar or turbulent flow.

Experimental results have been obtained by Bott and Gudmundsson (1977a) for a flowing system where paraffin wax-kerosene solutions were cooled in tubular heat exchangers. It was found that the overall heat transfer resistance increased rapidly to some average value that fluctuated at random with time. These fluctuations were apparently caused by continuous buildup and break-down processes of the wax deposit. The creation of planes of weakness and the increase in shear stress at the wall as deposits build up were probably the main factors causing break-down and removal.

Bott and Gudmundsson (1977b) have studied the factors affecting the deposition of paraffin wax from its solution with hydrocarbons onto surfaces in pipelines and process equipment. Deposition studies showed that the amount of paraffin deposited increases with time to an asymptotic value. The asymptotic value showed significant fluctuations around the mean value with time.

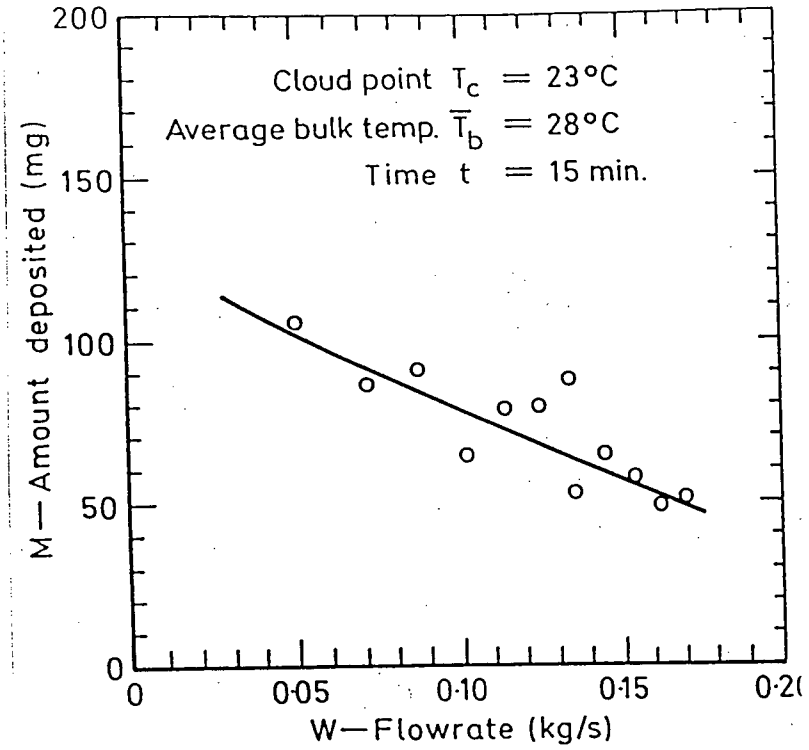

Fig. 2. Typical curve of amount of wax deposited vs. flowrate by Bott and Gudmundsson (1977b).

It was suggested that paraffin deposition is controlled by the cohesive properties of the wax. For the given studies, there appeared to be a critical deposit thickness at which deposits break up and slough away, giving rise to the fluctuating condition. The equipment used by Bott and Gudmundsson essentially consisted of two closed circulation loops where paraffin wax from wax- kerosene mixtures flowing in a rectangular duct was allowed to deposit on a copper plate cooled by water. A long entry section to the duct was provided to ensure that the velocity profile in the experimental section had been fully developed before the plate was reached by the fluid. The bulk temperature of the paraffin wax-kerosene solution was kept 5 ^{o}C above its cloud point temperature. The solution flowrate varied from about 0.04 kg/s to 0.18 kg/s such that Reynolds number was greater than 5000 and the flow conditions therefore turbulent. The amount of paraffin deposition was determined by weighing. The deposition decreased with increasing flowrate (Fig. 2)

and bulk temperature but increased with concentration. The asymptotic fouling resistance varied inversely as Re squared.

Surface properties

Since deposition and particularly the adhesion of the deposit onto a surface will be a function of the surfaces properties, investigations into the effects of different surfaces have been carried out.

Jessen and Howell (1958) report that crude oil field observations have indicated that plastic coated pipe not only reduced paraffin accumulation but in some cases eliminated deposition completely. However, data were needed to demonstrate the relative effectiveness of plastic materials. Steel, butyrate, rigid PVC, kralastic resin type plastic pipes and aluminum pipe were tested. The rate of paraffin deposition at all velocities and temperatures was greatest in steel pipes but considerable paraffin deposition was also found in butyrate pipe. The least amount of paraffin accumulation was noted in the rigid PVC and kralastic pipe. All plastic pipes tested showed less tendency for accumulation of paraffin than did steel or aluminum pipe, as shown in Fig. 3.

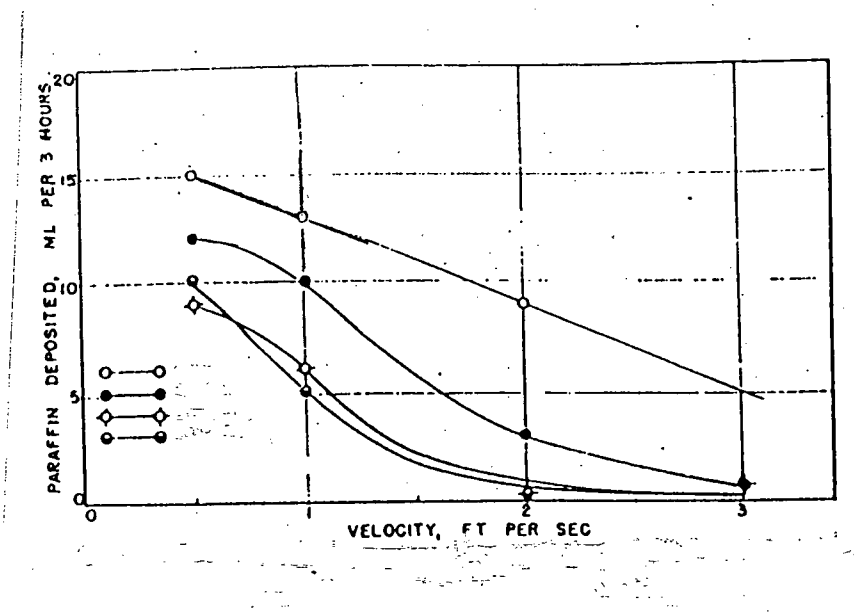

Fig. 3. Effect of velocity on rate of deposition of Delhi DU-184-1 crude oil at 106 ^{O}F.

In laminar flow, a gradual increase in the rate of paraffin deposition was obtained with increased velocity, the maximum rate being reached when the flow changed from viscous to turbulent flow. At higher velocities the rate of deposition decreased rapidly. At Re greater than 4,000, the plastic pipe surfaces were free of any paraffin accumulation. The tendency for the rate of paraffin deposition to increase with velocity to velocities approximately equal to the transition velocity (Re=1980) was clearly shown for the steel pipe. Fig 3 shows the turbulent case. Paraffin deposited at high rate of flow was found to be considerably harder than paraffin deposited at low flow rates.

Hunt (1962) studied the effect of roughness on paraffin deposition and concluded that deposits do not adhere to metals themselves but are held in place by surface roughness. A cold finger assembly was immersed in a wax-oil slurry contained in a 300

ml beaker surrounded by water at 120 ^{O}F. The temperature of the water circulating through the cold finger was lowered from a temperature just above the slurry temperature at a constant rate of 1.2 ^{O}F/hour over a period of 15 1/2 hours. An increased deposit was found on sand-blasted stainless steel compared to polished cold-rolled steel. The deposit did not adhere to plastic coatings such as epoxy-phenolic, isophthalic ester, coal tar-epoxy and epoxy.

Jorda (1966) found that paraffin deposition increased with surface roughness. A wax-oil solution composition of 25 percent by weight of refined petroleum wax in a refined petroleum solvent at a temperature of 41^{O}C and 300 rpm was used. It was observed that the weight of the paraffin deposit increased as the temperature of the deposition surface decreased from 2, 6, 8, and 10^{O}C below the cloud point. Roughness was found to play an important role as can be seen in Figure 4. Sliding of paraffin on polished surfaces and flaking on roughened surfaces was also observed. Smooth phenol-formaldehyde (roughness <2μ), epoxy-phenolic (<5μ) and polyurethane (<3μ) have shown less deposit compared to surfaces covered by mill scale (30-40μ). Tetra-fluoroethylene provides a zero micron surface roughness, which was expected to provide a superior surface for paraffin control; however, in the tests with tetra-fluoroethylene, polyethylene and polypropylene surfaces, massive deposits of paraffin of extreme hardness were collected.

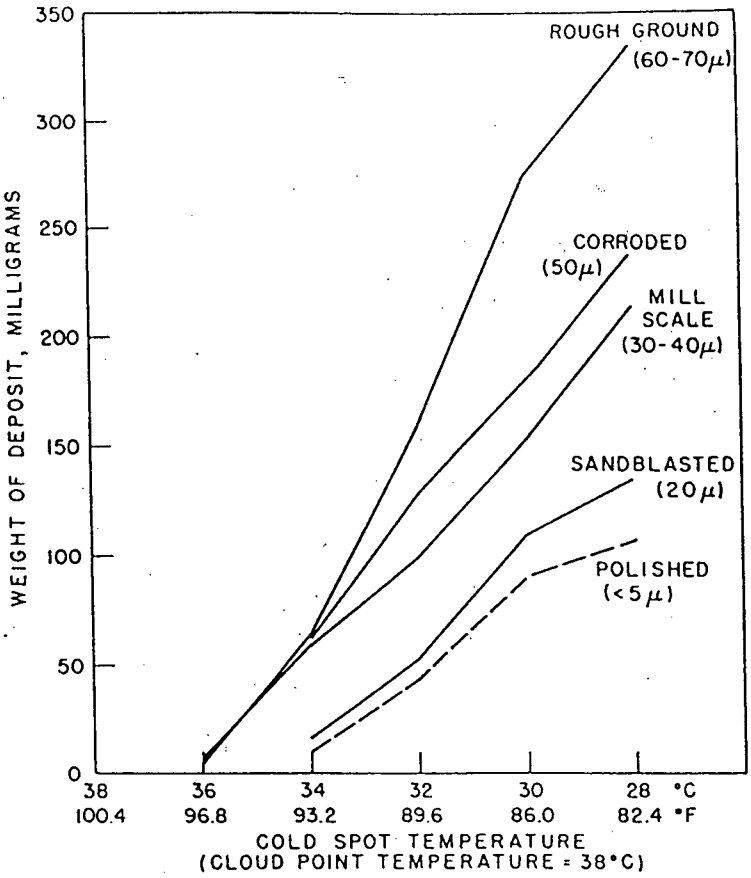

Fig. 4. Weights of paraffin deposited on polished, sand-blasted, mill-scaled, corroded and rough-ground steel as a function of deposition surface temperature (roughness factors in parentheses).

Patton and Casad (1970) performed similar studies and concluded that no correlation could be observed between surface roughness and amount of deposit. However, they argued that the adhesion bond at a surface should be proportional to the total contact area and therefore related to surface roughness. An experiment done using 10-percent RHI wax-soltrol 170 solution is shown in Table 1. Plastic coatings resulted in about a 30 % reduction in deposit weight over 6 hours.

TABLE I — EFFECT OF SURFACE PREPARATION ON DEPOSITION
10 PERCENT RHI WAX — SOLTROL 170 SOLUTION

ΔT_c = 4°C
Stirring Rate = 300 rpm

Preparation	Deposit Wt. (mg) 6 hours	Percent Change	Deposit Wt. (mg) 16 hours	Percent Change
Polished	86.6	—	119.0	—
240-Grit	90.0	+ 3.9	113.5	− 4.6
50-Grit	90.3	+ 4.3	103.2	−13.3
Coating X	59.8	−30.9	81.9	−31.2
Coating Y	55.3	−36.7	74.4	−37.5
Coating Y*	60.4	−30.2	84.5	−29.0
Coating Z			78.3	−34.2 (22 hours)

*Roughened with 50-grit paper.

$$\text{Percent Change} = \frac{\text{Wt. Deposited} - \text{Wt. Deposited on Polished Surface}}{\text{Wt. Deposited on Polished Surface}}$$

Coating X = Unmodified phenolic
Coating Y = Epoxy-phenolic
Coating Z = Polyurethane

Summary of literature review

The key studies on velocity, temperature and concentration effects are listed in Table 2.

Table 2. Summary of literature review of R_f^* vs. wax-solvent velocity, T_b and concentration effects.

	Jessen and Howell	Jorda	Toronov	Patton and Cassad	Eaton and Weeter	Bott and Gudmundsson
Velocity Effects	*	Not studied	*	*	±	*
Temperature Effects	Not studied	*	Not studied	Not studied	±	*
Concentration	Not studied	Not studied	Not studied	Not studied	Not studied	+

+ when indicated variable increases , R_f^* increases.

* when indicated variable increases, R_f^* decreases.

± when indicated variable increases, both an increase and decrease in R_f^* are observed.

Jorda reported that as the cold surface temperature was increased, the wax deposit decreased. Since the wax-kerosene solution temperature as reported was 41 ^{o}C, which was presumably the inlet bulk temperature, then it can be inferred that the bulk temperature of the solution inside the apparatus must have been increasing with increasing temperature of the cold surface. If the above assumption holds true, then it can be safely concluded that Jorda's results signify that as the bulk temperature of the wax-oil solution increased, the mass of wax deposit decreased, which is indicated in the above Table 2.

Eaton and Weeter presented their data as wax deposition vs. rpm. Therefore it was not possible to determine whether their experiment was in the laminar or turbulent region or both. The other four studies agree that R_f^* decreases with increasing velocity. Bott and Gudmundsson indicate that R_f^* decreases as T_b increases, but little was reported by others on temperature effects.

Four studies of surface effects were reviewed. It was concluded by most authors that plastics generally have lower deposits compared to metal surfaces. This was mainly attributed to smoothness of the surfaces. However, it was also found that ultra-smooth surfaces such as tetra-fluoroethylene showed a good adhesion to wax, and formation of hard deposits. On the other hand, when steel was compared with other rough surfaces

and plastic, the plastics and polished steel showed less deposit, persuading some researchers that wax is held by surface roughness. Therefore, adhesion of wax to surfaces must be both a function of roughness and material type.

Chapter 3

3. Experimental Setup

3.1. The Test Rig

The test rig included a tank, a pump, a chilled test section and associated flow meters. The annular test section consisted of a 750 mm long double pipe heat exchanger, which was opearted in counter-current flow. The hydrocarbon solvent containing wax flowed in the annular section, and the wax deposited on the outside surface of the inner tube through which the coolant flowed. The test rig is shown in Fig. 5. The test section and flow lines both from and to the supply tank were insulated. The flow lines and manometer lines were equipped with heating tapes to warm up the solution when the experiment was started.

3.1.1 Test section

The test section was composed of a 1/2-inch Type 316 stainless steel tube concentrically surrounded by a 1-inch pipe. The geometry of the test section was as follows:

Outer pipe: stainless steel with a transparent glass viewing section, ID=25.4 mm,

L=750 mm

Inner tube: stainless steel, wall thickness =1.245 mm

ID=9.96 mm, OD= 12.45 mm

Distance between inlet and outlet lines for the wax-kerosene mixture: 720 mm

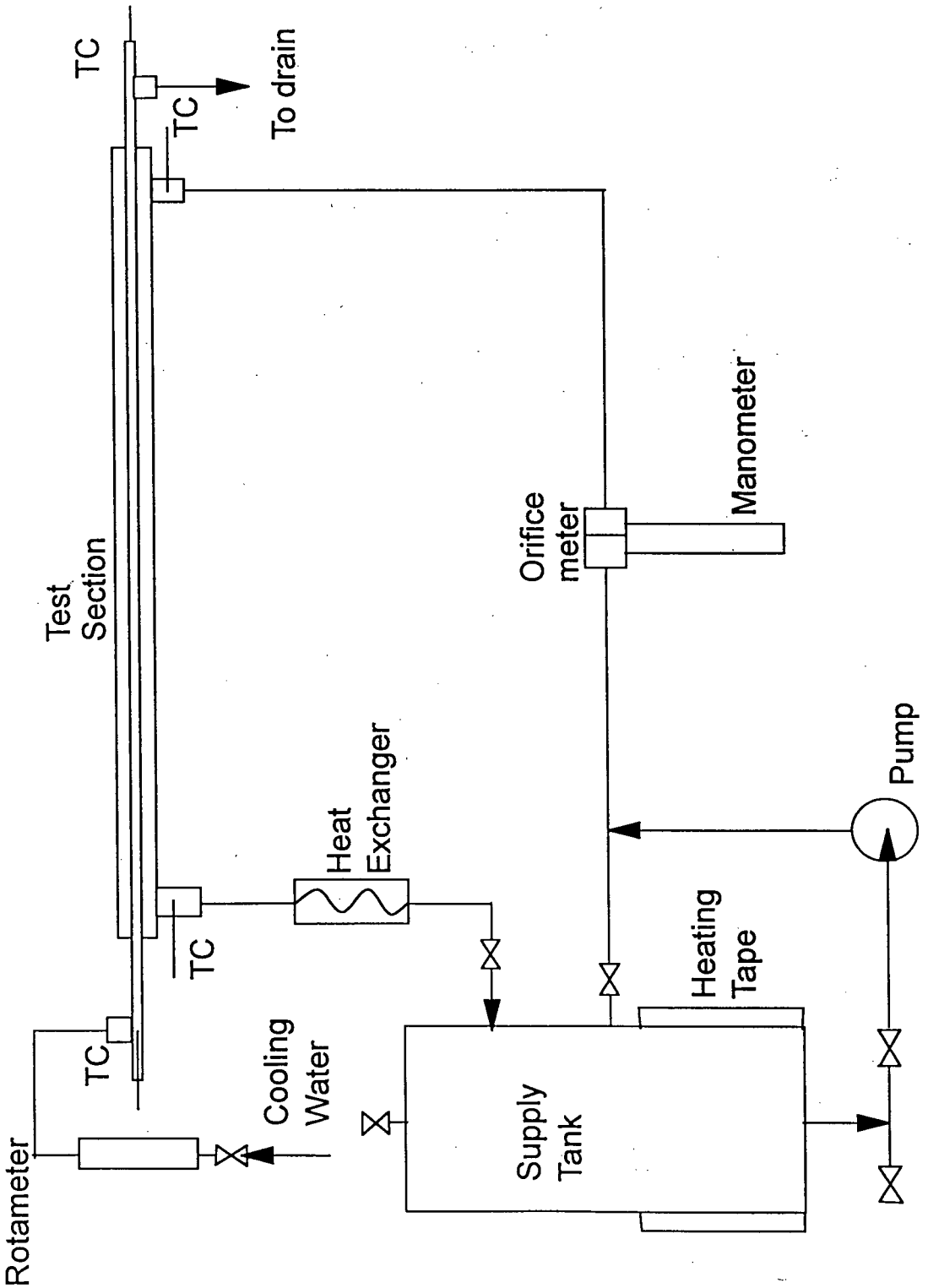

Fig. 5. Flow diagram of wax fouling.
TC=thermocouple

Samples of the stainless steel tubes (with roughness 2.5 μm) were sent to ESSO Petroleum Canada, and to Heresite Protective Coatings, Inc. for surface modification. ESSO provided a sand-blasted stainless steel tube (5 μm roughness), a chrome-plated stainless steel tube (0.5 μm), and tubes coated with n-C18 silane on stainless steel and on chrome-plated stainless steel. ESSO also provided the roughness values of the tubes. Heresite Protective Coatings, Inc. provided stainless steel coated with Heresite Si 57 E (shiny) and Heresite P-400/L-66 (dull). The Si series type of coating is produced from complex mixtures of liquid thermosetting plastics (phenol, formaldehyde, silicone, epoxide resins) and is produced with special flooding or spraying techniques. The Heresite P-400/L-66 is made of a phenolic coating. Both Si 57 E and P-400/L-66 have thicknesses of about 6-8 mils (152-203μm).

The tubes were tested in turn by substituting them for the original stainless steel tube in the unit. A Heresite Protective Coatings, Inc. brochure states: "The fact that Si 14 EG and Si 57 EG have practically no effect on heat transfer is important in practice. Tube bundles protected with such resin formulations do not, therefore, require to have increased surface area. This is confirmed by heat transfer figures:-

Steel tube drawn	422
Steel tube sandblasted	425
Steel tube, with Si 14 EG and Si 57 EG	396 "

No units were given for the numbers recorded above. The brochure also states that "By using suitable silicone formulations the frictional resistance to the flowing liquids is considerably lowered. It was shown that the frictional losses were lower compared to uncoated pipes." This indicates that the surface is more smooth than steel tubes. The surface smoothness is characterized by a smooth to enamel-like finish.

3.1.2. Pump

The pump used for circulating the wax-kerosene mixture was an ACE-5100 end suction mild steel centrifugal pump. Running with water, the specified head was 100 ft at a capacity of 12 US gallons/minute. The drive motor (Jl3509A), made by Baldor Electric Co., drew a current of 11A at 115V (or 5.5A at 230V).

3.1.3 Flow rate measurement

Measurements of flow rate were made for both the cooling water and the wax-kerosene mixture. A rotameter and an orifice meter, respectively, were used for the measurements.

Cooling water flow rate

The cooling water flow rate was measured by means of a rotameter upstream of the double pipe heat exchange tube. The calibration curve and its equation are given in Appendix A.

Wax-kerosene mixture flowrate

The flow rate of the wax-kerosene mixture was measured by an orifice meter. The volumetric flow rate was calculated from:

$$V = C_d A_{or} \sqrt{\frac{2\Delta P}{\rho_k (1-\beta^4)}} \tag{14}$$

where

$$\Delta P = h(\rho_{hg} - \rho_w)g$$

C_d, the discharge coefficient, was determined by calibration (Zhang, 1992) over the Re-range studied and was found to be 0.62 (confirmed at Reynolds No. of

orifice=4000). ΔP, the pressure drop across the orifice meter, was measured by using a manometer filled with mercury. To prevent wax deposition on the manometer and the pressure transmitting tubes, the wax-kerosene was separated from the water in small cylindrical pots (about 50 mm diameter by 110 mm height). The pots contained about half clean water and half kerosene solution. The clean water (transmission liquid) transmitted the pressure difference to the differential pressure manometer.

3.2 Temperature Measurement and Calibration

The following temperatures and temperature difference were measured:

- cooling water inlet temperature
- cooling water outlet temperature
- wax-kerosene mixture inlet temperature
- wax-kerosene mixture outlet temperature
- bulk temperature in the supply tank
- cooling water temperature rise

The thermocouples used were chromel (nickel-chromium)-constantan (copper-nickel) E type. All thermocouples were calibrated in the range 0°C to 60°C . The temperature-electrical voltage calibrations for the thermocouples used are given in Appendix B.

For temperature display a direct-reading digital thermometer was used (an OMEGA serial number 2170 digital thermometer and a 12-way selector switch). The automatic cold-junction-compensated thermometer had a range of -99.8 °C to 999.8 °C. Its resolution and repeatability were ±0.2 °C.

For temperature recording on the test rig, a Digitrend 235 data logger was used.

The datalogger could record either temperature or thermoelectric voltage . The temperature difference between the inlet and outlet of either the cooling water or the wax-kerosene mixture was normally about 1°C. This small differential temperature requires a high accuracy in the measurement to give a reasonable accuracy for heat flow calculations. Therefore, a ±0.5 μv or ±0.008 °C resolution was used, which was the best possible accuracy one could get from the datalogger. The differential temperature of the cooling water side was measured by connecting the chromel sides of the two chromel-constantan thermocouples together and the constantan sides to the datalogger, for measurement of the voltage difference. This voltage difference was converted to temperature rise by the calibration equation.

3.3. Cloud Point and Viscosity

3.3.1 Cloud Point

According to standards (ASTM D2500-91 and IP 219/93), the cloud point of a petroleum oil is the temperature at which paraffin wax or other solid substances start to crystallize out or separate from solution when the oil is chilled under definite prescribed conditions.The cloud point was determined in separate experiments so that the wax-kerosene solution inlet bulk temperature could be appropriately controlled to stay above the cloud point in the wax fouling experiments.

Apparatus :

The apparatus shown in Fig. 6 was designed to meet the specification of ASTM D2500-91 and IP 219/93. The components of the apparatus are as follows:

a) Test jar: A test jar, a, of clear glass , cylindrical form, 33 mm in inside diameter and

115 mm in height.

b) Thermometer: An ASTM cloud test thermometer, b, having a range -38 to + 50 ^{o}C (or -36 to 120 ^{o}F).

c) Cork: A cork, c, to fit the test jar, bored centrally to take the test thermometer.

d) Jacket: A jacket, d, of glass, water tight, of cylindrical form, flat bottom, about 114 mm in depth, with inside diameter 13.7 mm. greater than the outside diameter of the test jar.

e) Disk: A disk of cork , e, 6 mm in thickness, and of the same diameter as the inside of the jacket.

f) Gasket: A ring gasket, f, about 5 mm in thickness, to fit snugly around the outside of the test jar and loosely inside the jacket. This gasket was made of cork. The purpose of the ring gasket was to prevent the test jar from touching the jacket.

g) Bath: A cooling bath, g, made of a transparent glass cylinder of 152 mm diameter and 152 mm height with a transparent glass support for the jacket, d.

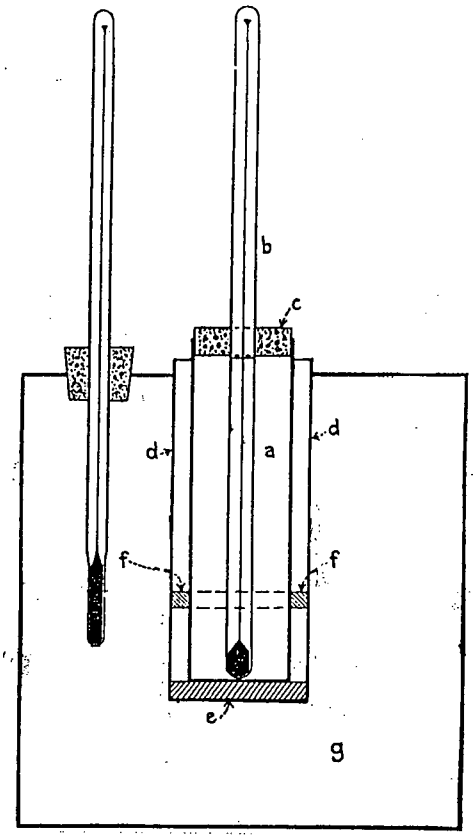

Fig. 6. Apparatus for cloud point measurement.

3.3.2 Viscometry

The flow behavior of waxy crudes is reported to be considerably modified by the crystallization of paraffins. Viscometer measurements were undertaken to determine whether the wax-kerosene solutions were Newtonian or non-Newtonian at their operating temperatures and, if Newtonian, to determine the viscosity.

A rotary viscometer was used to measure the shear stress vs. shear rate behaviour of the wax-kerosene mixtures at different concentrations and temperatures. The HAAKE Rotovisco is a computer-controlled rotary viscosity-testing apparatus. It consists of a stationary outer cup which contains the fluid to be tested. A motor-driven inner cup (rotor) is placed into the fluid and rotated. The torque of the rotor is measured by a force sensor and the data are logged to memory. The shear rate is measured as 1/second.

For a Newtonian fluid in the absence of turbulence, the rate of shear D [1/s] is directly proportional to the shear stress (τ_s). In this case the viscosity is defined by the Newtonian equation

$$\mu = \frac{\tau_s}{D} \tag{15}$$

If the rate of deformation (shear rate D) is not directly proportional to the shear stress (τ_s), then the fluid is said to be non-Newtonian.

Chapter 4

4. Experimental Procedures

4.1 System Cleaning

Before cleaning, the wax-kerosene mixture was drained out from the test rig via the drain valve at the bottom of the mixing tank. The test rig was washed with about 10 litres clean hot kerosene (50°C or less) by pumping this liquid through the flow loop for about 30 minutes. The whole system including the pump and filter was then drained.

4.2 Preparation of Wax-Kerosene Mixture

Wax concentration was determined in weight percent

$$i.e.\ concentration\ of\ wax-kerosene\ mixture\ (wt.\ \%) = \frac{wax\ weight}{wax\ weight\ +\ kerosene\ weight} * 100$$

The total volume of the mixing tank was about 30 liters. The general procedure was:

1) The tank was filled with 10 liters of kerosene (minus a portion set aside for washing).

2) The kerosene was recirculated by the pump and heated up to 40°C .

3) The melted wax was then poured into the tank. The funnel and fill port were washed with heated kerosene, which had been set aside for this purpose.

4) The mixture was recirculated for 10 minutes at 50°C before a test was started.

4.3 Fouling Test

The general protocol for the fouling runs is described as follows:

1) Power to the datalogger is turned on. The time and run number are put into the instrument. The functions of measuring points are programmed and the compensation voltage, E, of the datalogger is recorded.

2) All display instruments in the test rig are turned on. A particular temperature display

can be selected using the selector switch.

3) The pump is started and the wax-kerosene mixture is circulated through the test system.

4) The tank heating tape is turned on using the potentiometer (max. 13 amps.) if necessary.

5) The pipe heating tape can be turned on by using the switch but heating the pipe is optional depending on the wax-kerosene condition in the pipeline. Once the wax-kerosene starts to flow, power to the heating tape **must be stopped.**

5) The wax-kerosene flow rate is adjusted to the desired value using the two flow valves.

6) When the bulk temperature reaches a steady state, the readings of the manometer pressure drops are recorded.

7) The datalogger is started with a scanning sequence of 2 minutes.

8) The cooling water through the test section is set at 20% on the rotameter scale. The flow rate corresponding to this setting can be calculated using the calibration Eq. 43 in Appendix A.

9) Data are gathered over three hours, and visual observations of the wax deposit made. The run is then stopped by turning off all heating tapes and the data logger.

10) The cooling water is turned off, allowing the wax-kerosene mixture to heat up. If required, the system is washed by running hot liquid through the test rig.

11) The pump is stopped, and all power is shut off.

4.4. Cloud Point Test

Procedure for cloud point

Following is the procedure for measuring the cloud point temperature, using the

apparatus of Fig. 6.

a) The oil temperature to be tested was brought to a temperature of at least 14 °C above the approximate cloud point.

b) The clear oil was poured into the test jar, a , to a height of not less than 51 mm or more than 57 mm.

c) The test jar was tightly closed by the cork, c, carrying the test thermometer, b, in a vertical position in the center of the jar, with the thermometer bulb resting on the bottom of the jar.

d) The disk, e, was placed at the bottom of the jacket, d, and the test jar was inserted into the jacket with the ring gasket, f, 25 mm above the bottom.

e) The temperature of the cooling bath, g, was maintained at -1.1 to 1.7 °C.

f) At each test thermometer reading that is a multiple of 1.1 °C(2°F), the test jar was removed from the jacket, quickly but without disturbing the oil, inspected for cloud, and replaced in the jacket.

g) When such inspection first revealed a distinct cloudiness or haze in the oil at the bottom of the test jar, the reading of the test thermometer was recorded as the cloud point.

Chapter 5

5. Properties of Wax and Kerosene

5.1. Waxes

In this investigation, three waxes were used. A refined wax marketed by ESSO was purchased locally. ESSO Petroleum Canada, Research Department supplied two slack waxes from the Sarnia refinery, which were designated MCT-10 and MCT-30.

Waxes were characterized by measuring the amount of oil in the wax and obtaining a boiling point distribution using a GC chromatogram which permits identification of the normal paraffins present in the wax. The amount of oil is measured using the procedure ASTM (D3235). The results provided by ESSO for the two types of wax used, including important physical properties, are shown in Fig. 9 and Fig. 10. Slack wax is an intermediate product before refining. The figures show that both refined wax and slack wax MCT-10 contain mostly molecules with about 20 to 30 carbon atoms. MCT slack wax contains more branched hydrocarbons and oil compared to refined wax.

5.2 Kerosene

The kerosene utilized in these experiments was bought from ESSO. Commercial kerosene is defined by the ASTM as a "refined petroleum distillate suitable for use as illuminant when burned in a wick lamp" (Handbook of Petroleum Processing, 1967). The properties are summarized below:

Boiling point range	195-260 °C
Flash point	46 °C
Burning test	16 hr

Sulfur, % mass	0.13
Color, Saybolt chrom,	
no darker than	+21
Color, Saybolt chrom,	
after heating 16 hr,	
no darker than	+16
Cloud point	-15 °C
Specific gravity (15.6 °C)	0.80

5.3 Cloud Point of Wax-Kerosene Mixtures

The cloud point of a wax-kerosene mixture is the temperature at which paraffin wax or other solid substances start to crystallize out or separate from solution when the oil is chilled under definite prescribed conditions. The bulk temperature outside the heat exchanger was maintained above the cloud point. This would ensure that the wax precipitates only inside the heat exchanger. The cloud point measurements taken for refined wax, slack wax MCT-10 and MCT-30 are tabulated below.

Table 3. Cloud Point Temperature (°C) for Refined and Slack Waxes in Kerosene.

Conc (% by wt.)	Refined wax	MCT-10	MCT-30
5	15.6	15.0	31.1
10	21.1	21.1	36.7
15	25.6	23.3	40.0
20	28.9	27.8	42.2

5.4 Viscosity of Wax-Kerosene Mixtures

The wax-kerosene mixtures were found to be Newtonian near and above the cloud point. The test was made by using the Rotovisco mentioned in the previous two Chapters and the range of the shear rate used was from 0 to 468 1/s. Two typical graphs (Fig. 7

and Fig. 8) show shear stress vs. shear rate for refined wax at 10% by wt. concentration and slack wax MCT-10 at 5 % by wt. concentration. All the data points at each concentration and temperature were fitted using a linear equation of the form $\tau = b + aD$, an equation of the form $\tau = a + bD^n$ and a third equation of the form $\tau = bD^n$. The best fit was found in each case by the linear equation, which is equivalent to the second equation with n=1. For refined wax at 10 % by wt and a temperature of 21.1 °C, the standard deviation for the linear fit was 0.021 and the τ intercept was -0.007, so it could be inferred that the intercept was not significant and could be assumed to pass through zero, since the absolute value of the intercept was less than the standard deviation. The slack wax MCT-10 was tested at 5 % concentration and a temperature of 15 °C (Fig. 8), at which the standard deviation and the τ intercept for the linear fit were 0.023 and -0.008 respectively. As the absolute value of the intercept was again less than the standard deviation, it could again be stated that the significance of the intercept was negligible. Therefore, the wax-kerosene solution was taken to be Newtonian at the given temperature and concentration. The wax-kerosene solution viscosities were found from the slope of the best line passing through the origin, i.e. $\mu = \frac{\tau}{D}$.

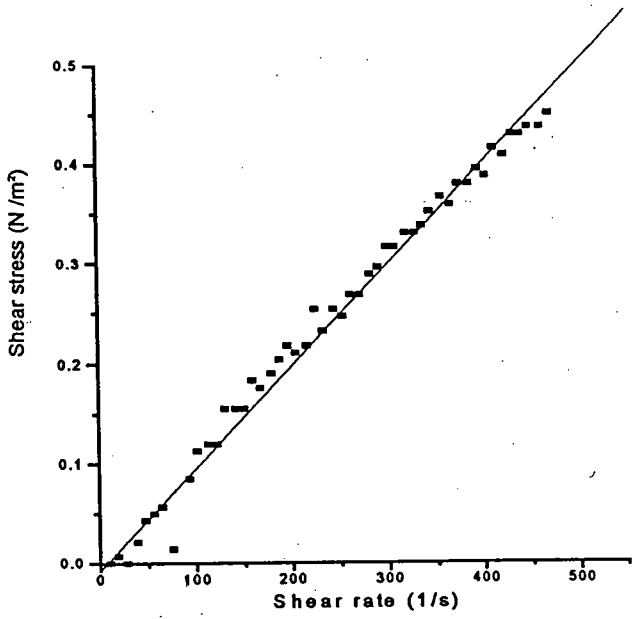

Fig. 7. Typical graph of shear stress vs. shear rate for refined wax in kerosene at 10 % by wt. and 21.1 °C. Cloud point of solution= 21.1 °C

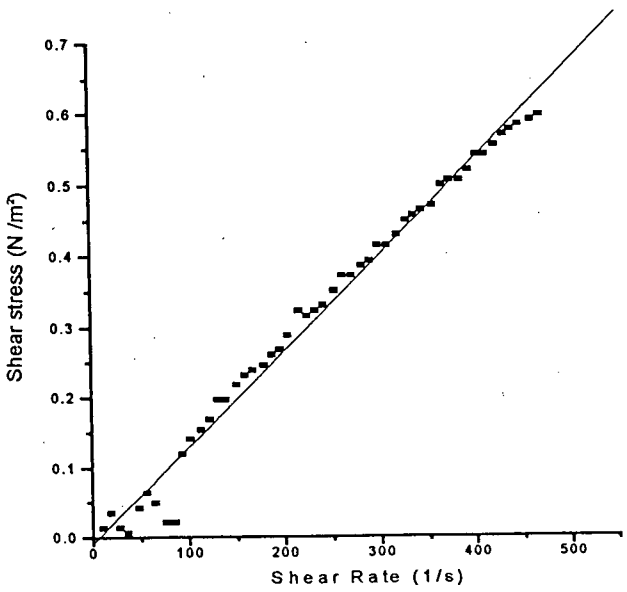

Fig. 8. Typical graph of shear stress vs. shear rate for slack wax MCT-10 in kerosene at 5 % by wt. and 15.0 °C. Cloud point of solution=15.0 °C

Viscosity was measured as a function of temperature for wax-kerosene mixtures as described in section 3.3.2. The viscosity runs taken at some intervals of temperature starting near the cloud point are tabulated below.

Table 4: Viscosity runs for refined wax at 5 % by wt. in kerosene.

T [°C]	15.6	25.0	30.0	35.0	40.0
μ [Pa.s].10^{-3}	1.30	0.89	0.82	0.76	0.78

Table 5: Viscosity runs for refined wax at 10% by wt. in kerosene.

T [°C]	21.1	25.0	30.0	35.0	40.0
μ [Pa.s].10^{-3}	1.02	1.26	1.00	0.87	0.80

Table 6: Viscosity runs for refined wax at 15 % by wt. in kerosene.

T [°C]	25.6	30.0	35.0	40.0	
μ [Pa.s].10^{-3}	1.25	1.10	0.93	0.82	

Table 7: Viscosity runs for refined wax at 20 % by wt. in kerosene.

T [°C]	28.9	35.0	40.0		
μ [Pa.s].10^{-3}	1.10	1.00	0.80		

Table 8: Viscosity runs for slack wax MCT-10 at 5 % by wt. in kerosene.

T [°C]	15.0	20.0	25.0	30.0	35.0	40.0
μ [Pa.s].10^{-3}	1.37	1.03	1.03	0.90	0.90	0.81

Table 9: Viscosity runs for slack wax MCT-10 at 10 % by wt. in kerosene.

T [°C]	21.1	25.0	30.0	35.0	40.0	45.0
μ [Pa.s].10^{-3}	1.27	1.14	1.07	0.95	0.87	0.81

Table 10: Viscosity runs for slack wax MCT-10 at 15 % by wt. in kerosene.

T [°C]	23.3	30.0	35.0	40.0	45.0	
μ [Pa.s].10^{-3}	1.40	1.10	0.98	0.84	0.78	

Table 11: Viscosity runs for slack wax MCT-10 at 20 % by wt. in kerosene.

T [°C]	27.8	35.0	40.0	45.0	
μ [Pa.s].10^{-3}	1.04	0.91	0.81	0.80	

The physical properties which are used in the heat transfer and flow computations involve densities, viscosity, and heat capacities of the wax-kerosene mixture.

The properties of water were regressed using data obtained from the Handbook of Chemistry and Physics(1987). The accuracy of the equations has not been given.

Density of water (kg/m^3)

$$\rho_w = (999.83952 + 16.945176 t_b - 7.9870401 \times 10^{-3} t_b^2 - 46.170461 \times 10^{-6} t_b^3 + 105.56302 \times 10^{-9} t_b^4 - \frac{280.54253 \times 10^{-12} t_b^5}{(1 + 16.879850 t_b)}$$

for 0 °C $< t_b <$ 20 °C

Viscosity of water (Pa.s)

$$\log_{10} \mu_w 10^3 = \frac{1301}{998.333 + 8.1855(t_b - 20) + 0.00575(t_b - 20)^2} - 1.30233$$

t_b in °C

Heat capacity of water (kJ/kg °C)

$$C_{pw} = 4.21765 - 3.74987 \times 10^{-3} t_b + 1.49921 \times 10^{-4} t_b^2 - 3.35545 \times 10^{-6} t_b^3 + 4.27292 \times 10^{-8} t_b^4 - 2.30244 \times 10^{-10} t_b^5$$

where

$$t_b = \frac{t_1 + t_2}{2} \quad (^{\circ}C)$$

The density and heat capacity of the wax-kerosene mixtures were experimentally measured

by Zhang (1992) using refined wax. The results are as follows.

Density (kg/m^3): $\rho_k = 816.25 - 0.74892T_b$, T_b in ^oC

The presence of different concentrations of wax in kerosene did not change the density of the mixture much, so the above equation was used for all concentrations. The wax-kerosene solutions were measured from about 25 to 80 ^oC.

Heat capacity (kJ/kg ^oC): $C_{pk} = 1.18143 + 0.012246T_b$, where $T_b = \frac{T_1 + T_2}{2}$, T_b in ^oC

The effect of wax on the wax-kerosene specific heat capacity was minimal, so the above equation was used for all concentrations.

Viscosity: $\mu_k = a\exp\left(\frac{b}{RT_b}\right)$, T_b in K.

The above equation for viscosity was fitted using data from Tables 4-7 for refined wax and Tables 8-11 for slack wax MCT-10. The corresponding values of a and b are given in Tables 12 and 13 for refined wax and MCT-10 slack wax, respectively.

Table 12: Viscosity Coefficients a and b for Refined Wax.

Wax concentration (wt. %)	5	10	15	20
a	1.83×10^{-6}	7.58×10^{-6}	1.27×10^{-7}	1.65×10^{-7}
b	15525	12147	22830	22171

Table 13: Viscosity Coefficients a and b for MCT-10 Slack Wax.

Wax concentration (wt %)	5	10	15	20
a	4.16×10^{-6}	3.80×10^{-6}	1.86×10^{-7}	5.92×10^{-7}
b	13676	14160	21993	18820

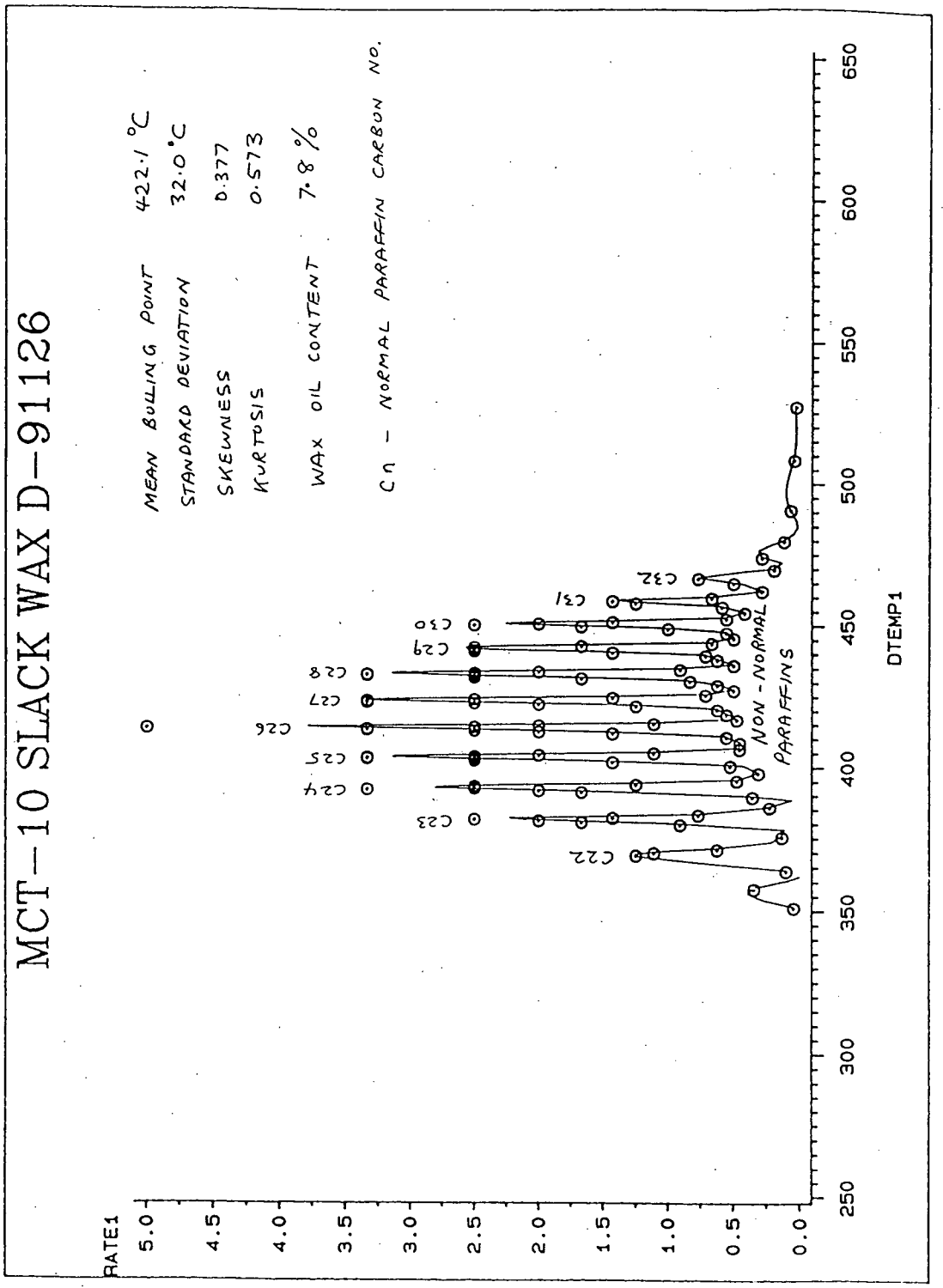

Fig. 9. GC chromatogram for refined wax.

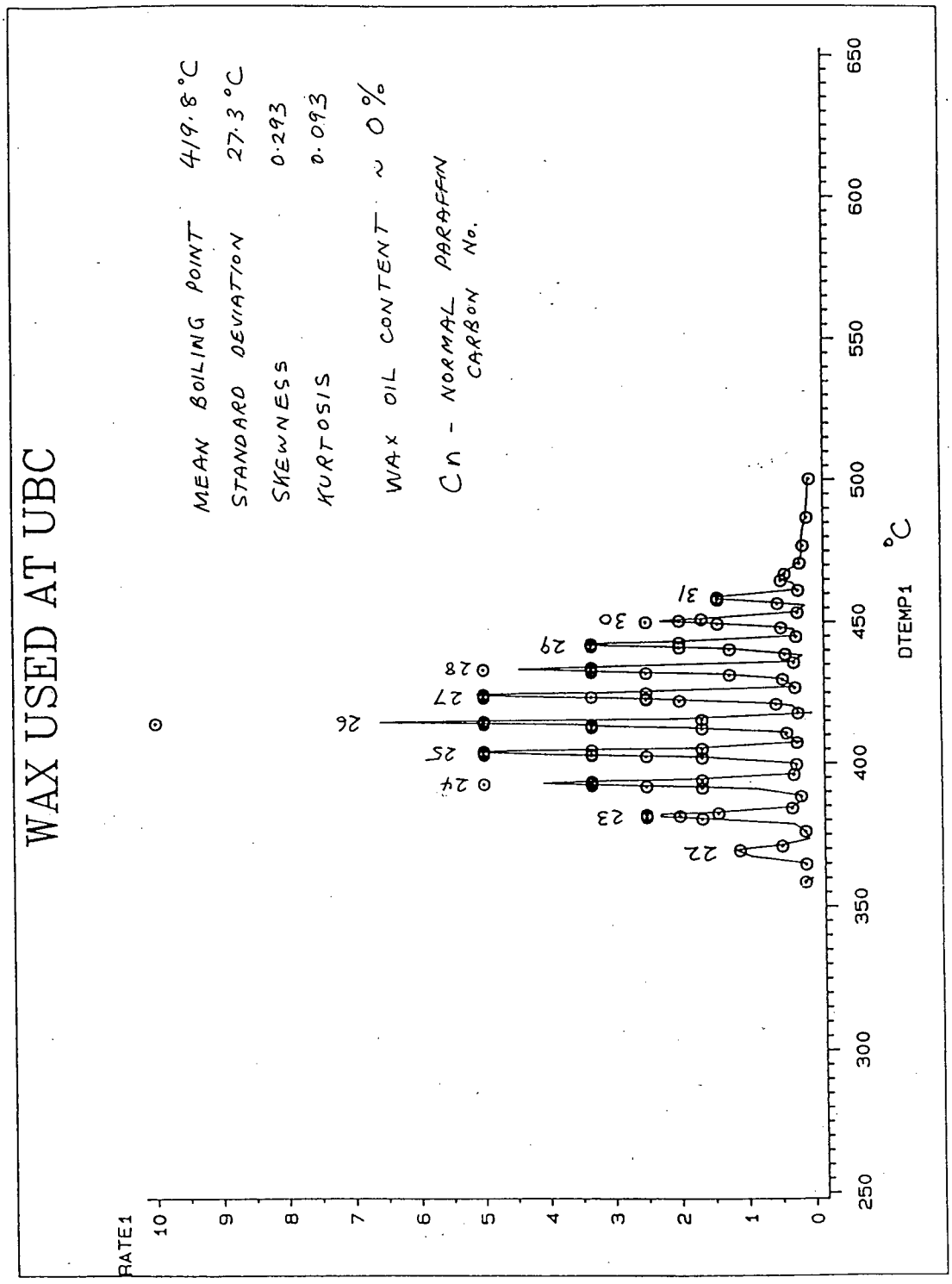

Fig. 10. GC chromatogram of slack wax MCT-10.

Chapter 6

6. Data Analysis

The computations arising from wax fouling tests included calculation of the fouling resistance as a function of time, and fitting these data to the Kern-Seaton equation.

6.1 Calculation of fouling resistance

The heat gained by the cooling water can be determined from

$$Q_w = \dot{m} C_{pw} (t_2 - t_1) \tag{16}$$

or by using the directly measured Δt (the differential temperature rise) for accuracy

$$Q_w = \dot{m} C_{pw} \Delta t \tag{17}$$

Equation (17) was preferred since the measurement of Δt was more accurate than that of $(t_2 - t_1)$. Because of uncertainties in the heat capacity for the wax-kerosene mixture the heat lost by this stream was not used in the calculation of Q. The overall heat transfer coefficient based on the inside surface of the inner tube was determined at time θ as

$$U = \frac{Q_w}{\Delta T_{lm} A_i} \tag{18}$$

where

$$\Delta T_{lm} = \frac{(T_1 - t_2) - (T_2 - t_1)}{\ln \dfrac{(T_1 - t_2)}{(T_2 - t_1)}} \tag{19}$$

The inside area was used because even with the coated tubes, A_i was constant for all tubes. The fouling resistance at any time θ was then given by

$$R_f = \left\{ \frac{1}{U} - \frac{1}{U_o} \right\} \frac{A_o}{A_i} \tag{20}$$

where U_o is the clean overall coefficient at θ=0.

The Reynolds number of wax-kerosene solution was calculated as

$$\mathrm{Re} = \frac{\rho d_h u}{\mu_k} \tag{21}$$

where d_h is the hydraulic diameter for the annulus, and u is the actual velocity in the annulus.

6.2. Data Fitting and Determination of Parameters

From the fouling tests, it was found that most plots of R_f^* vs. θ followed asymptotic behaviour, i.e. the deposit was built up at a falling rate and eventually reached a constant value. Even without constancy of m_d and the other assumptions underlying Eq. (6), this type of behaviour can be represented by the well known Kern-Seaton equation Eq. (7), which can be rewritten as

$$R_f = R_f^*(1-e^{-\frac{\theta}{\theta_c}}) \tag{22}$$

where $R_f = \frac{m}{\rho_f k_f}$, and was calculated via Equation (20).

A computer program (Appendix C) was developed which fitted the experimental data by a non-linear least squares method to the above equation and found the two parameters R_f^* and θ_c. Given a set of data points (θ_i, R_{f_i}), where i=1,....N, the values of R_f^* and θ_c were calculated to minimize the sum,

$$Sum = \sum_{i=1}^{N} \left\{ R_{f_i} - [\ R_f^*(1-e^{-\frac{\theta_i}{\theta_c}})\ ] \right\}^2 \tag{23}$$

Uncertainty

The uncertainty in the fouling resistance caculation has been explicitly derived by Crittenden et al. (1992) for crude oil fouling. The heat transferred in the heat exchanger can be calculated using Eq. (17), and the fouling resistance using Eq.(20). From Eq. (20), it is clear that the error in the calculated value of R_f is dependent upon the errors in the calculated values of both U_o and U. For the function

$$R_f = R_f(U_o, U) \tag{24}$$

$$dR_f = \frac{\partial R_f}{\partial U_o} dU_o + \frac{\partial R_f}{\partial U} dU \tag{25}$$

If the errors in U_o and U are δU_o and δU respectively, and are small relative to U_o and U, then the error induced in R_f is given by:

$$\delta R_f = \frac{\partial R_f}{\partial U_o} \delta U_o + \frac{\partial R_f}{\partial U} \delta U \tag{26}$$

The worst possible value of δR_f occurs when all of the terms on the right hand side of the equality are either positive or negative. Thus, taking δU_o and δU to be positive,

$$\delta R_f = \left|\frac{\partial R_f}{\partial U_o}\right| \delta U_o + \left|\frac{\partial R_f}{\partial U}\right| \delta U \tag{27}$$

From Eq. (20),

$$\frac{\partial R_f}{\partial U_o} = \frac{1}{U_o^2} \frac{A_o}{A_i} \tag{28}$$

$$\frac{\partial R_f}{\partial U} = -\frac{1}{U^2} \frac{A_o}{A_i} \tag{29}$$

Thus

$$\delta R_f = \left(\frac{\delta U_o}{U_o^2} + \frac{\delta U}{U^2} \right) \frac{A_o}{A_i} \tag{30}$$

Errors in U depend upon the accuracy of the heat exchanger data and are related solely to errors in Q, A_o and LMTD (Eq. 19).

Errors in operating parameters

In the following analysis the worst scenario is considered, that is, the errors in each of the four end temperatures and in each of the two flowrates compound, rather than eliminate each other. The instantaneous coefficient U is given by:

$$U = \frac{Q_w \ln\left\{ \frac{T_1 - t_2}{T_2 - t_1} \right\}}{A_i \left[(T_1 - t_2) - (T_2 - t_1) \right]} \tag{31}$$

Thus neglecting errors in the calculation of A_i,

$$\delta U = \left| \frac{\partial U}{\partial Q_w} \right| \delta Q_w + \left| \frac{\partial U}{\partial t_1} \right| \delta t_1 + \left| \frac{\partial U}{\partial t_2} \right| \delta t_2 + \left| \frac{\partial U}{\partial T_1} \right| \delta T_1 + \left| \frac{\partial U}{\partial T_2} \right| \delta T_2 \tag{32}$$

Hence

$$\frac{\delta U}{U} = \frac{\delta Q_w}{Q_w} + \frac{1}{W} \left\{ \left| \frac{Z}{\ln X} - 1 \right| \delta t_1 + \left| 1 - \frac{Y}{\ln X} \right| \delta t_2 + \left| \frac{Y}{\ln X} - 1 \right| \delta T_1 + \left| 1 - \frac{Z}{\ln X} \right| \delta T_2 \right\} \tag{33}$$

where

$$W = (T_1 - t_2) - (T_2 - t_1) \tag{34}$$

$$X = \left\{ \frac{T_1 - t_2}{T_2 - t_1} \right\} \tag{35}$$

$$Y = \frac{W}{(T_1 - t_2)} \tag{36}$$

$$Z = \frac{W}{(T_2 - t_1)} \tag{37}$$

Error in the duty

The instantaneous thermal duty Q_w is given by Eq. (16). Assuming that there is no error in C_{pw}, then, based on individual measurement of t_1 and t_2,

$$\delta Q_w = \left|\frac{\partial Q_w}{\partial \dot{m}}\right|\delta \dot{m} + \left|\frac{\partial Q_w}{\partial t_1}\right|\partial t_1 + \left|\frac{\partial Q_w}{\partial t_2}\right|\partial t_2 \tag{38}$$

or

$$\delta Q_w = C_{pw}(t_2 - t_1)\delta \dot{m} + \dot{m}C_{pw}\delta t_1 + \dot{m}C_{pw}\delta t_2 \tag{39}$$

and

$$\frac{\delta Q_w}{Q_w} = \frac{\delta \dot{m}}{\dot{m}} + \frac{\delta t_1 + \delta t_2}{(t_2 - t_1)} \tag{40}$$

The uncertainty as a percentage can be written by modifiying Eq. (30)

$$\frac{\delta R_f}{R_f} = \left(\frac{1}{U_o}\frac{\delta U_o}{U_o} + \frac{1}{U}\frac{\delta U}{U}\right)\frac{A_o}{A_i}\frac{1}{R_f} * 100\% \tag{41}$$

$\delta U/U$ is given by combining Eq. (40) and (33), i.e.

$$\frac{\delta U}{U} = \frac{\delta \dot{m}}{\dot{m}} + \frac{\delta t_1 + \delta t_2}{(t_2 - t_1)} + \frac{1}{W}\left\{\left|\frac{Z}{\ln X} - 1\right|\delta t_1 + \left|1 - \frac{Y}{\ln X}\right|\delta t_2 + \left|\frac{Y}{\ln X} - 1\right|\delta T_1 + \left|1 - \frac{Z}{\ln X}\right|\delta T_2\right\} \tag{42}$$

$\delta U_o/U_o$ can be calculated from the corresponding values at time θ=0, the mass flowrate, $\dot{m}$, remaining constant throughout an experiment. The values for δt_1, δt_2, δT_1, δT_2 = 0.008 °C for all cases. $\delta \dot{m}/\dot{m}$ was taken to be 1% from experimental observation. The uncertainty in the fouling resistances, $\delta R_f / R_f$, was calculated by finding $\delta U_o/U_o$ and $\delta U/U$ from Eq. (42) and inserting the values in Eq. (41). This result is reported in the next Chapter in %, which is the maximum error one can get in R_f. A slightly smaller maximum would have been reported if the above calculation were based on a single measurement of t_1-t_2 or Δt.

Chapter 7

7. Results and Discussion

After addressing reproducibility, the results are presented in five sections, namely, the effect of velocity, the effect of bulk temperature, the effect of surface condition, the concentration effect, and deposit removal and sliding phenomena. Two types of wax were used, refined wax and slack wax MCT-10, the properties of which are summarized in Chapter 5.

6.1 Test of Reproducibility

A test was carried out twice to check for reproducibility. The test was carried out for the chrome-plated stainless steel with slack wax at 20 % by wt concentration.

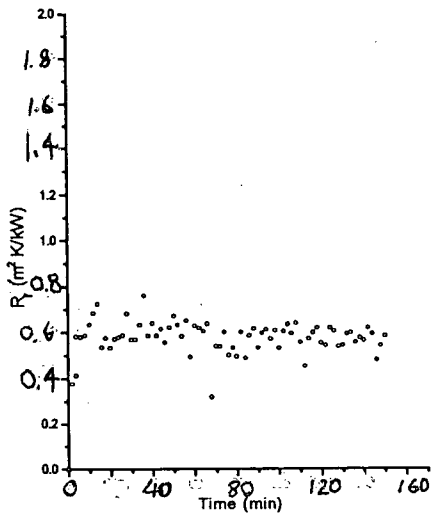

Fig. 11. Result for slack wax at 20% by wt on chrome-plated stainless steel tube, Re=9224 and T_b=31.2 °C.
$R_f = 0.6031(1-e^{-\frac{\theta}{21}})$

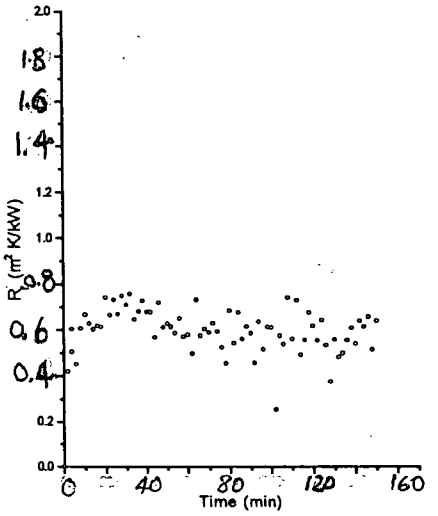

Fig. 12. Result for slack wax at 20% by wt. on chrome-plated stainless steel tube, Re=9208 and T_b=31.2 °C.
$R_f = 0.5814(1-e^{-\frac{\theta}{22}})$

As shown by Figures 11 and 12, the fouling resistance recorded as a function of time increased rapidly in the first 5-10 minutes and then assumed a constant fouling resistance. These results show that wax deposition is a rapid process with a small time constant θ_c . Table 16 lists results for R_f^* and θ_c. For the two experiments, $\overline{R}_f^*$=0.592 m² K/kW and the total range of R_f^* was 0.022 m² K/kW, which is less than 4 % of the mean. The time constants were 2.1 and 2.2 minutes, respectively, a disagreement of less than 5 %. The uncertainty was 15.4 % for Fig. 11 and 15.6 % for Fig. 12. The two graphs are representative for all the data except for those at the highest Re.

7.2. Fouling Results

7.2.1 Effect of Velocity

For slack wax MCT-10 at 20 % by wt., Fig. 13 a-e shows R_f versus time plots and the corresponding fitted curves. It is apparent that at lower velocity, the R_f values are larger. Table 15 shows that as the Reynolds number is roughly doubled from 6645 to 14,430, the R_f^* value decreases by a factor of 1.5. For refined wax at 10 % by weight, the above trend with Reynolds number was similar for the same tube and in this case the time constant, θ_c, also decreases as Re increases, i.e. the fouling resistance takes less time to reach 63 % of R_f^* at higher flow velocities, as seen in Table 14. Figure 14 shows the Reynolds No. effect on R_f^* for the refined wax runs. R_f vs. θ data are shown in Appendix D.

It was found that the asymptotic fouling resistance decreases with increasing flow velocity for all surface types and both waxes. The slack wax even at 20 wt. % concentration gave slightly lower values than did the refined wax at 10 wt. % concentration. For each tube the decreasing trend of R_f^* with velocity was evident, but the time constants showed little in the way of trends with velocity. Conditions of 37

experimental runs with slack wax and values of the fitted parameters are given in Tables 15- 21. The Reynolds number effect on R_f^* is plotted for all surfaces in Figure 15a. The lines were determined by fitting a quadratic equation to the data points for each surface. The effect of velocity appears stronger with some surfaces than with others. For example, with the n-C18 silane-coated chrome-plated stainless steel tube, R_f^* appears almost independent of Re at Re>9000, whereas with both Heresite coated stainless steel tubes, R_f^* drops markedly over the same range of Re. Fig. 15b shows a plot of log (R_f^*) vs. log (Re) for the data of Fig. 15a. The uncoated stainless steel (slope=-0.42), chrome-plated stainless steel (-0.61), sand-blasted stainless steel (-0.81), n-C18 silane-coated chrome-plated stainless steel (-0.58) and n-C18 silane coated stainless steel (-0.84) each show a straight line fit on this plot. However, the two Heresite-coated tubes did not show this straight line fit. From the data of Bott and Gudmundsson (1977b) for a sand-blasted copper plate shown in Figure 2, log (R_f^*) vs. log (Re) would yield a slope of about -0.5. For the five straight line fits obtained on Fig. 15b, the slopes ranged from -0.4 to -0.8, while the average slope of the two curves for the Heresite-coated tubes was approximately -2.6.

One reason for the decrease in R_f^* with velocity may be the increased shear acting on planes of weakness in the deposit such that as Re increases, progressively thinner wax layers can exist. The Kern and Seaton model, Eq. (7), suggests that removal increases with deposit thickness for this very reason. Another possible reason for the decrease is that as the flow velocity increases, the surface temperature where the wax deposition occurs increases.

Taking the derivative of Eq. (22) with respect to time yields the initial fouling rate

$$\left.\frac{dR_f}{d\theta}\right|_{t=0} = \frac{R_f^*}{\theta_c}$$

The results of the above equation were calculated and presented in Tables 14-28. While the trends of R_f^*/θ_c versus Re are widely scattered, this parameter tends to decrease as Reynolds increases for both types of waxes and for most tubes. Thus for refined wax at 10 % on stainless steel the initial fouling rate, R_f^*/θ_c, decreases with increasing Re (Table 14), i.e. lower initial rate of attachment. This was also found by Watkinson and Epstein (1969) for gas oil fouling. The same holds true for slack wax MCT-10 at 20 % on stainless steel, sand-blasted stainless steel and n-C18 silane-coated stainless steel (Tables 15, 16 and 21), but the two Heresite coated tubes do not show a consistent trend.

Table 14. Results for refined wax at 10 % by wt. using stainless steel. T_b =32.6±0.2°C, Cloud Point= 21.1 °C , t_b=9.5±0.5 °C, V_w=2.5 m/s.

Re	R_f^* (m² K/kW)	θ_c (min.)	Uncertainty (%)	R_f^*/θ_c (m² K/kW·min)
7093	2.1890	8.9	13.7	0.2460
11414	0.8896	5.5	30.0	0.1617
14812	0.5122	2.5	22.5	0.2049
17332	0.3363	2.6	27.5	0.1293
19053	0.2249	2.1	27.9	0.1071

Table 15. Results for slack wax MCT-10 at 20% by wt. using stainless steel. T_b =31.4±0.3 °C, Cloud Point= 27.8 °C , t_b=10.4±1.5°C, V_w=1.1 m/s.

Re	R_f^* (m² K/kW)	θ_c (min.)	Uncertainty (%)	R_f^*/θ_c (m² K/kW·min)	$R_{f,\,tot}^* = 1/U_o + R_f^*$ (m² K/kW)
6645	0.9293	8.0	11.9	0.1162	2.2666
8722	0.8244	10.8	11.4	0.0765	1.9197
10615	0.7926	13.2	8.9	0.0600	1.6597
12184	0.7244	18.1	9.2	0.0400	1.6142
14430	0.6668	10.3	7.8	0.0645	1.4867

Table 16. Results for slack wax MCT-10 at 20% by wt. using chrome-plated stainless steel. T_b = 31.3±0.1°C ,Cloud Point=27.8 °C , t_b=7.6±0.4°C, V_w=1.1 m/s.

Re	R_f^* (m² K/kW)	θ_c (min.)	Uncertainty (%)	R_f^*/θ_c (m² K/kW·min)	$R_{f,tot}^* = 1/U_o + R_f^*$ (m² K/kW)
6586	0.8238	2.1	17.8	0.3980	2.5841
9224	0.6031	2.1	15.4	0.2900	1.9377
9208	0.5814	2.2	15.6	0.4184	1.9258
11015	0.5941	1.4	11.6	0.3910	1.6754
13156	0.5240	1.3	9.8	0.0749	1.4183
14428	0.4817	6.4	9.6	0.2692	1.3076

Table 17. Results for slack wax MCT-10 at 20% by wt. using sand-blasted stainless steel. T_b = 31.2±0.1 °C, Cloud Point= 27.8°C , t_b=11.4±0.6 °C, V_w=1.1 m/s.

Re	R_f^* (m² K/kW)	θ_c (min.)	Uncertainty (%)	R_f^*/θ_c (m² K/kW·min)	$R_{f,tot}^* = 1/U_o + R_f^*$ (m² K/kW)
6418	1.2187	5.9	10.1	0.2066	2.3548
8734	0.8227	9.3	11.7	0.0863	1.9047
11340	0.7614	8.9	7.6	0.0856	1.5304
12732	0.6609	7.6	7.7	0.0870	1.3919
14440	0.6016	7.3	6.7	0.0824	1.2142

Table 18. Results for slack wax MCT-10 at 20% by wt. using n-C18 silane-coated chrome- plated stainless steel. T_b =31.3±0.1 °C, Cloud Point=27.8°C , t_b=13.6±0.7°C, V_w=1.1 m/s.

Re	R_f^* (m² K/kW)	θ_c (min.)	Uncertainty (%)	R_f^*/θ_c (m² K/kW·min)	$R_{f,tot}^* = 1/U_o + R_f^*$ (m² K/kW)
6629	0.7407	7.9	15.9	0.0938	2.0159
8773	0.4854	20.9	19.4	0.0232	1.7455
11314	0.4605	4.1	11.5	0.1123	1.2891
12888	0.4572	6.3	9.6	0.0726	1.1567
14642	0.4527	12.1	8.1	0.0374	1.0383

Table 19. Results for slack wax MCT-10 at 20% by wt using Heresite Si 57 E coated stainless steel. T_b =31.3±0.2 °C, Cloud Point=27.8 °C , t_b=13.5±0.9 °C, V_w=1.1 m/s.

Re	R_f^* (m² K/kW)	θ_c (min.)	Uncertainty (%)	R_f^*/θ_c (m² K/kW·min)	$R_{f,\,tot}^* = 1/U_o + R_f^*$ (m² K/kW)
6567	0.4406	3.2	21.0	0.1377	1.4979
8819	0.4056	5.0	15.8	0.0811	1.3169
11215	0.2263	2.1	18.2	0.1078	0.9410
12697	0.1534	3.2	24.1	0.0479	0.8162
14207	0.0700	9.4	55.6	0.0074	0.7314

Table 20: Results for slack wax MCT-10 at 20% by wt. using Heresite P-400/L-66 coated stainless steel. T_b= 31.2±0.1 °C, Cloud Point=27.8°C , t_b=13.2±0.4 °C, V_w=1.1 m/s.

Re	R_f^* (m² K/kW)	θ_c (min.)	Uncertainty (%)	R_f^*/θ_c (m² K/kW·min)	$R_{f,\,tot}^* = 1/U_o + R_f^*$ (m² K/kW)
6616	0.5552	6.4	21.1	0.0868	1.8305
8803	0.3804	2.0	17.2	0.1902	1.3111
8765	0.3671	2.3	16.3	0.0517	1.2295
11042	0.1912	3.7	28.2	0.0163	1.0458
12674	0.1288	7.9	47.2	0.0106	0.9277
14432	0.0520	4.9	155.1	0.1596	0.8425

Table 21. Results for slack wax MCT-10 at 20% by wt. using monolayer n-C18 silane coated stainless steel. T_b =31.5±0.1 °C, Cloud Point=27.8 °C , t_b=13.2± 0.2°C, V_w=1.1 m/s.

Re	R_f^* (m² K/kW)	θ_c (min.)	Uncertainty (%)	R_f^*/θ_c (m² K/kW·min)	$R_{f,\,tot}^* = 1/U_o + R_f^*$ (m² K/kW)
6631	0.7016	4.4	14.4	0.1595	1.8546
8734	0.4639	14.2	15.7	0.0327	1.4491
11084	0.4496	10.0	11.5	0.0450	1.2543
12672	0.3753	4.2	11.6	0.0894	1.1197
14147	0.3574	6.9	9.0	0.0518	1.0402

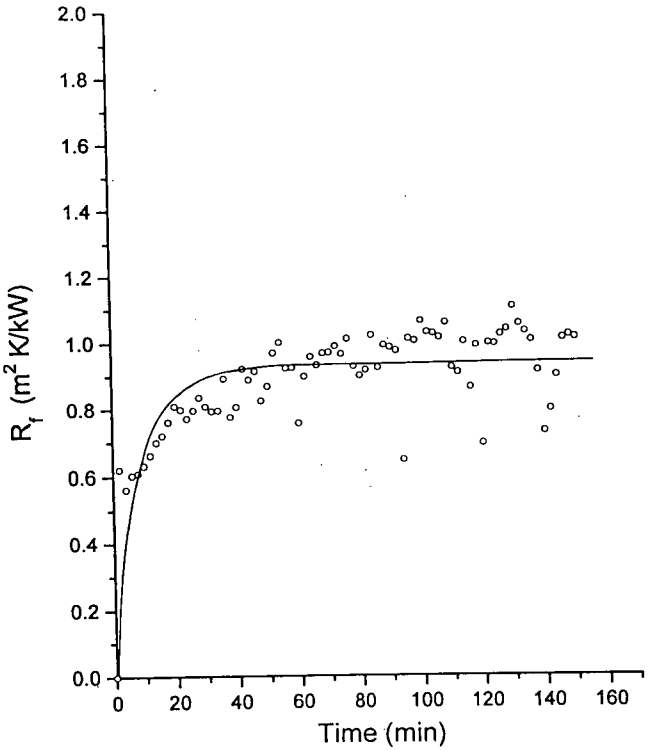

Fig. 13a. R_f vs. time for slack wax MCT-10 at 20 % by wt. using stainless steel. Re = 6645, T_b=31.4 °C, Cloud Point = 27.8°C.

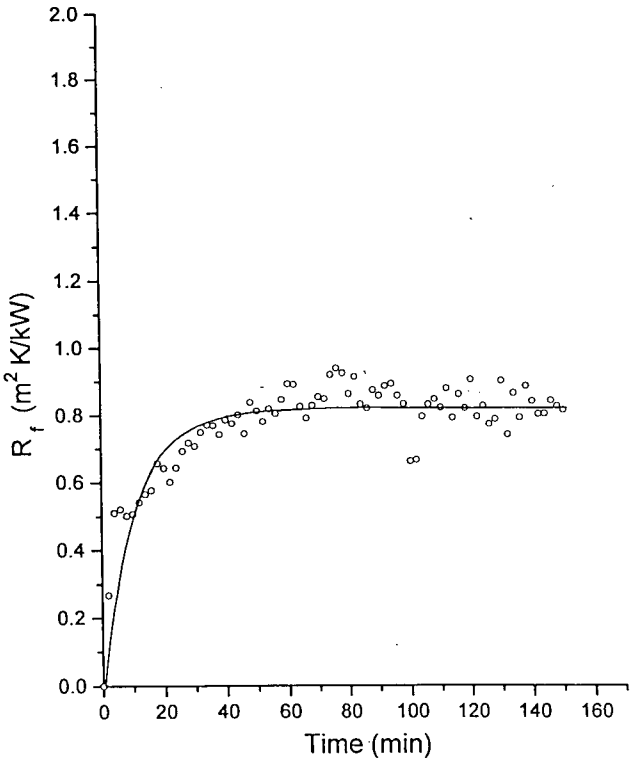

Fig. 13b. R_f vs. time for slack wax MCT-10 at 20 % by wt. using stainless steel. Re = 8722, T_b=31.4 °C, Cloud Point = 27.8°C.

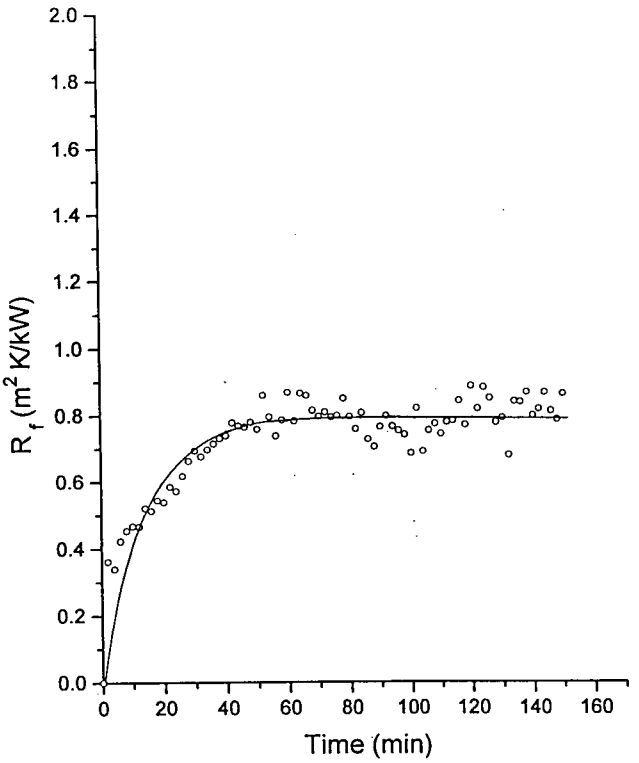

Fig. 13c. R_f vs. time for slack wax MCT-10 at 20 % by wt.using stainless steel. Re=10615, T_b=31.4 °C, Cloud Point=27.8°C.

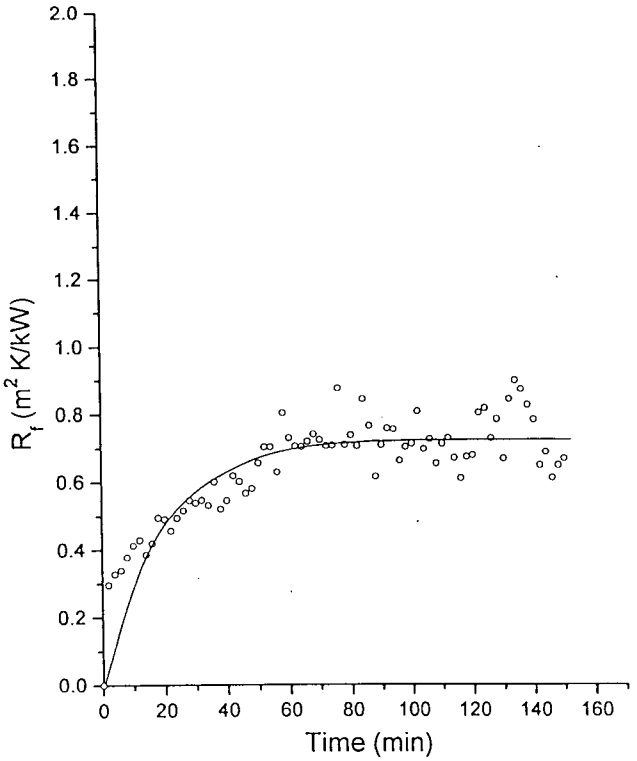

Fig. 13d. R_f vs. time for slack wax MCT-10 at 20 % by wt.using stainless steel. Re=12184, T_b=31.4 °C, Cloud Point=27.8°C.

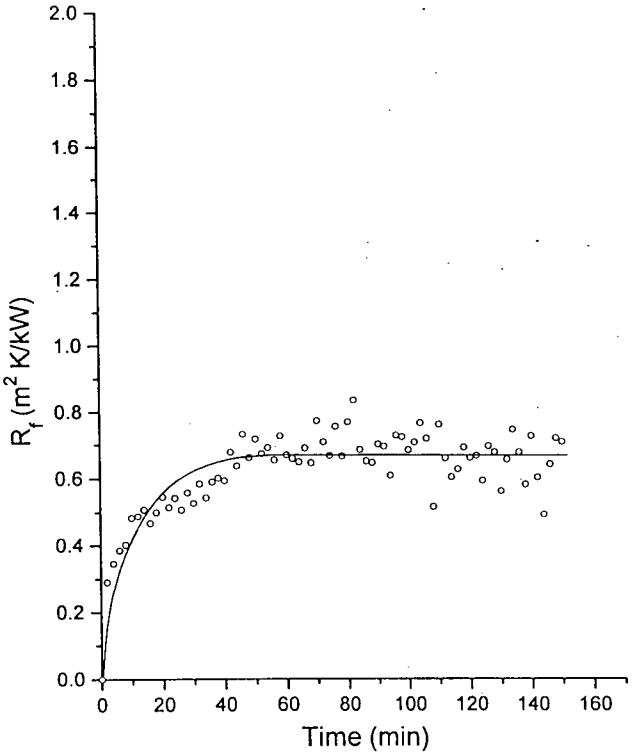

Fig. 13e. R_f vs. time for slack wax MCT-10 at 20 % by wt.using stainless steel. Re=14430, T_b=31.4 °C, Cloud Point=27.8°C.

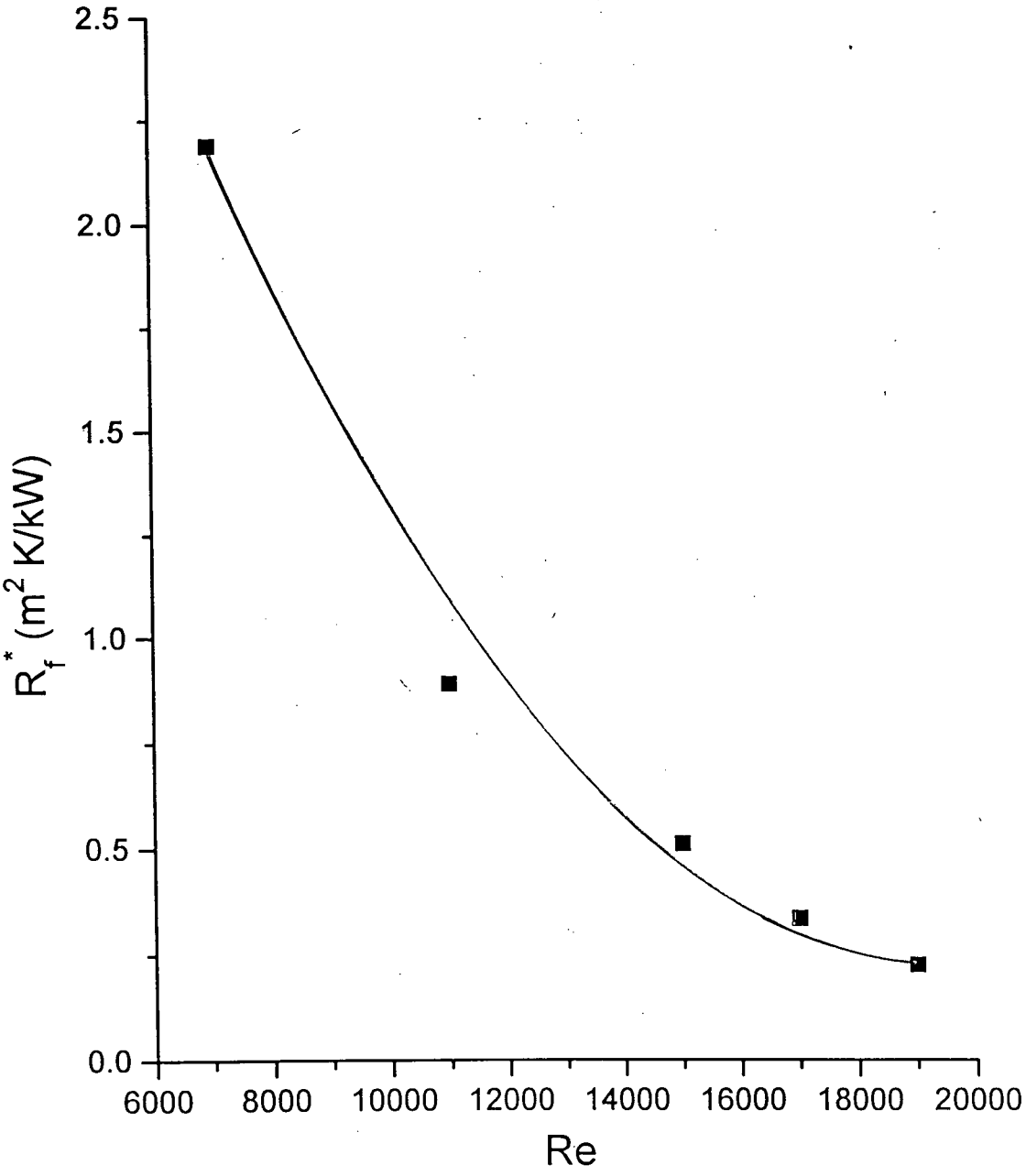

Fig. 14. Results for refined wax at 10% by wt. on uncoated stainless steel tube. T_b=32.6°C.

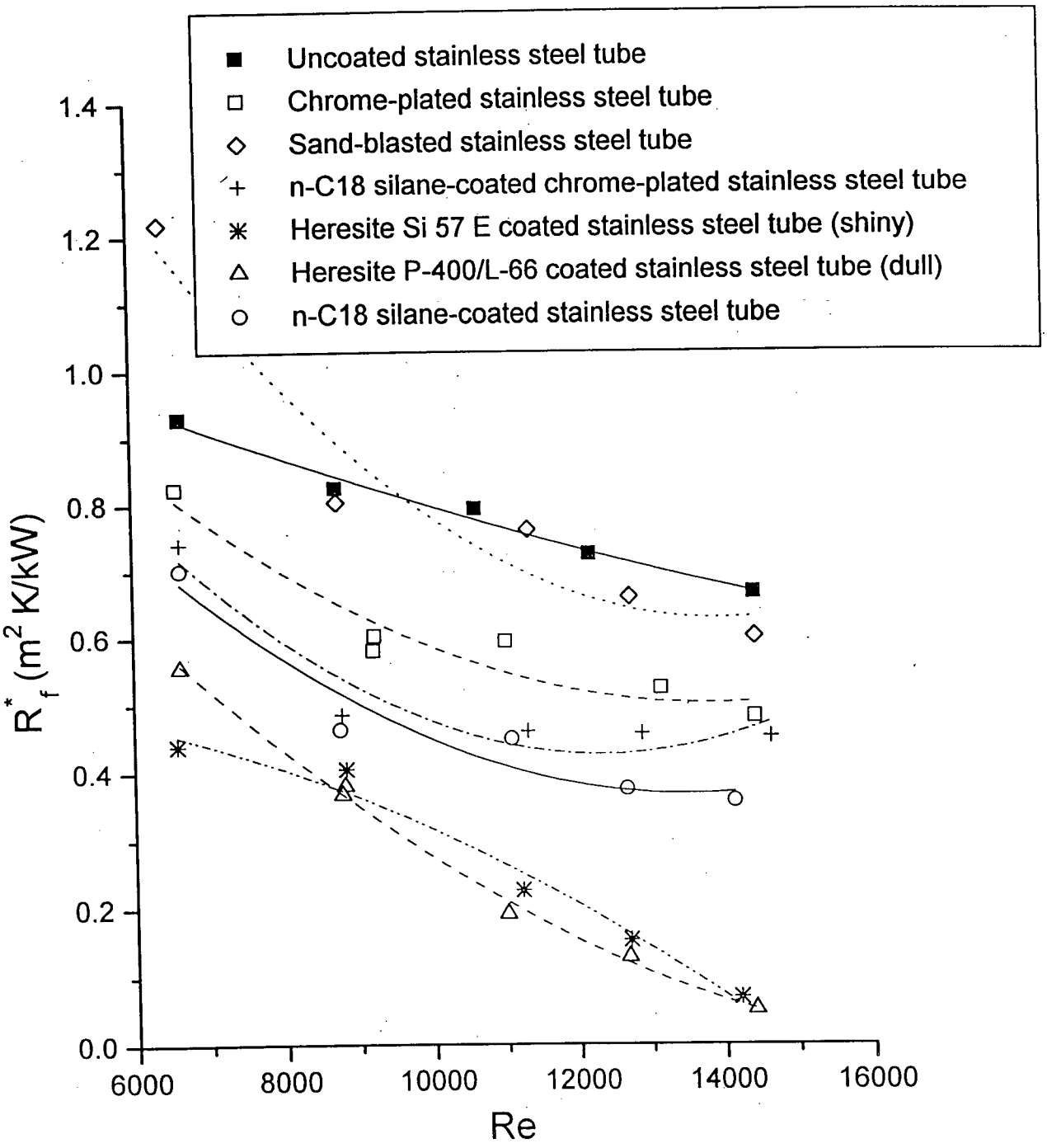

Fig. 15a. Result of R_f^* vs. Re for MCT-10 slack wax, 20% by wt at T_b=31.3±0.2 °C for different surfaces.

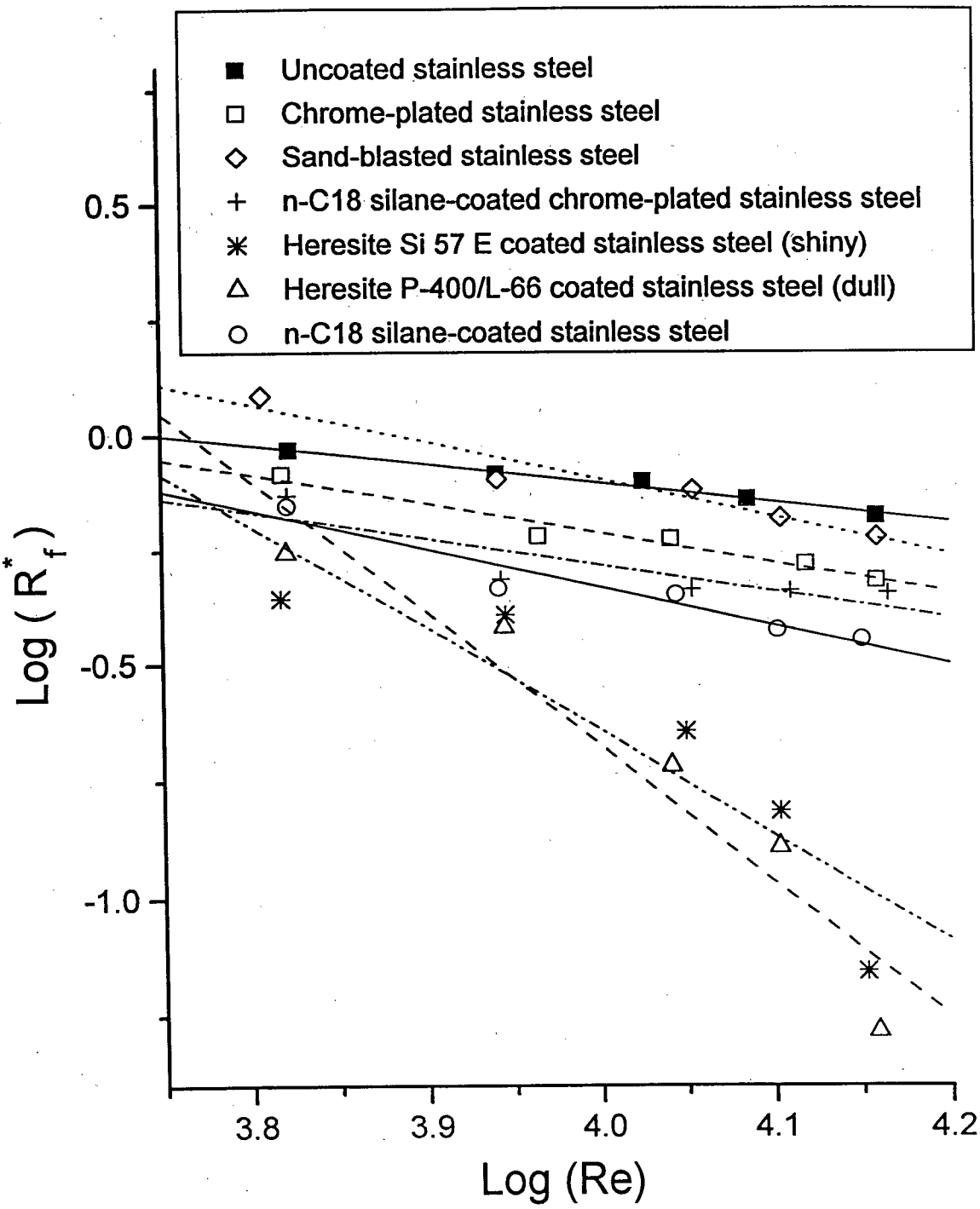

Fig. 15b. Result of Log (R_f^*) vs. Log (Re) for MCT-10 slack wax, 20% by wt at T_b=31.3±0.2 °C for different surfaces.

7.2.2 Effect of Bulk Temperature

The bulk temperature here refers to the average of inlet and outlet bulk temperature of the wax-kerosene flow as defined in Chapter 5. The inlet and outlet temperatures typically differed by 1 °C. The bulk temperature was varied from near the cloud point of the mixture to about 40 °C . The effect of the bulk temperature was determined for refined wax on the stainless steel tube, and for slack wax on a total of four tubes. Figure 16a-e shows the R_f versus time curves for the case of slack wax. The trends shown in this figure are representative for the other tubes as indicated in Tables 22-26. At bulk temperatures near the cloud point, wax deposition was heaviest, and decreased with increasing bulk temperature as expected. For example, in Fig. 16a, at T_b=28.7 °C, R_f^* =1.5 m^2 K/kW, whereas in Fig. 16d at T_b=38.1 °C, R_f^* =0.22 m^2 K/kW. Fig 17. and Fig.18 show the trends of R_f^* with T_b. The most significant drop in R_f^* occurs between the data near the cloud point and those at some 5 °C higher, where R_f^* has decreased by almost an order of magnitude. While R_f^* decreased sharply with increasing bulk temperature for all cases, the time constant did not show any consistent trend. Near the cloud point, θ_c values tended to be high, and usually decreased with increasing temperature. In Table 23, for slack wax fouling on the stainless steel tube, a consistent drop in θ_c with increasing temperature is observed, whereas in other cases (Table 22 and Table 26) there appears to be an increase in θ_c at the highest temperatures. The initial fouling rate, R_f^*/θ_c, for refined wax at 10 % on stainless steel showed a decrease with bulk temperature (Table 22).

The principal explanation for a decrease in R_f^* with increasing T_b is that the higher the value of T_b, the smaller the zone of the hydrocarbon flow which is between the cloud point and the heat transfer surface, and hence the smaller the degree of wax crystallization.

This effect is enhanced by the steeper temperature gradient near the surface where the temperature is higher.

Table 22. Results for refined wax at 10% by wt. using stainless steel and wax-kerosene Re=12155±1909. Cloud Point=21.1 °C , t_b=10.0±0.3 °C, u=1.6 m/s, V_w=2.5 m/s.

T_b(°C)	R_f^* (m² K/kW)	θ_c (min.)	Uncertainty (%)	R_f^*/θ_c (m² K/kW·min)
28.7	3.6474	12.0	21.0	0.3040
32.4	0.8896	5.5	30.0	0.1617
36.4	0.4632	6.6	27.3	0.0702
40.0	0.3435	4.4	18.6	0.0781
44.2	0.3070	111	14.2	0.0277

Table 23. Results for slack wax MCT-10 at 20% by wt. using stainless steel and Re=9430±1166, Cloud Point=27.8 °C , t_b=7.9±0.5°C, u= 1.6 m/s, V_w=1.1 m/s.

T_b(°C)	R_f^* (m² K/kW)	θ_c (min.)	Uncertainty (%)	R_f^*/θ_c (m² K/kW·min)
28.9	1.5241	16.2	11.0	0.0943
31.2	0.8244	10.8	11.1	0.0765
34.0	0.3788	5.2	13.1	0.0727
38.1	0.2205	2.7	16.7	0.0832
40.6	0.3916	2.3	7.9	0.1733
40.8	0.2359	1.0	14.1	0.2359

Table 24. Results for slack wax MCT-10 at 20% by wt. using chrome-plated stainless steel and Re= 9629±626. Cloud Point=27.8°C , t_b=9.6±1.5 °C, u=1.6 m/s, V_w=1.1 m/s

T_b(°C)	R_f^* (m² K/kW)	θ_c (min.)	Uncertainty (%)	R_f^*/θ_c (m² K/kW·min)
31.2	0.6031	2.1	15.6	0.2900
35.9	0.2409	3.4	23.3	0.0713
37.3	0.2056	1.3	42.5	0.1619
40.9	0.1187	2.3	21.8	0.0514

Table 25. Results for slack wax MCT-10 at 20% by wt. using sand-blasted stainless steel and Re= 9357±877.Cloud Point= 27.8°C , t_b=11.7±0.8°C, u=1.6 m/s, V_w=1.1 m/s

T_b(°C)	R_f^* (m² K/kW)	θ_c (min.)	Uncertainty (%)	R_f^*/θ_c (m² K/kW·min)
31.3	0.8027	9.3	11.7	0.0863
33.6	0.4572	1.1	20.2	0.4011
37.1	0.3645	12.8	11.6	0.0285
40.2	0.2664	7.8	11.2	0.0342

Table 26. Results for slack wax MCT-10 at 20% by wt. using n-C18 silane-coated chrome-plated stainless steel and Re=9391±940. Cloud Point=27.8°C , t_b=12.8±0.5 °C, u=1.6 m/s, V_w=1.1 m/s

T_b(°C)	R_f^* (m² K/kW)	θ_c (min.)	Uncertainty (%)	R_f^*/θ_c (m² K/kW·min)
31.5	0.4854	20.9	19.4	0.0232
33.5	0.3180	4.5	16.6	0.0707
36.9	0.2098	5.7	20.6	0.0368
41.0	0.0640	12.5	60.6	0.0051

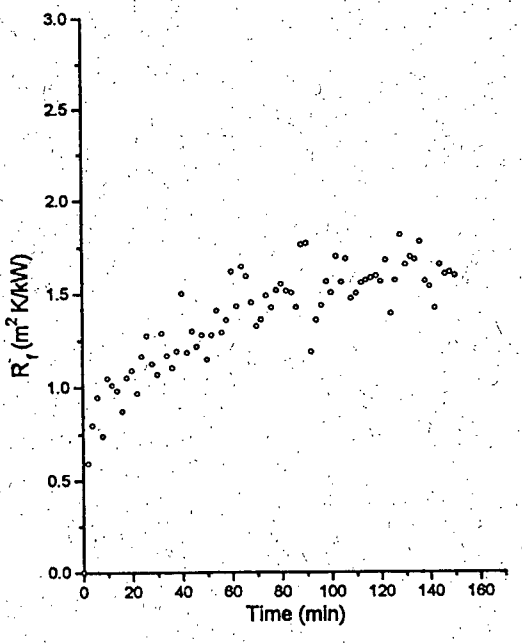

Fig. 16a. of R_f vs. time for slack wax MCT-10 at 20 % by wt.using stainless steel. Re=8391, T_b= 28.9 °C, Cloud Point=27.8°C.

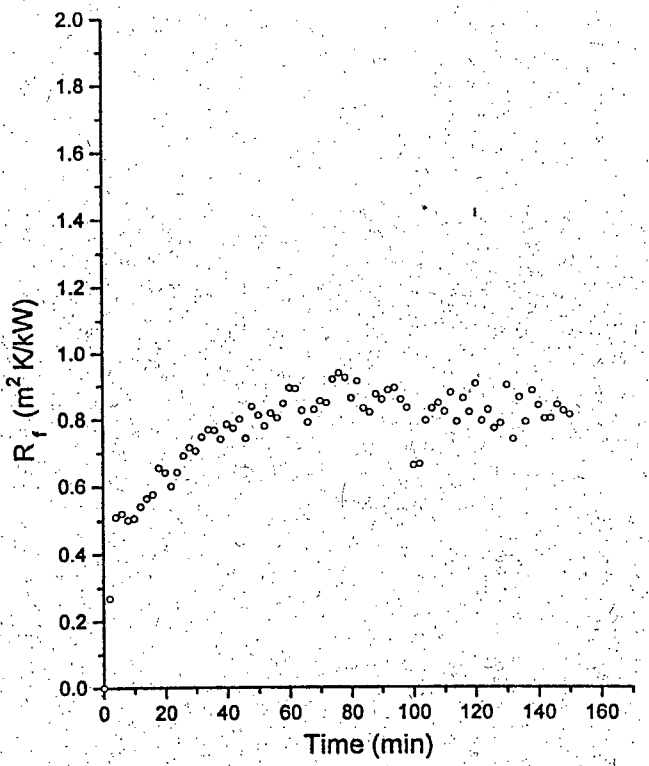

Fig. 16b. R_f vs. time for slack wax MCT-10 at 20 % by wt.using stainless steel. Re=8722, T_b= 31.2 °C, Cloud Point=27.8°C.

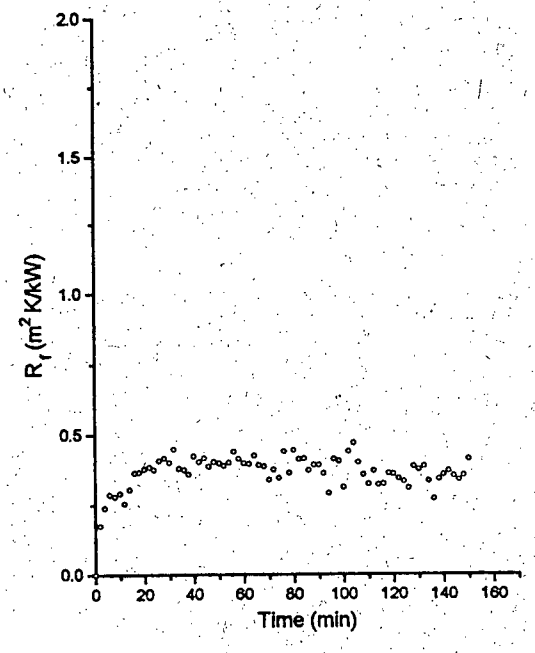

Fig. 16c. R_f vs. time for slack wax MCT-10 at 20 % by wt.using stainless steel. Re=9372, T_b= 34.0 °C, Cloud Point=27.8°C.

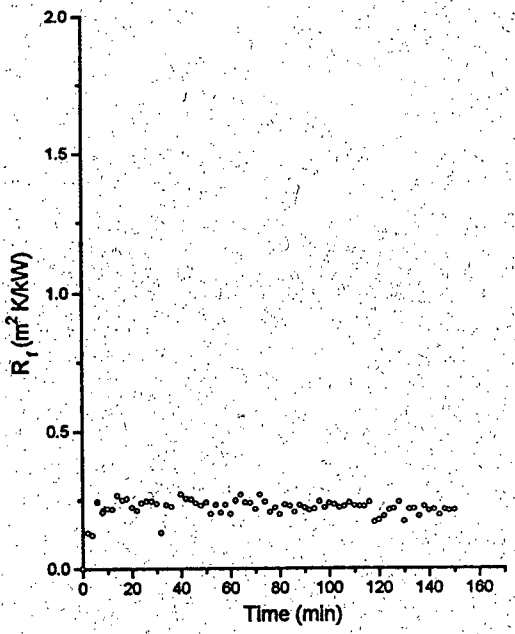

Fig. 16d. R_f vs. time for slack wax MCT-10 at 20 % by wt.using stainless steel. Re=9841, T_b= 38.1 °C, Cloud Point=27.8°C.

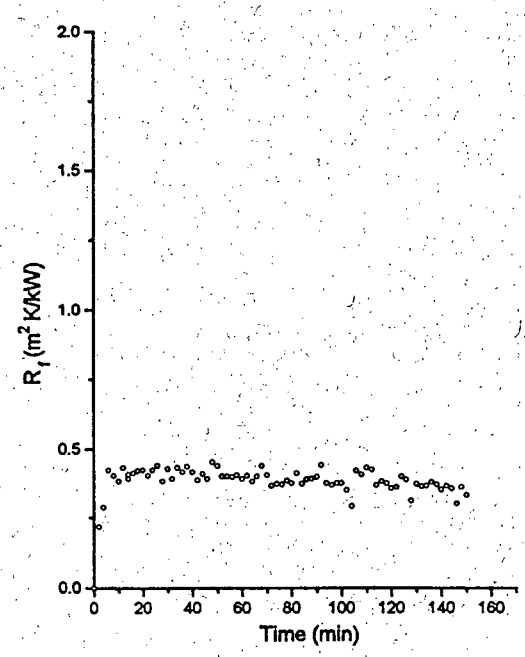

Fig. 16e. R_f vs. time for slack wax MCT-10 at 20 % by wt.using stainless steel. Re=10115, T_b=40.6 °C, Cloud Point=27.8°C.

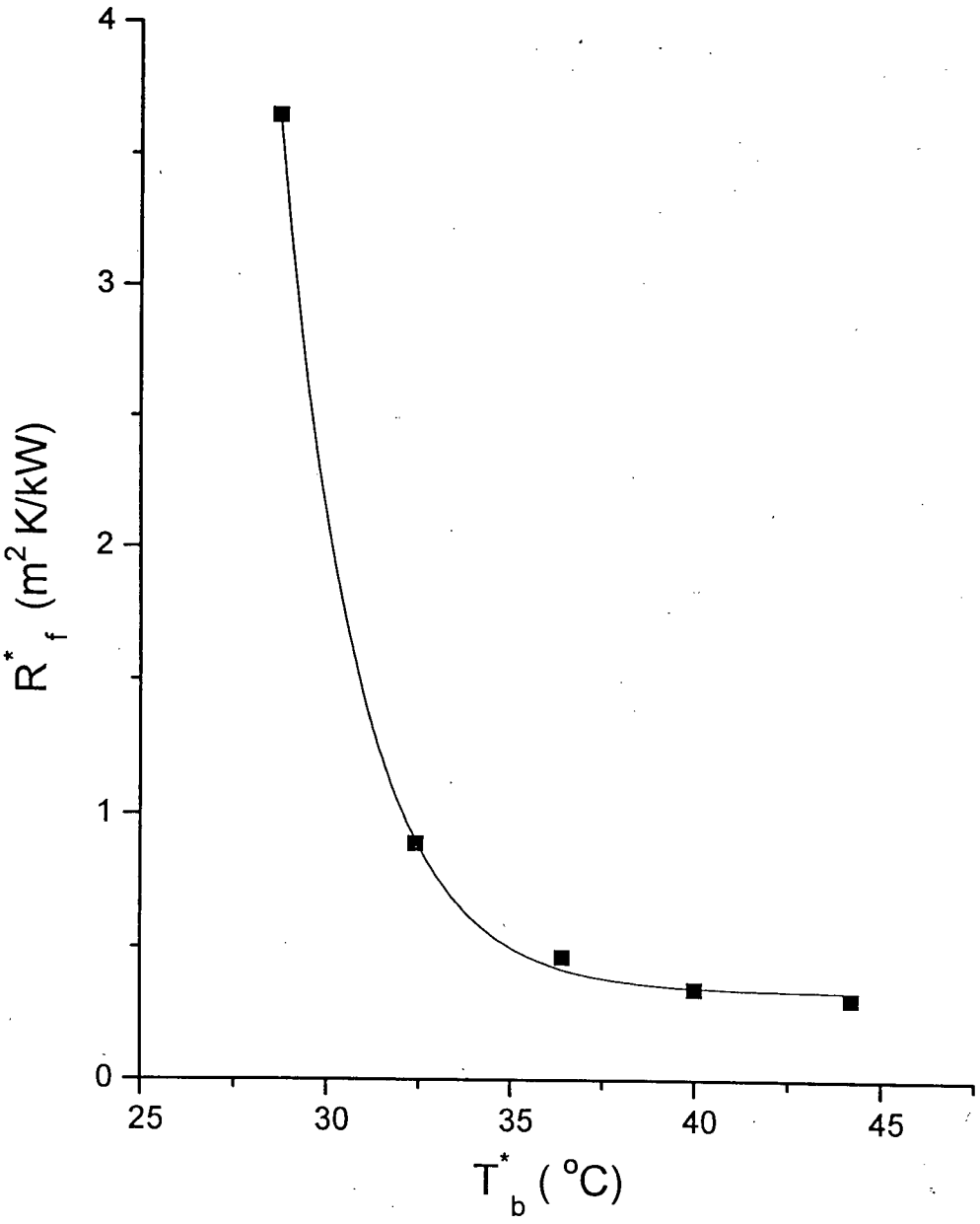

Fig. 17. Results for refined wax at 10% by wt. on stainless steel tube at Re=12155.

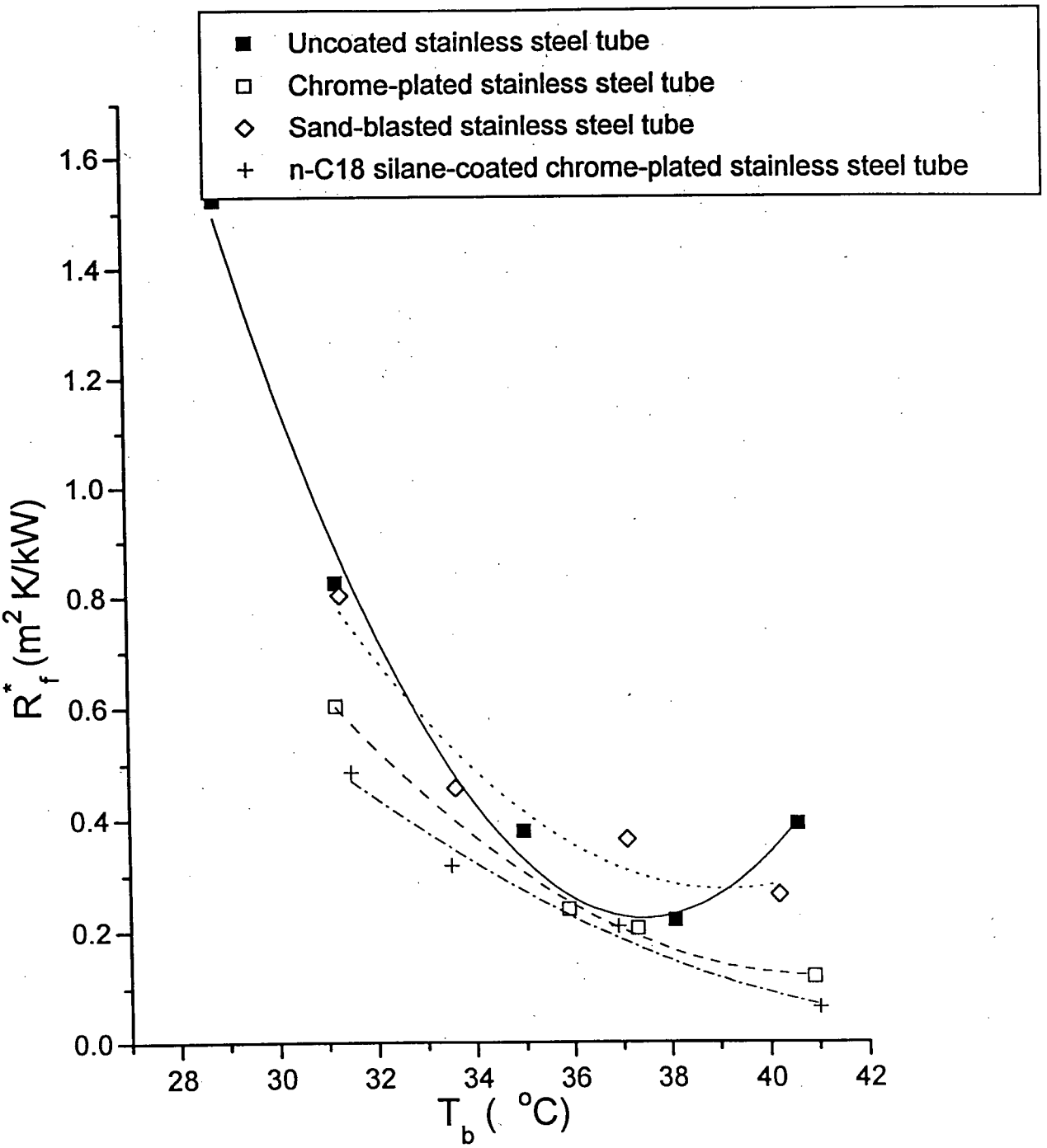

Fig. 18. Results for MCT-10 slack wax at 20% by wt. and Re =9363 ± 277 for different surfaces.

7.2.3 Effect of Surface Conditions

Figure 15a shows that the general ranking of tubes from the best to the worst in terms of increasing R_f^* is both Heresite coated stainless steel tubes < n-C18 silane coated stainless steel < n-C18 silane-coated chrome-plated stainless steel < chrome-plated stainless steel < uncoated stainless steel <sand-blasted stainless steel. It can also be seen that the two Heresite-coated tubes show a lower asymptotic fouling resistance compared to the others at all Reynolds numbers tested. These results agree with prior studies, in which it has been shown that plastic coatings give a lower wax deposit (Jessen and Howell, 1958), and it can be recalled that Jorda (1966) has attributed this phenomenon to the general smoothness of plastics. Jorda has argued that smooth plastics do not harbor wax crystals as easily as a rough tube. Evidence of poor adhesion of wax is described in the next section where sliding of wax was observed to occur on the chrome-plated stainless steel, n-C18 silane-coated chrome-plated stainless steel tube and the n-C18 silane-coated stainless steel tube, indicating that they are very smooth. Both silane-coated tubes have shown a lower fouling resistance compared to the uncoated stainless steel, the sand-blasted stainless steel and the chrome-plated stainless steel tubes.

Because the plastic coatings will increase the overall thermal resistance, it is useful to compare surfaces according to their total thermal resistance, i.e. original plus fouling resistance. Data are listed in Tables 15-21 and shown plotted versus Reynolds number in Figure 19. On this basis the Heresite coated tubes again proved superior, the Heresite Si 57 E (shiny) outclassing the Heresite P-400/L-66 (dull) slightly; and the silane coated tubes next best. The chrome plated tube was essentially no better than the standard and the sand-blasted stainless tube, although the chrome-plated stainless steel has a lower asymptotic fouling resistance compared to both the stainless steel and the sand-blasted stainless steel tubes (Fig. 15a). This phenomenon conforms to the traditional reasoning

that the higher the thermal resistance, the lower the heat transfer, which brings about a lower wax deposit.

Considering only the roughness factor (in brackets), the chrome-plated stainless steel tube (0.5μm) has a lower R_f^* compared to the uncoated stainless steel (2.5μm), which again has a lower R_f^* at lower Re when compared to the sand-blasted stainless steel tube (5.0μm). It does not follow, however, that a lower wax deposit is necessarily obtained by using a smooth surface, as wax deposit is a function of several factors. The Heresites were said to have enamel-like finish surfaces according to manufacturer's brochure (Heresite Protective Coatings, Inc.), but no roughness figures were given.

Wax fouling is also a function of the material type inasmuch as some materials can form a weak hydrogen bond with the paraffin wax, which could enhance the wax deposit. It was shown in the literature survey that materials like tetra-fluoroethylene (Jorda, 1966) which have an ultra-smooth surface show an extreme adhesion to wax deposit, which is evidence that there might be some sort of bond between this type of surface and wax. A micro study of the type of adhesion which occurs between wax deposit and surface has yet to be done. However, in summary, wax deposition must be a function of thermal resistance of the surface material, its roughness and its intrinsic properties.

Four tests have been carried out to compare the different surfaces as a function of bulk temperature of the wax-kerosene (Fig. 18). The uncoated stainless steel and the sand-blasted stainless steel tubes show a higher wax deposit compared to the chrome-plated stainless steel and the n-C18 silane-coated chrome-plated stainless steel tubes. This is exactly the same hierarchy as shown by Fig. 15a for asymptotic fouling resistance vs. Re, and the same explanations can be applied.

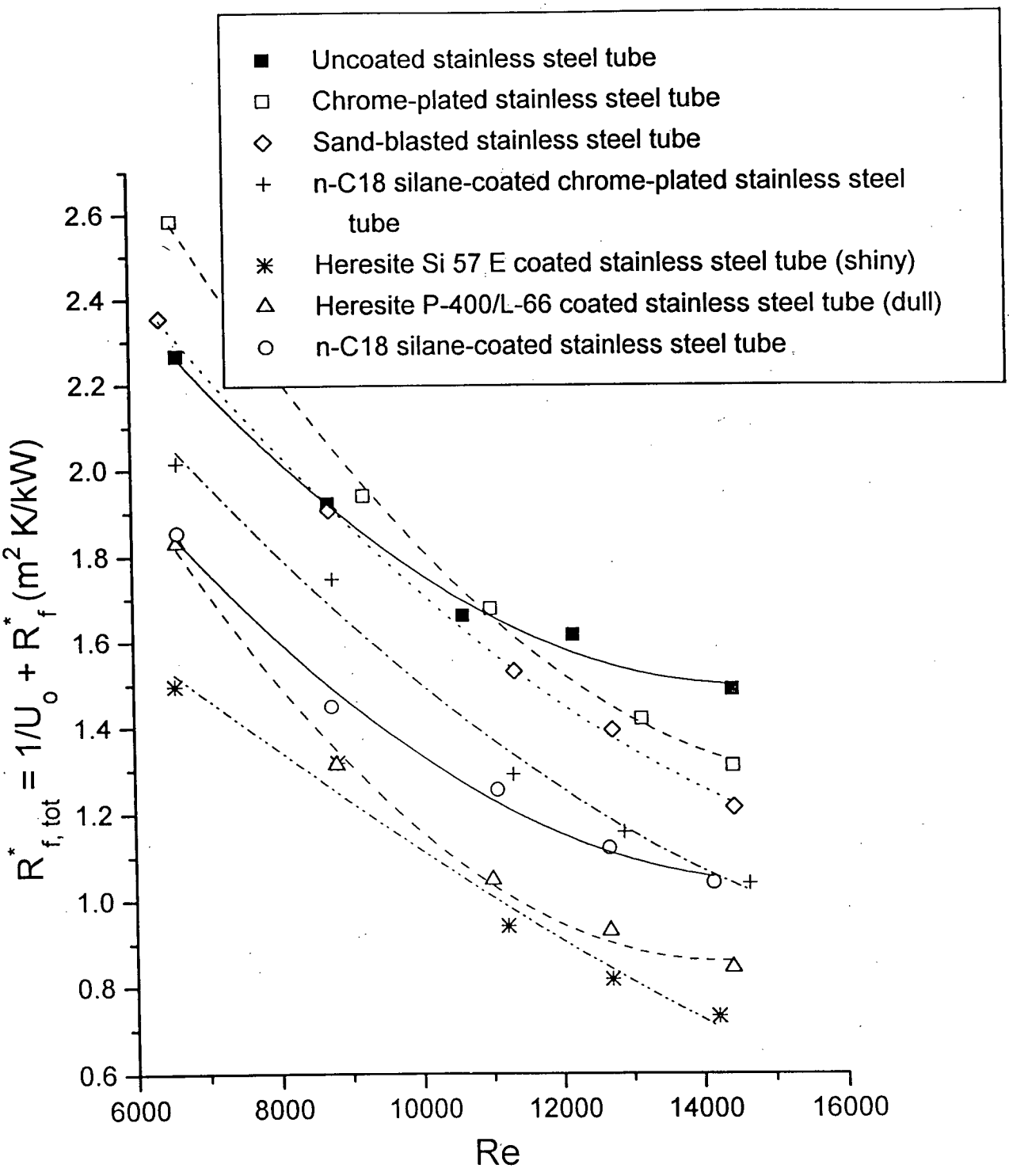

Fig. 19. Graph for slack wax MCT-10 at 20 % by wt. and t_b =31.3±0.2 °C for different surfaces.

7.2.4 Effect of wax concentration

The effects of wax concentration on the fouling resistance were also studied for both types of wax. Fig. 20a-d shows R_f vs. time data on the stainless steel tube for slack wax at concentrations from 5 to 20 % . A large increase in wax deposition with concentration is noted. At the highest wax concentration of 20 %, deposition was extremely heavy. Similar trends were apparent for the refined wax, although the amount of wax deposited was markedly higher. Tables 27 and 28 summarize the data. Figures 21 and 22 show strongly non-linear effects of concentration on R_f^*. At low concentrations there is little increase in R_f^* ; however above about 15 % concentration for refined wax, and above 10 % concentration for slack wax, R_f^* increases sharply. Doubling the concentration from 10 % to 20 % results in about a 13-14 fold increase in R_f^* for both refined and slack wax. Table 27 for refined wax shows no consistent trend of θ_c with concentration, but for slack wax MCT-10, it can be seen in Table 18 that there is an increase in θ_c with increasing wax concentration. Increased concentration of the wax-kerosene solution will increase the number of particles available for deposition on the surface as the driving force in Eq. (4) (the concentration difference) increases. From Fig. 23, a plot of R_f^* vs. $T_b - T_c$, as the concentration increases at a constant bulk temperature and flowrate of the wax-kerosene, $T_b - T_c$ decreases and therefore the cloud point temperature will move away from the tube surface, which leads to increased wax deposition.

An increase of initial fouling rate, R_f^*/θ_c, with concentration for refined wax has been observed (Table 27), which shows that the attachment rate for this wax is higher when the wax concentration driving force is higher. The slack wax MCT-10 (Table 28) showed smaller initial fouling rates compared to the refined wax at 10-20 wt. % concentrations, which indicates that slack wax displays lower adhesion to the stainless steel tube (Tables 27 and 28). In general, slack wax has shown smaller fouling resistances than the refined wax, even when its concentration has been higher.

Table 27. Results for refined wax using stainless steel at Re=10664±1902 and T_b=32.5± 0.1°C, t_b=9.3±0.5°C, u=1.6 m/s, V_w=2.5 m/s

Conc. (% by weight)	R_f^* (m² K/kW)	θ_c (min.)	Uncertainty (%)	R_f^*/θ_c (m² K/kW·min)	$T_b - T_c$ (°C)
5	0.5400	79.6	36.0	0.0068	17.0
10	1.2700	2.9	15.1	0.4379	11.4
15	2.8000	5.5	25.3	0.5091	6.9
20	17.1200	15.3	33.0	1.1190	3.5

Table 28. Results for slack wax MCT-10 using stainless steel at Re= 10003±1760 and T_b =29.2 ±0.1 °C, t_b=13.9±0.9 °C, u=1.6 m/s, V_w=1.1 m/s

Conc. (%) by weight	R_f^* (m² K/kW)	θ_c (min.)	Uncertainty (%)	R_f^*/θ_c (m² K/kW·min)	$T_b - T_c$ (°C)
5	0.0774	2.0	43.6	0.0387	14.0
10	0.0799	14.6	57.5	0.0055	8.0
15	0.4899	13.6	13.1	0.0360	5.9
20	1.1080	26.9	15.5	0.0412	1.5

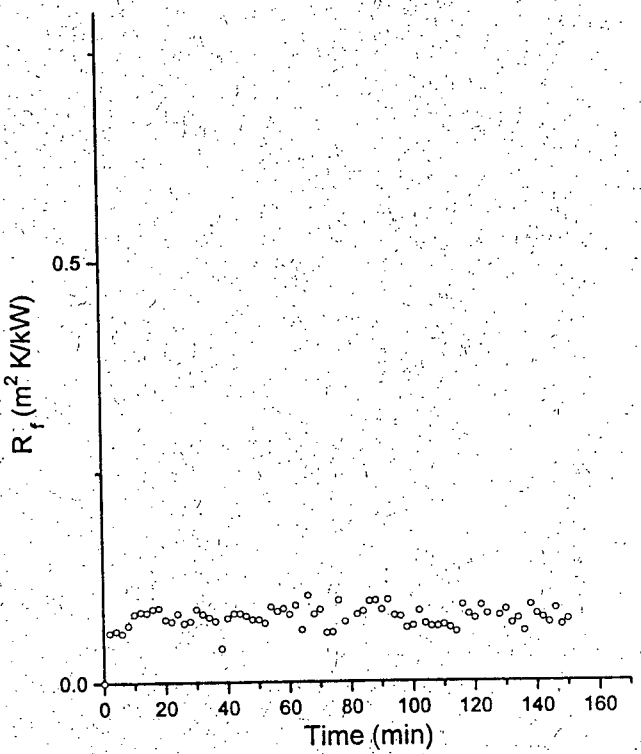

Fig. 20a. R_f vs. time for slack wax MCT-10 at 5 % by wt.using stainless steel. Re=11185, T_b=29.2 °C, Cloud Point=15.0°C.

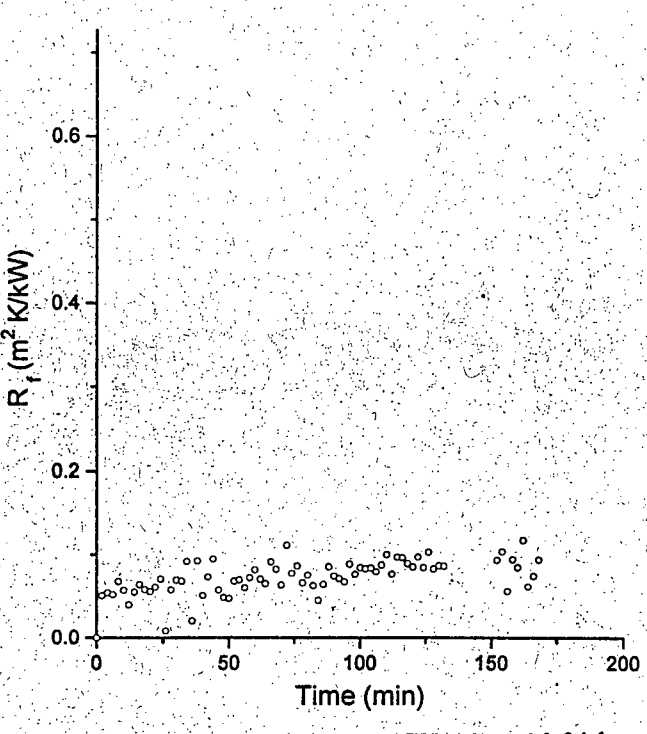

Fig. 20b. R_f vs. time for slack wax MCT-10 at 10 % by wt.using stainless steel. Re=10714, T_b=29.2 °C, Cloud Point=21.1°C.

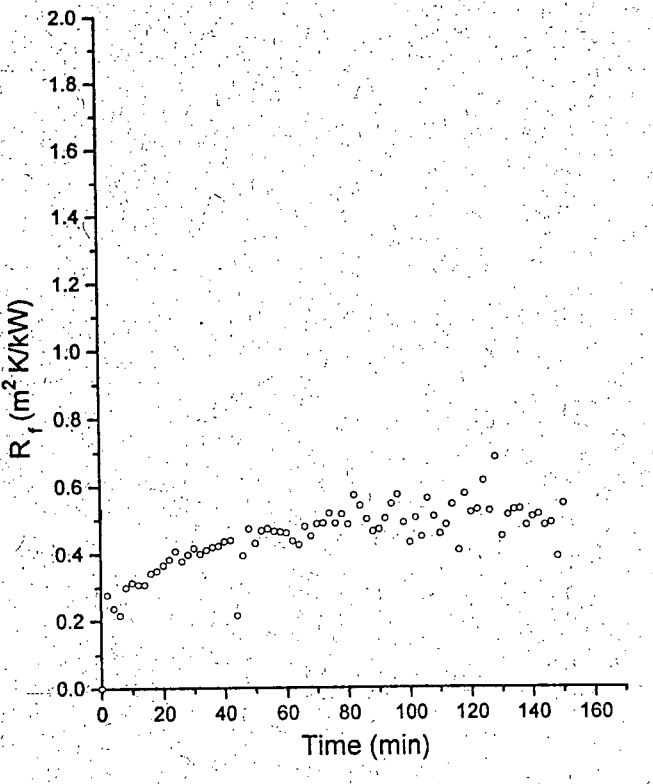

Fig. 20c. R_f vs. time for slack wax MCT-10 at 15 % by wt.using stainless steel. Re=9569, T_b=29.2 °C, Cloud Point=23.3°C.

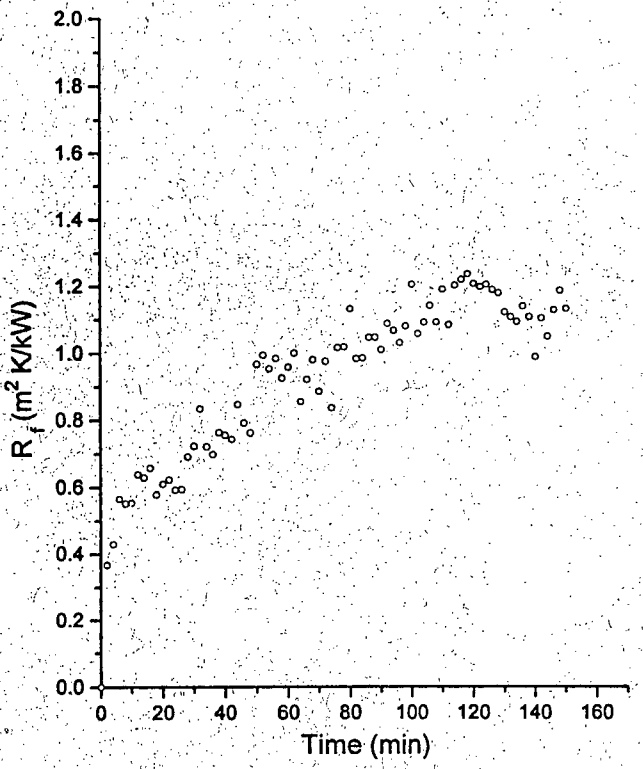

Fig. 20d. R_f vs. time for slack wax MCT-10 at 20 % by wt.using stainless steel. Re=8545, T_b=29.2 °C, Cloud Point=27.8°C.

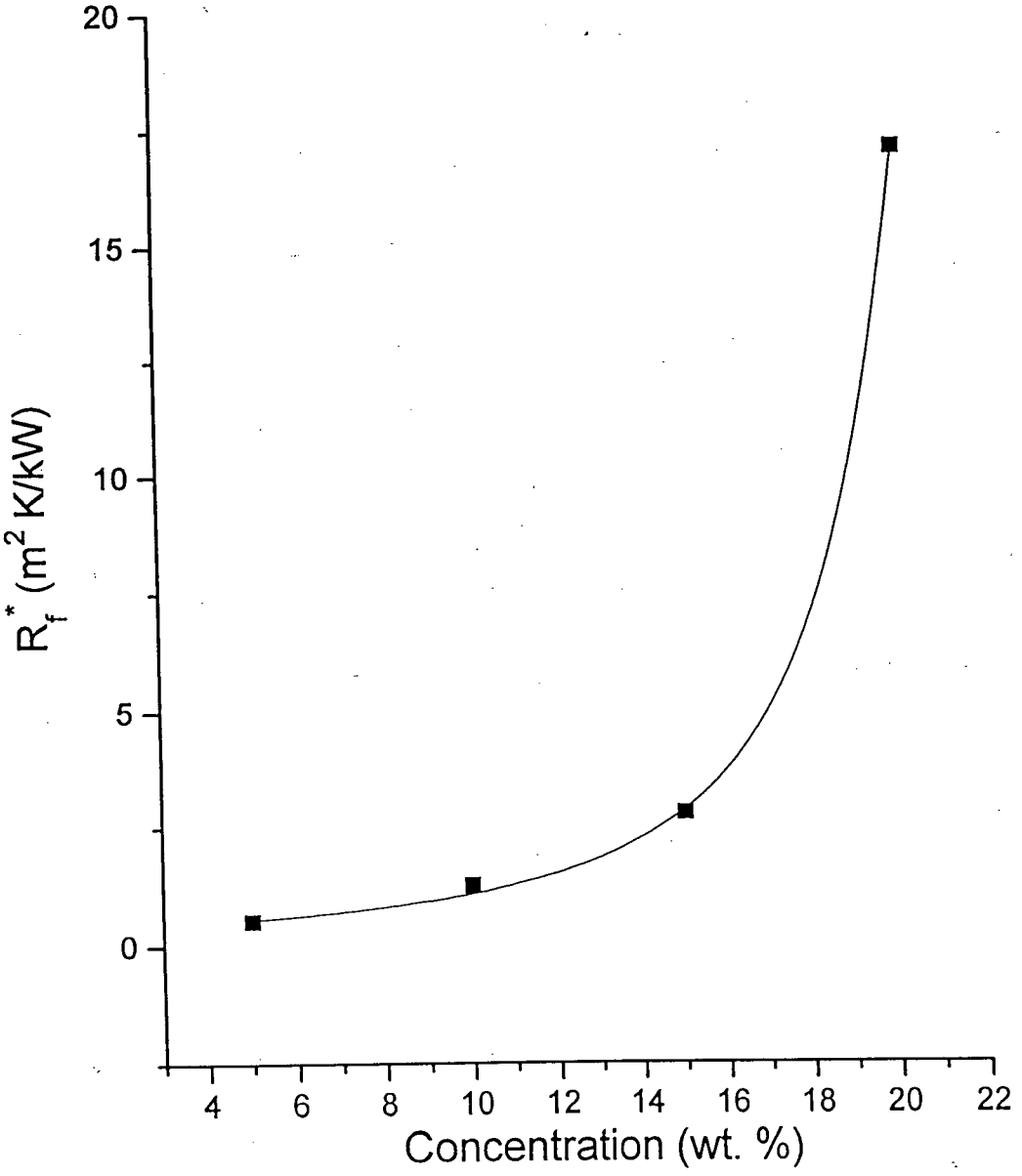

Fig. 21. Results for refined wax on uncoated stainless steel tube. Re=10664 and T_b =32.5°C.

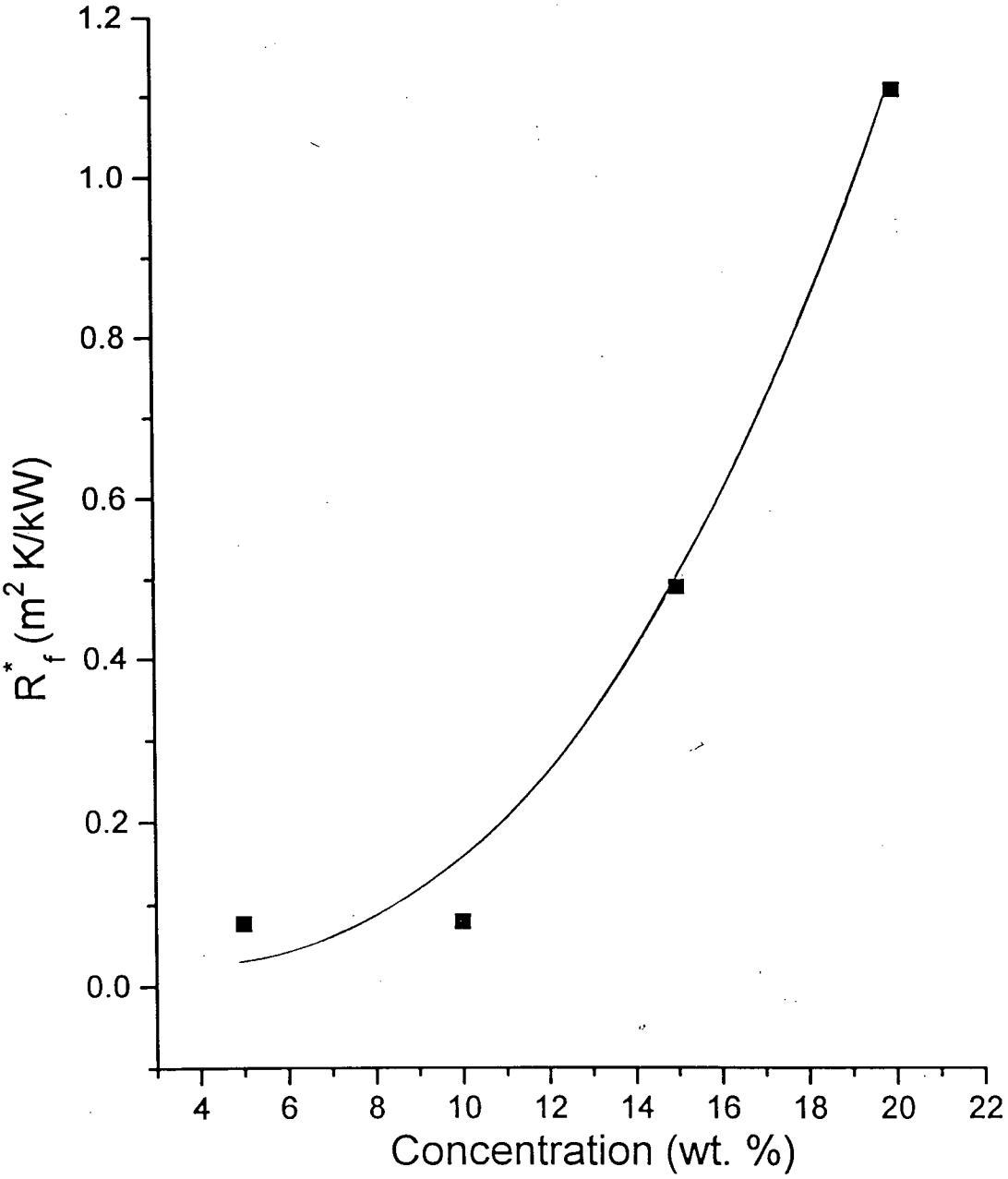

Fig. 22. Results for slack wax MCT-10 on uncoated stainless steel tube. Re= 10003 and T_b=29.2°C.

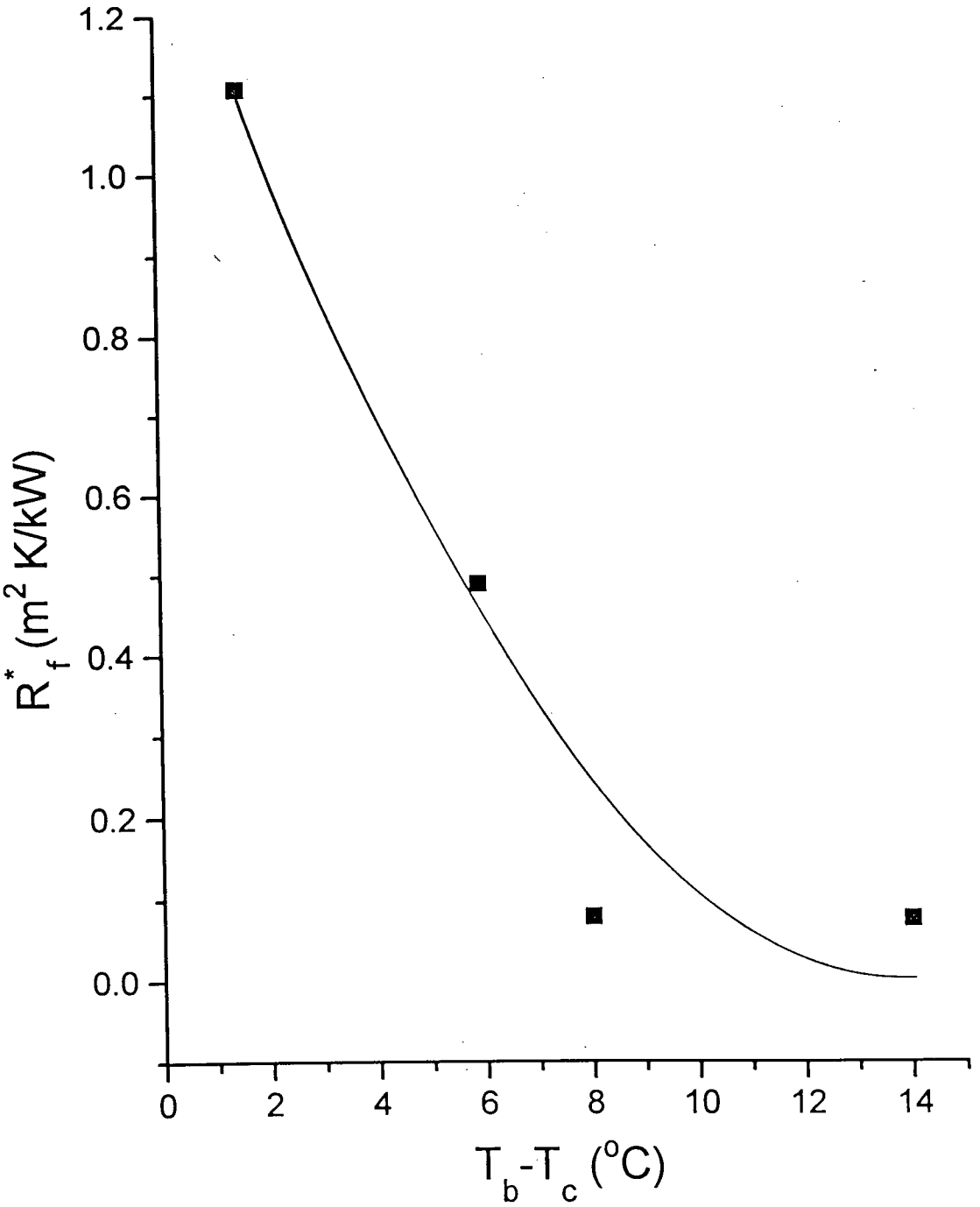

Fig 23. Graph of R_f^* vs. $T_b - T_c$ for slack wax MCT-10 on uncoated stainless steel tube. Re= 10003 and T_b=29.2°C.

7.2.5. Removal and Sliding of Fouling Deposit

The glass section on the double pipe heat exchanger shown in Fig. 5 permits the fouling process to be critically observed. Removal was not observed at the micro level, but relatively large chunks (max. 5 mm size) of both wax types were seen to be removed by the flowing fluid, resulting in small patches of free exposed surface. This phenomenon appeared to happen randomly approximately after 60 minutes from startup until the end of an experiment for some of the tubes. The patches were randomly located. These observations are supported by Bott and Gudmundsson (1977b), who found that wax deposition reaches an asymptotic value that fluctuates randomly around a mean constant value. Table 29 summarizes observations on deposit motion for the various tubes tested.

Sliding of wax chunks was also observed along the chrome-plated stainless steel, the n-C18 silane-coated chrome-plated stainless steel, and the n-C18 silane-coated stainless steel tubes. Values of sliding velocity measured for the chrome-plated stainless steel tube are shown below in Table 30. The sliding velocity (which refers to velocity of wax chunks along the tube) was measured manually through the glass section on the heat exchanger by using a ruler and timing a particular wax chunk movement from one marked point to the next. For the other two tubes, the sliding velocity was difficult to measure as the chunks were removed after a short distance of movement. The phenomena of sliding and wax chunk removal were also reported by other authors (Hunt, 1962; Jorda, 1966). It would be expected that the sliding velocity would increase with increasing liquid velocity, as the shear stress on the layer is increasing. The results, however, do not show a clearcut trend. An improved technique for measurement of sliding velocity might reveal a more consistent trend.

Table 29. Summary of removal and sliding of fouling deposit.

Type of tube	Wax removal/bare patches observed	Sliding
Uncoated stainless steel	Yes	No
Chrome-plated stainless steel	Very Small Patches	Yes
Sand-blasted stainless steel	No	No
n-C18 silane-coated chrome-plated stainless steel	Yes	Yes (but removed immediately)
Heresite Si 57 E coated stainless steel (shiny)	No	No
Heresite P-400/L-66 coated stainless steel (dull)	No	No
n-C18 silane-coated stainless steel	Yes	Yes (but removed immediately)

Table 30. Sliding velocity for chrome-plated stainless steel tube using slack wax MCT-10 at 20% by wt. T_b = 31.3±0.1°C ,Cloud Point=27.8 °C , t_b=7.6±0.4°C, V_w=1.1 m/s

Re	u(m/s)	Sliding velocity (m/s)
6586	1.17	0.68
9224	1.64	0.74
9208	1.64	0.70
11015	1.96	0.64
13156	2.35	1.00
14428	2.57	0.75

7.2.6. Uncertainty

Fouling resistance was determined from Eq. (20) as the small difference between two reciprocal values of the heat transfer coefficients, which are nearly equal large terms. Therefore precision is required in the experimental measurements to get satisfactory R_f results with little scatter. The major objective of uncertainty analysis is to identify those variables that have the greatest effect on the precision of the calculated result. Because of the scatter observed in early experiments the flowrate of water was adjusted to a lower value so that its temperature increase could be larger. Also, the

temperature measurement instruments were changed to higher precision thermocouples, and the water side thermocouples were arranged in such a way that the temperature rise was recorded directly.

It can be inferred that uncertainty is mainly affected by the cooling water side temperature rise, the thermocouple resolution, the magnitude of the fouling resistance, the initial overall heat transfer coefficient, and the cooling water mass flowrate fluctuation. A higher cooling water temperature rise, more precise thermocouple resolution, higher fouling resistance, higher overall heat transfer coefficient and lower fluctuation of cooling water mass flowrate from the set value will generally reduce the uncertainty.

There is no particularly set acceptable uncertainty level, but determination of uncertainty is useful to indicate how one can redesign the equipment or change the operational parameters in such a way as to improve precision. Crittenden et al. (1992) state that for the majority of their measurements the maximum error in R_f was in the order of 20%. However, this value is for a shell and tube industrial heat exchanger and higher values would be expected for the present laboratory equipment because of the smaller temperature changes. The average uncertainties as indicated in Tables14-29 which were calculated using Eq. (41) are acceptable, although there are sometimes high uncertainties at lower values of asymptotic fouling resistance. The high uncertainty occurs due to lower R_f^* , but nevertheless a consistent trend of R_f^* with Re and bulk temperature of wax-kerosene has been shown. As the water side flowrate is fixed, and the thermocouple resolution is also constant, it appears that the only variable in determining Q_w that could be improved is the cooling water side mass flowrate fluctuation. This fluctuation occurs as other users draw water from the same building water main, or turn the water flow off and on. This action changes the pressure and water flowrate in the cooling water line.

7.2.6. Prior work at UBC

Prior work was done by Guohong Zhang (1992) with refined wax in kerosene on the same equipment as shown in Fig. 5. These were preliminary test results, and the present work has been done with improved temperature measurements. Using a 10% refined wax in kerosene at about 30 °C bulk temperature, it was shown that R_f^* remains constant while the time constant decreases with increasing Re, which implies that at higher surface temperatures weaker deposits are formed. The effects of bulk temperature from 25 to 48°C for 10% refined wax was also determined. His results show that R_f^* decreases with increasing bulk temperature and that the time constant does not show any trend for this series. The effect of concentrations of 5, 10, 15, and 20 % by wt of refined wax was also determined. The results show that both R_f^* and the time constant first increase and then decrease with increasing wax concentration. Although this prior work had been done without improving the temperature measuring system, it provided a useful guide to the expected results. The range of values of these experiments agree with the present results, but the trends shown for R_f^* vs. Re and concentration are not the same. The trends of R_f^* vs. T_b, θ_c vs. Re and θ_c vs. concentration agree with the present results. θ_c vs. T_b does not show any consistent trend for both sets of experiments.

Chapter 8

8. Conclusions

One of the ultimate objectives of fouling research is to minimize deposition in industrial equipment. This research was undertaken to understand the role of process variables and tube wall materials on refinery chillers where the process of separation of wax from the rest of petroleum occurs by cooling. Two waxes were used–refined wax and slack wax MCT-10. Seven tubes with differing surfaces were tested. The following conclusions were drawn:

1. The wax-kerosene mixtures for both refined and slack wax MCT-10 were found to be Newtonian at the invetigated concentrations of 5 %, 10 %, 15 %, and 20 %. The cloud point measured for both waxes was found to be a function of concentration. The bulk temperature of the inlet wax-kerosene mixture was maintained above the cloud point.

2. The wax fouling showed a fouling resistance which increased with time to reach a fluctuating asymptotic value. In many cases, wax chunk removal leaving a bare patch was observed after approximately an hour. Also, sliding of wax along the tube was observed on the chrome-plated stainless steel, the n-C18 silane coated chrome-plated stainless steel and the n-C18 silane coated stainless steel tubes, although the sliding velocity was difficult to measure in the latter two tubes. These observations lead to the conclusion that there is less attachment between the wax and the surface of the tube for these cases, indicating that the surface is smooth enough not to harbor wax crystals from the flowing fluid. Smooth surfaces coupled with a low adhesion to wax could be good candidates for equipment to avoid wax fouling.

3. Graphs of asymptotic fouling resistance versus Reynolds number for all tubes and both waxes showed a decrease in R_f^* as flow velocity increased. The decrease was non-linear and was fitted by using a polynomial of degree two. The plot of R_f^* vs. Re for refined wax decreased sharply, and then almost assumed a constant value, showing that increased flow velocity does not decrease fouling by a large factor once past a critical velocity. For slack wax, the sand-blasted stainless steel, the chrome-plated stainless steel, the n-C18 silane coated chrome-plated stainless steel and the n-C18 silane coated stainless steel tubes showed a sharp decrease and then also leveled off towards a constant value at high Re. The uncoated stainless steel and the two Heresite coated tubes showed a strong decrease with Re without any tendency to level off. These results appear logical, since the probability of getting planes of weakness among the deposited particles increases as deposit thickness increases, and the increase of flow velocity increases the shear stress on the deposit.

4. For both waxes, the asymptotic fouling resistance decreased non-linearly with increasing bulk temperature of the wax-kerosene mixture. The data points were fitted with a polynomial equation of degree 2. There was a sharp decrease in R_f^* with increasing temperature near the cloud point and then it slowly leveled off with increasing temperature for refined wax. For slack wax, a stronger decrease was observed at all bulk temperatures for the following four tubes: stainless steel, chrome-plated stainless steel, sand-blasted stainless steel and n-C18 silane-coated chrome-plated stainless steel.

5. In the range of Reynolds number employed (6418-14642), the asymptotic fouling resistance decreased among tubes tested in the following order: sand-blasted stainless steel, uncoated stainless steel, chrome-plated stainless steel, n-C18 silane-coated chrome-plated stainless steel, n-C18 silane coated stainless steel tube, and the two Heresite-coated tubes. The decreasing order in terms of the asymptotic fouling resistance vs. the bulk

temperature was sand-blasted stainless steel, uncoated stainless steel, chrome-plated stainless steel, and n-C18 silane-coated chrome-plated stainless steel, which thus shows the same hierarchy as R_f^* against Re.

6. Roughness (bracketed values) seems to play an important role in wax fouling. It was shown that the chrome-plated tube (0.5 μm) had a lower R_f^* compared to the uncoated stainless steel (2.5 μm), which had again a lower value of R_f^* compared to the sand-blasted stainless steel tube (5.0 μm) for a part of the Re range employed. It was reported in the Heresite Protective Company brochure that the two Heresite-coated tubes have enamel-like smooth surfaces, and both were found to have the lowest wax deposit. This indicates that a lower roughness decreases wax deposit.

7. For both waxes the asymptotic fouling resistance increased with concentration of wax in the wax-kerosene mixture on stainless steel. There was a small increase at low concentration and then a sharp increase at the higher concentrations. The slack wax shows less wax deposit as compared to refined wax at all concentrations.

8. Trends of the time constant, θ_c, in the Kern-Seaton equation with process variables were often poorly defined. According to Kern and Seaton (1959), the time constant is inversely proportional to the shear stress and, according to Taborek et al. (1972), it is proportional to the deposit strength. In most cases, the time constant showed little trend with Re, bulk temperature or concentration. But it was noted that the time constant decreased with increasing Re for the refined wax, indicating that the wax shows less firm attachment with increasing Re. The slack wax MCT-10 tested on stainless steel also showed a decrease of time constant with increasing bulk temperature of the wax-kerosene mixture. In addition, the time constant showed an increase with concentration for the slack

wax MCT-10 using stainless steel, but showed a high value with refined wax using stainless steel both at the lowest and the highest concentrations.

9. The thinnest MCT-10 slack wax deposits were observed on the two Heresite-coated stainless steel tubes, the performance of which were comparable. In practical situations, it may be difficult to affect the temperature or concentration of a solution, but the flowrate can easily be affected by installing a pump or an agitator. A lower wax deposit can therefore be obtained by operating a heat exchanger at increased flow velocity or turbulence, and using a smooth surface which has a low affinity for wax.

Nomenclature

A_i = inner surface area of inner tube, m^2

A_o = outer surface area of inner tube, m^2

A_{or} = cross-sectional area of orifice, m^2

B = constant in Eq. (5)

C = constant in Eq. (11)

C_b = bulk concentration, kg/m^3

C_d = discharge coefficient of orifice

C_{pk} = specific heat capacity of wax-kerosene, kJ/kg K

C_{pw} = specific heat capacity of water, kJ/kg K

C_s = interface concentration, kg/m^3

d_h = hydraulic diameter of the annulus where wax-kerosene flows, m

D = shear rate, 1/s

g = gravitational acceleration, m/s^2

h = the level difference between the high and low side of manometer, m

h_i = inner heat transfer coefficient, kW/m^2 K

h_o = outer heat transfer coefficient, kW/m^2 K

k_f = thermal conductivity of wax deposit, kW/m K

k_t = turbulent mass transfer coefficient, m/s

m = mass of deposit per unit area, kg/m^2

m^* = mass of asymptotic wax deposit per unit area, kg/m^2

$\dot{m}$ = mass flow rate, kg/s

$\dot{m}_d$ = deposition flux, $kg/s.m^2$

$\dot{m}_r$ = removal flux, $kg/s.m^2$

Q_w = heat gained by cooling water, kW

R_b = deposit bond resistance

R_f = fouling resistance at a given time, m^2 K/kW

R_f^* = asymptotic fouling resistance, m^2 K/kW

R_{fi} = calculated experimental fouling resistance at the time θ_i, m^2 K/kW

R_w = thermal resistance of the wall, m^2 K/kW

Re = wax-kerosene Reynolds No.$=\frac{\rho_k d_h u}{\mu_k}$

t_1 = inlet cooling water temperature, °C

t_2 = outlet cooling water temperature, °C

t_b = average bulk temperature of water, °C

T_1 = inlet temperature of wax-kerosene, °C

T_2 = outlet temperature of wax-kerosene, °C

T_b = average bulk temperature of wax-kerosene, °C

T_c = cloud point temperature of wax-kerosene mixture, °C

T_s = initial surface temperature of tube, °C

Δt = temperature rise of cooling water, °C

Δt_{lm} = log mean temperature difference, °C

u = velocity of wax-kerosene mixture, m/s

u^* = friction velocity, m/s

U_o = initial overall heat transfer coefficient based on A_i, kW/m^2 K

U = instantaneous overall heat transfer coefficient based on A_i, kW/m^2 K

V = volumetric flowrate of wax-kerosene mixture, m^3/s

V_w = velocity of water, m/s

V_w = volumetric flowrate of water, m^3/s

x = thickness of wax deposit, m

β = orifice diameter / pipe diameter = 2/24.84=0.4831

θ = time, min

θ_c = time constant, min

θ_i = time from experimental data, min

μ_k = viscosity of wax-kerosene, Pa.s

μ_w = viscosity of water, Pa.s

ρ_f = density of wax deposit, kg/m^3

ρ_{Hg} = density of mercury, kg/m^3

ρ_k = density of wax-kerosene, kg/m^3

ρ_w = density of water, kg/m^3

τ_s = shear stress, N/m^2

ψ = deposit strength

References:

Armenski, E.A. et. al, Izv Vyssh Ucheb Zaved, Neft Gas, **14**, 71, (1971).

Bland, W. F. and Davidson, R. L. , "Petroleum Processing Hanbook", McGraw-Hill, Inc., pp. 11-51- 11-54, (1967).

Bott, T.R.. and Gudmundsson, J.S., "Deposition of Fouling Wax from Flowing Systems", Institute of Petroleum, **IP 77-007**, (1977a).

Bott, T.R. and Gudmundsson, J.S., "Deposition of Paraffin Wax from Kerosene in Cooled Heat Exchanger Tubes", Can. J. Chem. Eng., **55**, 381, (1977b).

Gudmundsson, J. S., Particulate Fouling, in "Fouling of Heat Transfer Equipment", eds. E. F. C. Somerscales and J. G. Knudsen, 357-387, Hemisphere, Washington, D.C., (1981).

Brod, M, Deane, B. C., and Rossi, F., "Field Experience with the Use of Additives in the Pipeline Transportation of Waxy Crudes", J. Inst. Pet., **57**, No. 554, 110, (1971).

Cleaver, J.W. and Yates, B., "The Effect of Reentrainment on Particle Deposition", Chem. Eng. Sci., **31**, 47-151, (1976).

Cleaver, J.W. and Yates, B.. "A Sublayer Model for the Deposition of Particles from Turbulent Flow", Chem. Eng. Sci, **30**, 983-992, (1975).

Crittenden, B.D., Kolaczkowski, S.T. and Downey, I.L., "Fouling of Crude Oil Preheat Exchangers", Trans IChemE, **70**, Part A, 555-557, (1992).

Dinkelacker, A., "Play Tornado-Like Vortices a Role in the Generation of Flow Noise?" Reprinted from Mechanics of Sound Generation in Flows, ed. E.-A. Muller, IUTAM/ICA/AIAA Symposium, Max-Planck-Institut fur Stromungsforschung, Gottingen, BRD, Springer-Verlag, Berlin, (1979).

Eaton, P.E. and Weeter, G.Y., "Paraffin Deposition in Flow Lines", Tretolite Division, presented at 16th Nat. Heat Transfer conf., Paper 76-CSME/CSChE-22, St. Louis, (1976).

Epstein, N,, "Thinking about Heat Transfer", Heat Transfer Engineering, **4**, No.1, 43-53, (1983).

Epstein, N., "Fouling of Heat Exchanger Surfaces", presented at GVC.VDI-Gesellschaft Verfahrenstechnik und Chemieingenieurwesen, 1.1-1.4, Munchen, Germany, (1990).

Frendenlund, J. H., Pedersen, K. S., Ronningsen, H. P., "A Thermodynamic Model for Predictions of Wax formation in Crude Oils", AIChE Journal, **34**, No. 12, 1937-1942, (1988).

Hansen, G. Arthur, "Fluid Mechanics", John Wiley & Sons, Inc., N.Y., (1967), pp. 438-440.

Holder, G.A. and Winkler, J., "Wax Crystalization from Distillate Fuels", Journal of Institute Petroleum, **51**, No. 499, 228, (1965).

Hunt, E.B., "Laboratory Study of Paraffin Deposition", Petroleum Transactions, 1259-1265, (Nov. 1962).

Jessen, F.W.and Howell, J.N., "Effect of Flowrate on Paraffin Accumulation in Plastic, Steel and Coated Pipe", Petroleum Transactions, AIME, **213**, 80-84, (1958).

Jorda, R.M., "Paraffin Deposition and Prevention in Oil Wells", J. Pet. Tech., **18**, 1605-1612, (Dec. 1966).

Kern, D.Q. and Seaton, R.E., "A Theoretical Analysis of Thermal Surface Fouling", British Chemical Engineering, **4**, No. 5, 258-262, (1959)

Majeed, A., Bringedal, B., Overa, S., "Model Calculates Wax Deposition for N. Sea Oils", Oil and Gas Journal, **88**, No. 25, 63-69, (1990).

Patton, C.C. and Casad, B.M., "Paraffin Deposition from Refined Wax-Solvent Systems", Soc. Pet. Engineers Journal, **10**, No. 1, 17-24, (March 1970).

Patton, C.C., and Jessen, F.W., " The Effect of Petroleum Residua on Paraffin Deposition from a Heptane-Refined Wax System", Soc. Pet. Engineers Journal, **5**, No. 1, 333, (1965).

Svendsen, J.A., "Mathematical Modeling of Wax Deposition in Oil Pipeline Systems", AIChE Journal, **39**, No.8., 1377-1387, (1993).

Weast, Robert C., Astle, Melvin J., Beyer, William H. , "Handbook of Physics and Chemistry", 68 th ed., CRC Press, Inc., Boca Raton, Florida, pp. D-171-172, F-10, F-39, (1987-1988).

Taborek, J., Aoki, T., Ritter, R.B. and Palen, J.W., Knudsen, J.G., "Predictive Methods for Fouling Behavior", Chemical Engineering Progress, **68**, No. 7, 69-74, (1972).

Taborek, J,, Aoki T, Ritter, R.B. and Palen, J.W.,"Fouling: The Major Unresolved Problem in Heat Transfer", Chemical Engineering Progress, **68**, No.2, 59-63, (1972).

Toronov, V.P., Tatar Neft Nauch-Issled Inst., **13**, 207, (1969).

Watkinson, A.P.and Epstein, N., "Gas oil Fouling in a Sensible Heat Exchanger", Chem. Eng. Prog. Symp. Ser., **65**, No. 92, 84-90, (1969).

Zhang, G., "Investigation of Paraffin Wax Fouling", report on work done at UBC, 45 pages, (1992).

Appendix A

Rotameter Calibration

The calibration curve and its equation for cooling water flow is:

$$\text{Flow Rate (U.S. gal/min.)} = 0.275 + 0.05\ S + 1*10^{-4}\ S^2 \qquad (43)$$

where S is the scale of the rotameter reading in %. See Fig. 24.

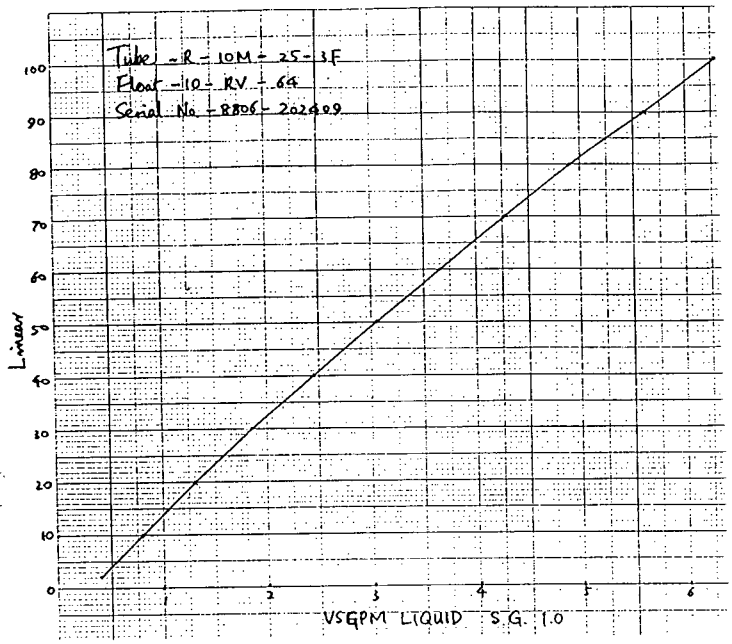

Fig. 24. Calibration curve of rotameter

Appendix B

Calibration equations for thermocouples:

No. 2 thermocouple (wax-kerosene mixture inlet)

$$T_1 = -0.21064 + 17.53609V_2 - 0.88371V_2^2 + 0.3139V_2^3 - 0.04991V_2^4$$

No. 3 Thermocouple (wax-kerosene mixture outlet)

$$T_2 = -0.0963 + 17.05522V_3 - 0.2259V_3^2 - 0.02855V_3^3 + 0.00832V_3^4$$

No. 4 Thermocouple(cooling water inlet)

$$t_1 = -0.32759 + 17.68791V_4 - 0.98792V_4^2 + 0.3553V_4^3 - 0.05466V_4^4$$

No. 5 Thermocouple (cooling water outlet)

$$t_2 = -0.33693 + 17.68651V_5 - 0.9769V_5^2 + 0.35688V_5^3 - 0.05611V_5^4$$

No. Thermocouple (differential temperature reading for water side)

$$\Delta t = (t_2 - t_1) = -0.00088 + 16.79067\Delta V$$

where $V_{i=2,3,4,5}$ is thermoelectric voltage in mV and T is temperature in ^{o}C

Appendix C

Computer Program

```
C  Purpose
C
C     This program fits data into a non-linear equation(Kern-Seaton)
C  finds the asymptotic value of fouling resistance and time constant.
C
C  Argument
C
C   M     Number of data
C   TKI   Inlet temperature of mixture
C   TKO   Outlet temperature of water
C   TWI   Inlet temperature of cooling water
C   TWO   Outlet temperature of cooling water
C   RHO   Densities
C         1=mixture
C         2=water
C   CP    Specific heat capacities
C         1=mixture
C         2=water
C   VIC   viscosities
C         1=mixture
C         2=water
C   V     Mixture flowrate
C   FL    Water flowrate
C   DELP  Pressure drop across orifice
C   DELT  Log-mean temperature difference
C   QW    Heat gain by water
C   QK    Heat loss by mixture
C   REW   Reynolds number of water side
C   REH   Reynolds number of mixture side
C   U(I)  Overall heat transfer coefficient
C   RF    Fouling resistance
C   T     Time
C   DI    Inner diameter of inner tube
C   DO    Outer diameter of inner tube
C   D     Inner diameter of outer tube
C   WT    Resolution of thermocouple
C   CD    Discharge coefficient
C   W     Length of tube
C   SUMU  Uncertainty
C   B2    Orifice diameter/pipe diameter
C   AOR   Area of orifice

      PROGRAM PROJEC
      IMPLICIT DOUBLE PRECISION (A-H,O-Z)
      EXTERNAL F,RHO,CP,VIC
      DIMENSION X(2),DX(2),A(2,3),TKI(300),TKO(300),TWI(300),TWO(300)
     *,TW(300),TK(300),UW(300),UK(300),RFW(300),RFK(300),TV(300),TR(300)
```

```
     *,DT(300),TI(300)
      COMMON RF(300),T(300),M
      DATA O1,O2,O3,O4,O5/3.785411D-3,.275D0,.05D0,1.D-4,60.D0/
      DATA CD,B2,AOR,RHOM,RHOW,G/.62D0,.4831D0,1.13D-4
     *    ,13.6D0,1.D0,9.8D0/
      DATA N,EPS,WT,W,DM/2,1.D-4,.008D0,.72D0,.01D0/

      DATA DI,DO,D/9.957D-3,12.446D-3,25.4D-3/

C  Files for data input and output

      OPEN(UNIT=4,FILE='wax49.dat')
      OPEN(UNIT=7,FILE='c:\f77\out49.dat')
      OPEN(UNIT=8,FILE='TEMP.DAT')
      M=76

C  Bulk concentration in %

      C=20

C  Manometer reading across orifice in inches

      Z=8.8
      Z=2.53D-2*Z

C  Rotameter reading in %

      S=20
      DO 20 I=1,M
       READ(4,10) T(I),TKI(I),TKO(I),TWI(I),TWO(I),DT(I),TI(I)
10     FORMAT(1X,F6.0,4F7.4,2F7.4)
20    CONTINUE

C  Converting the mV to  C

      DO 30 I=1,M
       TKI(I)=TKI(I)+TI(I)
       TKI(I)=-0.21064+17.53609*TKI(I)-0.88371*TKI(I)**2+0.3139
     *  *TKI(I)**3-0.04991*TKI(I)**4
       TKO(I)=TKO(I)+TI(I)
       TKO(I)=-0.0963+17.05522*TKO(I)-0.22591*TKO(I)**2-0.02855
     * *TKO(I)**3+0.00832*TKO(I)**4
       TWI(I)=-TWI(I)+TI(I)
       TWI(I)=-0.32759+17.68791*TWI(I)-0.98792*TWI(I)**2+0.3553
     * *TWI(I)**3-0.05466*TWI(I)**4
       TWO(I)=-TWO(I)+TI(I)
       TWO(I)=-0.33693+17.68651*TWO(I)-0.9769*TWO(I)**2+0.35688
     * *TWO(I)**3-0.05611*TWO(I)**4
       DT(I)=-0.00088+16.79067*DT(I)


       WRITE(8,300) I,TWO(I)-TWI(I)
300    FORMAT(1X,I8,F8.2)
30    CONTINUE
```

```
C  Outer and inner heat exchange area of tube.

      PI=4.D0*DATAN(1.D0)
      AI=PI*DI*W
      AO=PI*DO*W

C  Initializes the final fouling resistance X(1) and time consatnt X(2)

      X(1)=.7D0
      X(2)=10D0
      X(2)=1/X(2)
      SUMW=0.D0
      SUMK=0.D0
      SUMD=0.D0
      SUMQ=0.D0
      TAVW=0.D0
      TAVK=0.D0

C  Cooling water flowrate

      FL= O1*(O2+O3*S+O4*S**2)/O5
      DELP=1000.D0*G*Z*(RHOM-RHOW)

C  Finds bulk temperature and average temp. of fluid

      DO 40 I=1,M
       TW(I)=(TWO(I)+TWI(I))/2
       TK(I)=(TKO(I)+TKI(I))/2
       TAVW=TAVW+TW(I)
       TAVK=TAVK+TK(I)
40    CONTINUE

C  Flowrates, velocities, densities and viscosities are evaluated at
C  the average temperature for Re.

      TAVW=TAVW/M
      TAVK=TAVK/M
      V=CD*AOR*SQRT(2*DELP/(RHO(TAVK,1)*(1-B2**4)))
      VW=FL/(PI/4*DI**2)
      VK=V/(PI/4*(D**2-DO**2))

C  Finds the Reynolds number for both sides

      REW=RHO(TAVW,2)*VW*DI/VIC(C,TAVW,2)
      REK=RHO(TAVK,1)*VK*.012954D0/VIC(C,TAVK,1)

C  Writes the results into file

      WRITE(7,50) 'Bulk concentration (%)   ',C
50    FORMAT(1X,A26,F4.1)
      WRITE(7,60) 'Mixture Re               ',REK
60    FORMAT(1X,A26,F6.0)
```

```
      WRITE(7,70) 'Wate Re                ',REW
70    FORMAT(1X,A26,F6.0)
      WRITE(7,80) 'Water average Temp.( C)  ', TAVW
      WRITE(7,80) 'M. average Temp. ( C)    ', TAVK
80    FORMAT(1X,A26,F6.2)
      WRITE(7,80) '       '
      WRITE(7,90) 'Time','Fouling Res.','QW(kW)','EQ(%)'
      WRITE(7,90) '(min)', '(m K/kW) W.side'
90    FORMAT(1X,A15,A15,A15,A10)

C Determines the heat gain and loss.
C Also, the uncertainity is found by the following loop.

      DO 120 I=1,M
       QW=FL*RHO(TW(I),2)*CP(TW(I),2)*DT(I)
       SUMQ=SUMQ+QW
       V=CD*AOR*SQRT(2*DELP/(RHO(TK(I),1)*(1-B2**4)))
       QK=V*RHO(TK(I),1)*CP(TK(I),1)*(TKI(I)-TKO(I))
       EQ=(QK-QW)/QK*100
       DELH=TKI(I)-TWO(I)
       DELC=TWO(I)-TWI(I)
       DELL=TKO(I)-TWI(I)
       BH=DELH/DELL
       E=DLOG(BH)
       DELT=(DELH-DELL)/E

C For Crittenden

       WN=DELH-DELL
       YN=WN/DELH
       ZN=WN/DELL
       PRINT*,'M',DM
      UD=DM+2*WT/DELC+1/WN*(DABS(ZN/LOG(BH)-1)*WT+DABS(1-YN/DLOG(BH))*WT
     * +DABS(YN/DLOG(BH)-1)*WT+DABS(1-ZN/DLOG(BH))*WT)


C Finds the overall heat transfer coefficient
C Based on water side

       UW(I)=QW/(DELT*AI)

C Based on mixture side

       UK(I)=QK/(DELT*AO)

C The initial overall heat transfer coefficient belongs to the
C clean tube .
C Fouling resistance is 0 at time 0.

       IF (I.EQ.1) THEN
        UCN=UD
        PRINT*,'UCN',UCN
        UCW=UW(1)
        UCK=UK(1)
```

```
      CPWO=CP(TK(I),2)
      RHWO=RHO(TK(I),2)
      CPKO=CP(TK(I),1)
      RHKO=RHO(TK(I),1)
      RFW(1)=0.D0
      RFK(1)=0.D0
     ELSE

C Subsequent fouling res. at time T is calculated.

    RFW(I)=(1/UW(I)-1/UCW*CPWO/CP(TK(I),2)*RHWO/RHO(TK(I),2))*AO/AI
      RFK(I)=1/UK(I)-1/UCK*CPKO/CP(TK(I),1)*RHKO/RHO(TK(I),1)
      IF ((RFW(I).LE.0).OR.(RFK(I).LE.0)) THEN
        WRITE(6,100) ' Fouling resistance zero or negative'
100       FORMAT(1X,A35)
      END IF

C  The uncertainity for Crittenden

      UNCD=(UD/UW(I)+UCN/UCW)/RFW(I)

C  The uncertainity for the individual is added up and the average
C  is calculated.
C  For Crittenden

      SUMD=UNCD+SUMD

     END IF
     IF (I.EQ.1) THEN
       UNCD=0
     END IF
     WRITE(7,110) T(I),RFW(I),QW,EQ
110   FORMAT(1X,F15.1,F15.4,F15.3,F10.2)
120   CONTINUE

C  Finds the average uncertainity %
C  For Crittenden

     SUMD=100*SUMD/(M-1)

C  Finds the average heat transferred on the water side

     QAVW=SUMQ/M

C  Loop to find the surface temperature of the outer side
C  of tube.

     TC=0
     TF=TAVW
400   H=1057*(1.352+0.02*TF)*VW**0.8/DI**0.2
     TWSI=TF+QAVW*1000/(H*PI*DI*W)
     PRINT*,'***',TWSI
     AAV=(DI+DO)/2*PI
     DELX=(DO-DI)/2
```

```
      COND=(0.0135*TWSI+8)*1.73
      TWSO=QAVW*1000*DELX/(COND*AAV*W)+TWSI
      TF=(TWSI+TAVW)/2

      IF (DABS(TWSO-TC).GT.0.01) THEN
         TC=TWSO
         GO TO 400
      END IF
      PRINT*,'WSO',TWSO

C  Loop to find the parameters for water side.

        WRITE(7,130) '      '
        WRITE(7,130) 'Water side'
130       FORMAT(1X,A40)
        DO 140 I=1,M
         RF(I)=RFW(I)
140       CONTINUE

C  Determines the fitted parameters to an accuracy of EPS.

      DO 190 ITER=1,50
       DIFMAX=0.D0
       CALL COEFF(F,N,2,3,X,A)
       CALL GAUSS(A,N,2,3,DX,RNORM,IERROR)
       IF (IERROR.EQ.2) THEN
         WRITE(6,170) ' Zero entry in matrix'
170        FORMAT(1X,A20)
         STOP
       END IF
       DO 180 I=1,N
         X(I)=X(I)+DX(I)
         DIFMAX=DMAX1(DIFMAX,DABS(DX(I)))
180      CONTINUE

       PRINT*,'8',DIFMAX,DX(1),DX(2)
       PRINT*,X(1),X(2)
       IF (DIFMAX.LE.EPS) THEN
         PRINT*,'DONE'
         GO TO 200
       END IF
190    CONTINUE
200    WRITE(7,210) 'Fo.Res.','Time const.(min)','Unc(BDC)%','S. Temp'
210    FORMAT(1X,A15,A20,A15,A15)
      WRITE(7,220) ITER,X(1),1/X(2),SUMD,TWSO
220    FORMAT(1X,I4,F11.4,F20.2,F15.2,F15.2)

      END


C  Purpose
C
C      The subroutine is to find the argument of the matrix by
C  finite difference method.
```

```
C
C  Argument
C
C     X(J)   Parameters to be fitted
C     A(I,J)  Matrix of coefficients

      SUBROUTINE COEFF(F,N,NDR,NDC,X,A)
      IMPLICIT DOUBLE PRECISION (A-H,O-Z)
      DIMENSION X(N),A(NDR,NDC),DELX(10)
      NP=N+1
      DO 10 I=1,N
       DELX(I)=1.D-6*X(I)
10    CONTINUE
      DO 30 I=1,N
       DO 20 J=1,NP
        IF (J.NE.NP) THEN
          X(J)=X(J)+DELX(J)
          FUP=F(I,N,X)
          X(J)=X(J)-2.D0*DELX(J)
          FDOWN=F(I,N,X)
          X(J)=X(J)+DELX(J)
          A(I,J)=(FUP-FDOWN)/(2.D0*DELX(J))
        ELSE
          A(I,NP)=-F(I,N,X)
        END IF
20      CONTINUE
30    CONTINUE
      RETURN
      END

C
C  Purpose
C
C     Uses Gauss Jordan elimination with partial pivot selection
C  to solve simultaneous linear equation of form [A]*{X}={C}.
C
C  Argument
C
C     A       Augumented coefficient matrix.
C     N       Number of equtions to be solved.
C     NDR     First(row) dimension of A in calling program.
C     NDC     Second(column) dimension of A in calling program.
C     IERROR  Error flag
C             =1 Succesful Gauss elimination.
C             =2 Zero diagonal entry after pivot selection.
C     RNORM   If IERROR=1, measure size of residual error.
C           If IERROR=2, RNORM=0
C     X       Solution vector.
C

      SUBROUTINE GAUSS(A,N,NDR,NDC,X,RNORM,IERROR)
      IMPLICIT DOUBLE PRECISION (A-H,O-Z)
      DIMENSION A(2,3),X(N),B(50,51),S(50)
      NM=N-1
```

```
      NP=N+1

C  Sets up working matix.

      DO 20 I=1,N
       DO 10 J=1,NP
        B(I,J)=A(I,J)
10     CONTINUE
20    CONTINUE

C  Carry out elimination process N-1 times to determine the main
C  diagonal entry.

      DO 110 K=1,NM
       KP=K+1

C  Find for each row the column containing the largest coefficient.

       DO 40 I=K,N
        BIG2=ABS(B(I,K))
        IPIVOT=K
        DO 30 J=KP,N
         AB2=ABS(B(I,J))
         IF (AB2.GT.BIG2)THEN
          BIG2=AB2
          IPIVOT=J
         END IF
30       CONTINUE

C  For each row divide the first coefficient by the largest coefficient
C  in that row to find S(I).

        S(I)=B(I,K)/B(I,IPIVOT)
40     CONTINUE

C  Find the row having the largest S(I) represented by IPIVOT.

       BIG =ABS(S(K))
       IPIVOT=K
       DO 50 I=KP,N
        AB=ABS(S(K))
        IF (AB.GT.BIG) THEN
          BIG=AB
          IPIVOT=I
        END IF
50      CONTINUE

C  If IPIVOT.NE.K then interchange row K and IPIVOT.

       IF (IPIVOT.NE.K) THEN
         DO 60 J=K,NP
          TEMP=B(IPIVOT,J)
          B(IPIVOT,J)=B(K,J)
          B(K,J)=TEMP
```

```
60        CONTINUE
      END IF

C  Checks for zero entry in the main diagonal.

      IF (B(K,K).EQ.0) THEN
        IERROR=2
      END IF

C  Eliminate B(I,K) from rows KP through N

      DO 80 I=KP,N
       QUOT=B(I,K)/B(K,K)
       B(I,K)=0
       DO 70 J=KP,NP
        B(I,J)=B(I,J)-QUOT*B(K,J)
70     CONTINUE
80    CONTINUE

C  Eliminates B(I,KP) from K down to 1.

      DO 100 I=K,1,-1
       QT=B(I,KP)/B(KP,KP)
       DO 90 J=KP,NP
         B(I,J)=B(I,J)-QT*B(KP,J)
90     CONTINUE
100   CONTINUE
110   CONTINUE

C  Checks last diagonal element for zero entry. B(N,N)=0
C  causes an abnormal entry return with IERROR=2.

      IF (B(N,N).EQ.0) THEN
       IERROR=2
      END IF

C  Finds out the solution vector by dividing the r.h.s. coefficient
C  to the main diagonal entry for each column.

      DO 120 I=1,N
       X(I)=B(I,NP)/B(I,I)
120   CONTINUE

C  Calculates norm of the residual vector, C-A*X
C  Normal return with IERROR=1

      RSQ=0
      DO 140 I=1,N
       SUM=0
       DO 130 J=1,N
        SUM=SUM+A(I,J)*X(J)
130     CONTINUE
       RSQ=RSQ+(A(I,NP)-SUM)**2
140   CONTINUE
```

```
      RNORM=SQRT(RSQ)
      IERROR=1
      RETURN
      END


C Purpose
C     Finds the sum for regression of Kern-Seaton equation from
C T=0 to M
C
C Arguments
C     X(1)  Asymptotic fouling resistance.
C     X(2)  Time constant.

      DOUBLE PRECISION FUNCTION F(I,N,X)
      IMPLICIT DOUBLE PRECISION (A-H,O-Z)
      DIMENSION X(2)
      COMMON RF(300),T(300),M
      GO TO (10,20),I
10     SUM=0.D0
      DO 30 K=1,M
       SUM=SUM+(RF(K)-X(1)*(1-DEXP(-T(K)*X(2))))*
     *    (1-DEXP(-T(K)*X(2)))
30     CONTINUE
       F=SUM
      RETURN
20     SUM=0.D0
      DO 40 K=1,M
       SUM=SUM+(RF(K)-X(1)*(1-DEXP(-T(K)*X(2))))*
     *    X(1)*T(K)*DEXP(-T(K)*X(2))
40     CONTINUE
       F=SUM
      RETURN
      END

C Pupose
C
C   Function determines the density  at a given temperature for
C   both mixture and water.
C
C Argument
C
C   T  Teperature
C   K   =1 mixture
C       =2 water

      DOUBLE PRECISION FUNCTION RHO(T,K)
      IMPLICIT DOUBLE PRECISION (A-H,O-Z)
      GO TO (10,20),K
10     RHO=816.25-.74892*T
      RETURN
20     RHO=(999.83952+16.9451768*T-7.9870401D-3*T**2-46.170461D-6
     *  *T**3+105.56302D-9*T**4-280.54253D-12*T**5)/(1+16.87985D-3*T)
      RETURN
```

```
      END

C Purpose
C
C   Function determines the specific heat capacity of mixture
C   and water.
C
C Argument
C
C   T  Temperaure
C   K  =1 mixture
C      =2 water

      DOUBLE PRECISION FUNCTION CP(T,K)
      IMPLICIT DOUBLE PRECISION (A-H,O-Z)
      GO TO (10,20),K
10     CP=1.18143 + .012246*T
      RETURN
20     CP=4.21765-3.74987D-3*T+1.49921D-4*T**2-3.35545D-6*T**3+
     * 4.27292D-8*T**4-2.30244D-10*T**5
      RETURN
      END

C Purpose
C
C   Function determines viscosities of mixture and water
C
C Argument
C
C   T  Temperature
C   K  =1 mixture
C      =2 water
C
      DOUBLE PRECISION FUNCTION VIC(C,T,K)
      IMPLICIT DOUBLE PRECISION (A-H,O-Z)
      GO TO (10;20),K
10     IF (C.EQ.5) THEN
       A1=4.16D-6
       B1=13676.D0
       ELSEIF (C.EQ.10) THEN
         A1=3.80D-6
         B1=14160.D0
         ELSEIF (C.EQ.15) THEN
          A1=1.86D-7
          B1=21993.D0
          ELSEIF (C.EQ.20) THEN
            A1=5.92D-7
            B1=18820.D0
      ENDIF
      VIC=A1*EXP(B1/8.314/(273.15+T))
      RETURN
20     IF (T.LE.20) THEN
       VIC=1301/(998.333+8.1855*(T-20)+.00585*(20-T)**2)-1.30233
       VIC=10**VIC*1.D-3
```

```
  ELSEIF (T.LE.100) THEN
    VIC=(1.3272*(20-T)-.001053*(T-20)**2)/(T+105)
    VIC=10**(VIC*1.002)*1D-3
 END IF
 RETURN
END
```

Appendix D

Experimental data.

The following Table shows the run number listed in the appendix, the file number and name in a diskette, tube type, wax type used and the overall initial heat transfer coefficient for each run. The following abbreviation is used:

SS = Stainless steel

Table 31. Lists of run number, disk numbr, tube type, wax type and U_o

Run. No.	Disk No.	Tube Type	Wax Type	U_o (kW/m² K)	u(m/s)	T_s (°C)
1	out7.dat	SS	Refined	0.4644	1.2	11.3
2	out15.dat	"	"	0.5082	1.6	13.3
3	out5.dat	"	"	0.5145	2.1	12.9
4	out6.dat	"	"	0.5796	2.4	14.2
5	out9.dat	"	"	0.6538	2.7	15.8
6	out35.dat	"	Slack Wax	0.7478	1.2	15.0
7	out31.dat	"	"	0.9130	1.6	18.0
8	out32.dat	"	"	1.1533	1.9	19.2
9	out34.dat	"	"	1.1238	2.2	17.9
10	out36.dat	"	"	1.2197	2.6	17.5
11	out42.dat	Chrome-plated SS	"	0.5681	1.2	12.7
12	out46.dat	"	"	0.7493	1.6	14.5
13	out47.dat	"	"	0.7438	1.6	14.4
14	out43.dat	"	"	0.9248	2.0	15.8
15	out44.dat	"	"	1.1182	2.4	17.3
16	out45.dat	"	"	1.2108	2.6	18.4
17	out50.dat	Sand-blasted SS	"	0.8802	1.2	16.3
18	out49.dat	"	"	0.9074	1.6	16.9
19	out51.dat	"	"	1.3004	2.0	19.1
20	out52.dat	"	"	1.3680	2.3	19.7
21	out53.dat	"	"	1.6324	2.6	21.2
22	out58.dat	n-C18 silane chrome-plated SS	"	0.7842	1.2	18.8
23	out57.dat	"	"	0.7936	1.6	18.6
24	out59.dat	"	"	1.2069	2.0	21.3
25	out60.dat	"	"	1.4296	2.3	22.2
26	out61.dat	"	"	1.0777	2.6	23.5
27	out66.dat	Heresite Si 57 E SS	"	0.9458	1.2	22.1
28	out65.dat	"	"	1.0973	1.6	21.9
29	out67.dat	"	"	1.3992	2.0	24.8
30	out68.dat	"	"	1.5088	2.3	26.0
31	out69.dat	"	"	1.5120	2.5	26.7

Run. No.	Disk No.	Tube Type	Wax Type	U_o (kW/m² K)	u(m/s)	T_s (°C)
32	out71.dat	Heresite P-400/L-66 SS	"	0.7841	1.2	20.5
33	out70.dat	"	"	1.0745	1.6	22.3
34	out75.dat	"	"	1.1595	1.6	23.5
35	out72.dat	"	"	1.1701	2.0	24.7
36	out73.dat	"	"	1.2517	2.3	25.5
37	out74.dat	"	"	1.2651	2.6	22.8
38	out77.dat	n-C18 silane SS	"	0.8673	1.2	18.7
39	out76.dat	"	"	1.0150	1.6	20.3
40	out78.dat	"	"	1.2427	2.0	21.4
41	out79.dat	"	"	1.3433	2.2	22.2
42	out80.dat	"	"	1.4645	2.5	22.8
43	out10.dat	SS	Refined wax	0.3485	1.6	10.8
44 Same as run 2	out15.dat	"	"	0.5082	1.6	13.3
45	out11.dat	"	"	0.5261	1.6	14.9
46	out12.dat	"	"	0.5926	1.6	16.5
47	out14.dat	"	"	0.6975	1.6	18.7
48	out40.dat	"	Slack wax	0.7123	1.6	11.9
49 Same as run 7	out31.dat	"	"	0.9130	1.6	12.7
50	out37.dat	"	"	1.0341	1.6	19.5
51	out38.dat	"	"	1.1141	1.6	22.7
52	out39.dat	"	"	1.3886	1.6	24.2
53	out41.dat	"	"	1.1767	1.6	24.2
54 Same as run 12	out46.dat	Chrome-plated SS	"	0.7493	1.6	15.4
55	out48.dat	"	"	0.8818	1.6	18.7
56	out81.dat	"	"	1.2727	1.6	25.3
57	out82.dat	"	"	1.3512	1.6	28.8
58 Same as run 18	out49.dat	Sand-blasted SS	"	0.9074	1.6	16.9
59	out54.dat	"	"	1.0620	1.6	20.2
60	out55.dat	"	"	1.2528	1.6	23.9
61	out56.dat	"	"	1.3476	1.6	26.9
62 Same as run 23	out57.dat	n-C18 silane chrome plated SS	"	0.7936	1.6	18.6
63	out62.dat	"	"	1.0952	1.6	22.8
64	out63.dat	"	"	1.3638	1.6	27.1
65	out64.dat	"	"	1.3564	1.6	31.5
66	out3.dat	SS	Refined wax	0.5512	1.6	13.6
67	out4.dat	"	"	0.4994	1.6	11.2
68	out16.dat	"	"	0.2944	1.6	11.5
69	out18.dat	"	"	0.1699	1.6	10.4
70	out27.dat	"	Slack wax	1.4638	1.6	16.6
71	out28.dat	"	"	1.3223	1.6	16.0
72	out29.dat	"	"	1.1979	1.6	15.5
73	out30.dat	"	"	0.7437	1.6	14.8

Sample Calculations

The following sample calculation was done for slack wax MCT-10 at 20 % by using stainless steel. Re = 8722. The calculation has been done at time = 0 and time = 2 min.
The file is denoted by Run 7.

The reading from the data logger (or as stored in a diskette file) is:

V_2= 0.6195 mv V_3= 0.6585 mv V_4= -0.4060 mv V_5= -0.3485 mv ΔV = 0.0610 mv V = 1.2145 mv

The actual voltage is calculated by adding the reference voltage V to V_2, V_3, V_4, V_5
i.e.,

V_2= 1.8340 mv V_3= 1.8730 mv V_4 = -0.8085 mv V_5= -0.8660 mv ΔV = 0.0610 mv

Using the calibration equations in Appendix B

T_1= 31.52 °C, T_2= 30.97°C, t_1= 13.49°C, t_2= 14.45°C, Δt = 1.02 °C

The pipe diameters are:

D = 25.400 mm, D_i = 9.957 mm, D_o = 12.446 mm

The distance between the inlet and outlet of the flow line is =

0.72 m.

Wax-kerosene flow rate :

Manual reading from the mercury manometer is

Δh = 9 inches

Conversion to SI

Δh= 0.0253*9 = 0.228 m

$\Delta P = \rho g \Delta h$

= 1000(13.6-1)9.81.0.228

= 28182.2 Pa

The average wax-kerosene temperature for the whole run is

$T_{avg,k}$= 31.22 °C

$\rho_k = 816.25-0.7489T_{avg,k}$

= 792.9 kg/m³

C_d= 0.62

$A_{or}=\pi D^2/4=\pi 0.012^2/4=0.0001131$ m²

$\beta = 12/24.84 = 0.4831$

$$\dot{V} = C_d A_{or}\sqrt{\frac{2\ \Delta P}{\rho_k (1-\beta^4)}}$$

$V = 0.000607$ m³/s

The velocity of wax-kerosene mixture

$$u = \frac{\dot{V}}{(\pi/4)(D^2 - D_o^2)}$$

$= 1.58$ m/s

Water flow rate:

The Rotameter reading was S = 20 % for all runs.

Using the calibration equation

Flow Rate (U.S. gal/min.)= $0.275 + 0.05\ S + 1*10^{-4}\ S^2$

$= 3.78541.10^{-3}\ (0.275 + 0.05\ S + 1*10^{-4}\ S^2)/60$ m³/s

$\dot{V}_w = 8.296X10^{-5}$ m³/s

The velocity of water:

$$V_w = \frac{\dot{V}_w}{(\pi/4)D_i^2}$$

$=1.1$ m/s

Heat gained by water:

The bulk temperature of water is

$$t_b = \frac{t_1 + t_2}{2} = 13.97\ ^oC$$

$$C_{pw} = 4.21765 - 3.74987.10^{-3} t_b + 1.49921.10^{-4} t_b^2 - 3.35545.10^{-6} t_b^3 + 4.27292.10^{-8} t_b^4 - 2.30244.10^{-10} t_b^5$$

$= 4.1879$ kJ/kg °C

$$\rho_w = \frac{(999.83952 + 16.945176 t_b - 7.987040.10^{-3} t_b^2 - 46.170461.10^{-6} t_b^3 + 105.56302.10^{-9} t_b^4 - 280.54253.10^{-12} t_b^5}{1 + 16.879850.10^{-3} t_b}$$

= 999.37 kg/m³

$$Q_w = \dot{V}_w \rho_w C_{pw} \Delta t$$

= 8.296X10⁻⁵ X999.37X4.1879X1.02

= 0.355 kW

$A_i = \pi D_i L = 0.0225$ m²

$A_o = \pi D_o L = 0.0282$ m²

The log-mean temperature difference

$$\Delta t_{lm} = \frac{(T_1 - t_2) - (T_2 - t_1)}{\ln\left(\frac{T_1 - t_2}{T_2 - t_1}\right)}$$

=17.27°C

$$U_o = \frac{Q_w}{A_i \Delta t_{lm}}$$

= 0.9136 kW/m² K

Overall heat transfer coefficient at time = 2 min.:

V_2= 0.6195 mv V_3= 0.6585 mv V_4= -0.4060 mv V_5= -0.3485 mv ΔV= 0.0610 mv V= 1.2145 mv

The same calculation done above can be used to get the temperature in °C and the results are

T_1=31.26 °C, T_2=30.74 °C, t_1=12.63 °C, t_2=13.46 °C, Δt=0.89 °C

Heat gained by water:
(the volume flow rate of water is constant throughout the experiment)

ρ_w= 999.37 kg/m³

C_{pw} = 4.1879 kJ/kg°C

$$Q_w = \dot{V}_w \rho_w C_{pw} \Delta t$$

= 0.309 kW

Δt_{lm}= 17.95 °C

$$U = \frac{Q_w}{A_i \Delta t_{lm}}$$

= 0.7651 kW/m² K

From previous calculation

U_o = 0.9130 kW/m² K

The fouling resistance at time = 2 min. is

$$R_f = \frac{A_o}{A_i}\left(\frac{1}{U} - \frac{1}{U_o}\right)$$

= 0.2662 m² K/kW

Re of wax-kerosene mixture:

The density and viscosity are evaluated at the average bulk temperature

$T_{avg,k}$ = 31.22 °C

$$Re_k = \frac{\rho_k d_h u}{\mu_k}$$

= 8722

Re of water:

The density and viscosity are calculated at the average bulk temperature of water for the run

$T_{avg,w}$ =12.27 °C

$$Re_w = \frac{\rho_w D_i V_w}{\mu_w}$$

= 8648

Run 1

Bulk concentration (%)	10.0
Mixture Re	9093.
Water Re	18344.
Water average Temp.(°C)	9.40
M. average Temp. (°C)	32.59

Q_W at θ=0 = 0.392 kW

Time (min)	Fouling Res. (m^2 K/kW)	Time (min)	Fouling Res. (m^2 K/kW)
0	0.0000	92	2.2196
1	0.2561	93	2.2265
2	0.4490	94	1.8213
3	0.5095	95	1.8436
4	1.1698	96	1.8622
5	1.0993	97	1.7220
6	1.3197	98	2.6964
7	1.7163	99	2.7093
8	1.8020	100	2.1562
9	1.5293	101	2.1699
10	1.4995	102	2.2193
11	1.8804	103	2.1997
12	1.9004	104	2.1671
13	1.9441	105	2.1801
14	1.0008	106	2.1807
15	1.9138	107	2.2088
16	1.9380	108	2.2391
17	1.9806	109	1.7668
18	1.9461	110	1.7631
19	1.9786	111	1.7781
20	1.6339	112	1.4500
21	1.6053	113	2.2045
22	1.6254	114	2.2153
23	2.0284	115	1.2036
24	2.0495	116	2.2196
25	1.6500	117	2.1910
26	2.5202	118	2.1954
27	2.0039	119	2.1959
28	2.5703	120	2.2240
29	2.5787	121	1.7874
30	2.5495	122	2.2149
31	2.5776	123	2.2280
32	2.5973	124	1.4745
33	3.2498	125	1.4909
34	3.2347	126	1.8583
35	3.2559	127	1.8827
36	3.3044	128	2.1967
37	2.5740	129	2.7146
38	2.0885	130	2.7328
39	2.6624	131	2.7907
40	2.6575	132	2.2080
41	2.1031	133	2.2149
42	2.1083	134	1.8151
43	2.1537	135	2.1665
44	1.7385	136	2.7750
45	3.3329	137	2.7959
46	2.5744	138	2.2102

47	2.6195	139	1.1865
48	4.8699	140	2.2692
49	2.6545	141	2.3019
50	2.6185	142	1.5156
51	2.0780	143	2.2299
52	2.6500	144	2.2406
53	2.1272	145	2.2582
54	2.6699	146	2.3068
55	2.1558	147	1.8147
56	2.6970	148	2.2670
57	2.6500	149	2.2758
58	2.6720	150	2.2846
59	2.1410	151	2.2430
60	2.1389	152	2.2516
61	2.6600	153	1.8073
62	2.1293	154	2.2867
63	1.7526	155	1.8469
64	2.0076	156	2.2451
65	2.0315	157	2.2015
66	2.0549	158	2.2384
67	2.1028	159	2.2408
68	2.1328	160	1.8319
69	1.7317	161	1.8545
70	1.7593	162	1.5257
71	1.7630	163	2.2670
72	1.7398	164	2.2495
73	1.1763	165	1.8300
74	1.7618	166	2.2802
75	1.7225	167	2.2911
76	2.1520	168	2.2516
77	2.1486	169	1.8241
78	1.7593	170	1.8431
79	2.1991	171	2.3024
80	1.7630	172	1.8488
81	1.7990	173	2.3068
82	2.1829	174	1.8488
83	2.1850	175	1.8317
84	2.1649	176	1.8393
85	1.7457	177	1.8431
86	2.1770	178	2.8925
87	2.1942	179	2.3021
88	2.1440	180	1.8187
89	2.7092		
90	2.7272		
91	2.7631		

$R_f^*(m^2K/kW)$	θ_c *(min)*	Unc(B.D. Crittenden)%
2.1890	8.88	13.65

Run 2

Bulk concentration (%)	10.0
Mixture Re	11414.
Wate Re	18807.
Water average Temp.(°C)	10.27
M. average Temp. (°C)	32.38
Q_w at θ=0	= 0.451 kW

Time (min)	Fouling Res. (m^2 K/kW)	Time (min)	Fouling Res. (m^2 K/kW)
0	0.0000	86	0.8589
1	0.0702	87	0.8357
2	0.1180	88	1.1355
3	0.2458	89	1.1463
4	0.4585	90	0.9487
5	0.4917	91	0.9581
6	0.7193	92	0.9535
7	0.8924	93	1.1750
8	0.7585	94	0.9875
9	0.8923	95	0.8260
10	0.7474	96	0.9738
11	0.6291	97	0.9809
12	0.6341	98	0.9701
13	0.7722	99	1.1776
14	0.7873	100	0.9755
15	0.9312	101	0.8150
16	0.7612	102	0.9845
17	0.9273	103	0.8332
18	0.9392	104	0.8394
19	0.7828	105	0.8370
20	0.6557	106	0.8491
21	0.6611	107	0.8552
22	0.7888	108	0.8565
23	0.8868	109	0.7214
24	0.8828	110	0.7218
25	0.8828	111	0.8735
26	0.8933	112	0.7307
27	0.9132	113	0.9524
28	0.9224	114	0.9217
29	0.7678	115	1.1200
30	0.9330	116	0.9283
31	1.1131	117	0.7738
32	0.9238	118	0.9511
33	0.9290	119	0.9591
34	0.9236	120	0.9628
35	1.1160	121	0.9722
36	0.9251	122	0.8117
37	0.9317	123	0.8214
38	0.9383	124	0.8274
39	0.9408	125	0.6922
40	0.9487	126	0.8407
41	0.9566	127	0.5873
42	0.9700	128	0.5924
43	0.9737	129	0.8577
44	0.8253	130	0.6017
45	0.8254	131	0.6023
46	0.6976	132	0.6064

47	0.9345	133	0.6105
48	1.1058	134	0.6146
49	1.3505	135	0.6849
50	1.1213	136	0.9546
51	0.9415	137	0.7923
52	0.9308	138	0.9532
53	0.9348	139	0.9708
54	1.1361	140	0.9788
55	0.7887	141	0.9855
56	0.9493	142	0.9961
57	0.9535	143	0.8359
58	0.9588	144	0.8420
59	0.9668	145	0.8286
60	0.8103	146	1.1296
61	0.9872	147	1.1065
62	0.8249	148	1.3642
63	1.0032	149	0.9200
64	0.9832	150	1.1302
65	0.0475	151	0.9495
66	0.8065	152	0.9588
67	0.8101	153	0.9599
68	0.9805	154	0.6639
69	0.8188	155	0.9742
70	0.8541	156	0.8191
71	1.0015	157	0.8288
72	0.8419	158	0.8348
73	0.8346	159	0.8408
74	0.8297	160	0.8469
75	0.9698	161	0.7155
76	0.9631	162	0.7200
77	0.9728	163	0.8698
78	0.9711	164	0.6109
79	0.9791	165	0.7292
80	0.8247	166	0.7366
81	1.0023	167	0.6201
82	0.6969	168	0.7466
83	0.6973	169	0.7488
84	0.8528	170	0.7522
85	0.8528	171	0.7909
		172	1.1073
		173	1.1141
		174	0.9203
		175	1.1183
		176	0.9388
		177	0.9508
		178	0.9615
		179	0.9708

$R_f^*(m^2K/kW)$	θ_c (min)	Unc(BDC)%
0.8896	5.45	30.00

Run 3

Bulk concentration (%) 10.0
Mixture Re 14812.
Wate Re 18018.
Water average Temp.(°C) 8.78
M. average Temp. (°C) 32.58
Q_w at θ=0 = 0.573 kW

Time (min)	Fouling Res. (m^2 K/kW)	Time (min)	Fouling Res (m^2 K/kW)
0	0.0000	90	0.5066
1	0.2802	91	0.5076
2	0.3303	92	0.5085
3	0.2985	93	0.6057
4	0.3851	94	0.4215
5	0.3885	95	0.5135
6	0.3996	96	0.5154
7	0.4047	97	0.6143
8	0.4830	98	0.7328
9	0.4779	99	0.6200
10	0.6905	100	0.6210
11	0.6926	101	0.6220
12	0.5828	102	0.6220
13	0.5892	103	0.6277
14	0.5867	104	0.5209
15	0.4887	105	0.6259
16	0.4875	106	0.6259
17	0.5896	107	0.6259
18	0.4954	108	0.4309
19	0.4973	109	0.6242
20	0.5004	110	0.6242
21	0.5935	111	0.5264
22	0.4991	112	0.6242
23	0.4898	113	0.5264
24	0.4960	114	0.5264
25	0.4153	115	0.6299
26	0.4198	116	0.6249
27	0.4053	117	0.6163
28	0.0922	118	0.6210
29	0.4809	119	0.6200
30	0.3985	120	0.6143
31	0.4827	121	0.6163
32	0.4836	122	0.6200
33	0.4846	123	0.6143
34	0.4855	124	0.6163
35	0.4864	125	0.6163
36	0.4026	126	0.6182
37	0.4026	127	0.6220
38	0.1451	128	0.7370
39	0.4043	129	0.6240
40	0.4878	130	0.6287
41	0.4878	131	0.6297
42	0.4878	132	0.5260
43	0.4896	133	0.6317
44	0.3312	134	0.6317
45	0.4896	135	0.5297
46	0.4955	136	0.6317

47	0.4924	137	0.6337
48	0.4111	138	0.5330
49	0.4982	139	0.4392
50	0.4084	140	0.4392
51	0.4951	141	0.4355
52	0.3360	142	0.5264
53	0.4026	143	0.4363
54	0.3992	144	0.5223
55	0.4855	145	0.5232
56	0.4846	146	0.4363
57	0.4885	147	0.5264
58	0.5879	148	0.4363
59	0.4904	149	0.5273
60	0.4913	150	0.5283
61	0.5918	151	0.5255
62	0.4922	152	0.5980
63	0.5974	153	0.5893
64	0.5021	154	0.4951
65	0.2086	155	0.5043
66	0.5089	156	0.5131
67	0.5089	157	0.5168
68	0.6106	158	0.5195
69	0.5149	159	0.5140
70	0.5158	160	0.5191
71	0.4238	161	0.5167
72	0.5177	162	0.5209
73	0.5126	163	0.4329
74	0.5144	164	0.4337
75	0.4301	165	0.5237
76	0.5144	166	0.5246
77	0.5144	167	0.5246
78	0.4301	168	0.5246
79	0.5154	169	0.5246
80	0.4309	170	0.4392
81	0.4318	171	0.4392
82	0.4318	172	0.1185
83	0.4318	173	0.4372
84	0.4318	174	0.5241
85	0.4249	175	0.4900
86	0.5103	176	0.5167
87	0.4189	177	0.5200
88	0.6037		
89	0.5034		

$R_f^*(m^2K/kW)$	θ_c *(min)*	Unc(BDC)%
0.5122	2.47	22.48

Run 4

Bulk concentration (%)	10.0
Mixture Re	17332.
Wate Re	18263.
Water average Temp.(°C)	9.25
M. average Temp. (°C)	32.71
Q_w at θ=0	= 0.616 kW

Time (min)	Fouling Res. (m^2 K/kW)	Time (min)	Fouling Res. (m^2 K/kW)
0	0.0000	92	0.2833
1	0.0378	93	0.2763
2	0.1421	94	0.3333
3	0.2049	95	0.3333
4	0.1705	96	0.3348
5	0.2702	97	0.2777
6	0.4420	98	0.2798
7	0.4083	99	0.3372
8	0.2998	100	0.2303
9	0.3723	101	0.3387
10	0.2959	102	0.3387
11	0.5019	103	0.2798
12	0.5100	104	0.3320
13	0.4372	105	0.2745
14	0.5188	106	0.3348
15	0.5379	107	0.3313
16	0.4620	108	0.2236
17	0.5439	109	0.2763
18	0.4653	110	0.2763
19	0.4628	111	0.2738
20	0.4670	112	0.3328
21	0.3412	113	0.2745
22	0.3379	114	0.2727
23	0.4080	115	0.2745
24	0.3452	116	0.2752
25	0.3419	117	0.3342
26	0.4073	118	0.2791
27	0.4653	119	0.2748
28	0.4603	120	0.3385
29	0.5375	121	0.3385
30	0.4553	122	0.2830
31	0.4528	123	0.2830
32	0.4578	124	0.2812
33	0.3899	125	0.2812
34	0.4653	126	0.3420
35	0.3333	127	0.2851
36	0.4033	128	0.2833
37	0.2862	129	0.2802
38	0.4104	130	0.3303
39	0.4127	131	0.2703
40	0.3526	132	0.3266
41	0.4017	133	0.2685
42	0.4696	134	0.3253
43	0.2203	135	0.2706
44	0.3994	136	0.3283
45	0.4779	137	0.2720
46	0.4080	138	0.2717

47	0.4150	139	0.2749
48	0.4662	140	0.2749
49	0.4621	141	0.3313
50	0.4688	142	0.2738
51	0.4739	143	0.2720
52	0.3414	144	0.2220
53	0.4102	145	0.2727
54	0.4149	146	0.2713
55	0.4204	147	0.2727
56	0.3571	148	0.0896
57	0.3039	149	0.1756
58	0.3981	150	0.3322
59	0.4622	151	0.2791
60	0.5462	152	0.2805
61	0.4672	153	0.1784
62	0.4007	154	0.2812
63	0.3386	155	0.2830
64	0.3459	156	0.2837
65	0.4172	157	0.2819
66	0.3520	158	0.2819
67	0.3537	159	0.2320
68	0.4205	160	0.2855
69	0.2912	161	0.2844
70	0.2884	162	0.2826
71	0.3412	163	0.2320
72	0.3388	164	0.2869
73	0.3338	165	0.2310
74	0.3984	166	0.2303
75	0.3284	167	0.2303
76	0.3289	168	0.2320
77	0.3252	169	0.2320
78	0.3194	170	0.2819
79	0.3826	171	0.2303
80	0.4520	172	0.2303
81	0.3154	173	0.2819
82	0.3778	174	0.2801
83	0.3787	175	0.2801
84	0.3857	176	0.2819
85	0.3889	177	0.2826
86	0.3284	178	0.1796
87	0.3915	179	0.2819
88	0.3318	180	0.2819
89	0.3340		
90	0.2777		
91	0.2805		

$R_f^*(m^2K/kW)$	θ_c *(min)*	Unc(BDC)%
0.3363	2.55	27.50

Run 5

Bulk concentration (%)	10.0
Mixture Re	19053.
Water Re	18590.
Water average Temp.(°C)	9.86
M. average Temp. (°C)	32.68

Q_w at θ=0 = 0.733 kW

Time (min)	Fouling Res. (m^2 K/kW)	Time (min)	Fouling Res. (m^2 K/kW)
0	0.0000	90	0.2094
1	0.0811	91	0.2087
2	0.1272	92	0.2119
3	0.1364	93	0.1733
4	0.2118	94	0.2575
5	0.1804	95	0.2150
6	0.2206	96	0.1750
7	0.2206	97	0.1396
8	0.2596	98	0.1762
9	0.3025	99	0.2193
10	0.2996	100	0.2180
11	0.2523	101	0.2206
12	0.2563	102	0.2193
13	0.2591	103	0.2618
14	0.2576	104	0.2205
15	0.2589	105	0.0788
16	0.2137	106	0.2645
17	0.2163	107	0.1827
18	0.2150	108	0.2057
19	0.1768	109	0.1608
20	0.1750	110	0.2014
21	0.2561	111	0.2452
22	0.2562	112	0.2912
23	0.2137	113	0.2082
24	0.2137	114	0.2524
25	0.2588	115	0.3025
26	0.2162	116	0.2106
27	0.2162	117	0.2556
28	0.2175	118	0.0744
29	0.1762	119	0.2169
30	0.2143	120	0.2131
31	0.2174	121	0.2181
32	0.2174	122	0.2130
33	0.2131	123	0.2162
34	0.2517	124	0.2634
35	0.1301	125	0.2219
36	0.2982	126	0.2225
37	0.2075	127	0.2212
38	0.3001	128	0.2224
39	0.3015	129	0.0532
40	0.3028	130	0.2250
41	0.3035	131	0.2256
42	0.3582	132	0.2230
43	0.3085	133	0.1768
44	0.3610	134	0.1709
45	0.1402	135	0.2094
46	0.2522	136	0.2094

47	0.2025	137	0.1709
48	0.2450	138	0.2119
49	0.2456	139	0.2131
50	0.2462	140	0.1697
51	0.2088	141	0.1709
52	0.2113	142	0.2093
53	0.2556	143	0.2087
54	0.2150	144	0.1697
55	0.2595	145	0.2106
56	0.2188	146	0.2118
57	0.2493	147	0.2093
58	0.2375	148	0.1709
59	0.2408	149	0.2118
60	0.2064	150	0.2149
61	0.2565	151	0.2149
62	0.2943	152	0.1757
63	0.2454	153	0.1397
64	0.2454	154	0.1762
65	0.2945	155	0.2167
66	0.2966	156	0.1774
67	0.2948	157	0.1757
68	0.2491	158	0.1763
69	0.2524	159	0.1774
70	0.2536	160	0.1751
71	0.2549	161	0.1727
72	0.0705	162	0.1727
73	0.2554	163	0.2062
74	0.3064	164	0.2043
75	0.2156	165	0.2474
76	0.2553	166	0.2487
77	0.2137	167	0.2068
78	0.3060	168	0.2068
79	0.3060	169	0.2486
80	0.2613	170	0.2080
81	0.2994	171	0.1709
82	0.2885	172	0.2105
83	0.3380	173	0.2118
84	0.3380		
85	0.2885		
86	0.2045		
87	0.2051		
88	0.2057		
89	0.2075		

$R_f^*(m^2K/kW)$	θ_c (min)	Unc(BDC)%
0.2249	2.12	27.91

Run 6

Bulk concentration (%)	20.0
Mixture Re	6645.
Water Re	7906.
Water average Temp.(°C)	9.10
M. average Temp. (°C)	31.87
Q_w at θ=0	= 0.347 kW

Time (min)	Fouling Res. (m^2 K/kW)	Time (min)	Fouling Res. (m^2 K/kW)
0	0.0000	86	0.9223
2	0.6206	88	0.9899
4	0.5618	90	0.9834
6	0.6027	92	0.9727
8	0.6083	94	0.6458
10	0.6315	96	1.0091
12	0.6615	98	1.0020
14	0.6996	100	1.0616
16	0.7194	102	1.0275
18	0.7600	104	1.0238
20	0.8083	106	1.0120
22	0.7979	108	1.0560
24	0.7704	110	0.9215
26	0.7954	112	0.9065
28	0.8345	114	0.9992
30	0.8074	116	0.8623
32	0.7936	118	0.9879
34	0.7951	120	0.6927
36	0.8917	122	0.9944
38	0.7753	124	0.9915
40	0.8054	126	1.0207
42	0.9212	128	1.0351
44	0.8882	130	1.1040
46	0.9136	132	1.0518
48	0.8240	134	1.0292
50	0.8682	136	1.0035
52	0.9680	138	0.9117
54	0.9999	140	0.7287
56	0.9219	142	0.7957
58	0.9233	144	0.8974
60	0.7557	146	1.0092
62	0.8967	148	1.0183
64	0.9561	150	1.0111
66	0.9302		
68	0.9664		
70	0.9679		
72	0.9876		
74	0.9640		
76	1.0092		
78	0.9271		
80	0.8981		
82	0.9153		
84	1.0198		

$R_f^*(m^2K/kW)$	θ_c (min)	Unc(BDC)%
0.9293	8.02	11.94

Run 7

Bulk concentration (%)	20.0
Mixture Re	8722.
Water Re	8648.
Water average Temp.(°C)	12.27
M. average Temp. (°C)	31.22
Q_w at θ=0	= 0.355 kW

Time (min)	Fouling Res. (m^2 K/kW)	Time (min)	Fouling Res (m^2 K/kW)
0	0.0000	86	0.8185
2	0.2683	88	0.8731
4	0.5102	90	0.8564
6	0.5203	92	0.8849
8	0.5012	94	0.8912
10	0.5061	96	0.8568
12	0.5413	98	0.8316
14	0.5649	100	0.6608
16	0.5765	102	0.6642
18	0.6564	104	0.7943
20	0.6415	106	0.8302
22	0.6015	108	0.8464
24	0.6428	110	0.8203
26	0.6916	112	0.8778
28	0.7168	114	0.7902
30	0.7059	116	0.8602
32	0.7482	118	0.8188
34	0.7691	120	0.9036
36	0.7675	122	0.7931
38	0.7414	124	0.8251
40	0.7848	126	0.7703
42	0.7731	128	0.7856
44	0.8001	130	0.9006
46	0.7427	132	0.7397
48	0.8363	134	0.8636
50	0.8114	136	0.7902
52	0.7789	138	0.8840
54	0.8166	140	0.8399
56	0.8027	142	0.8006
58	0.8455	144	0.8020
60	0.8916	146	0.8418
62	0.8900	148	0.8248
64	0.8244	150	0.8127
66	0.7896		
68	0.8275		
70	0.8531		
72	0.8475		
74	0.9177		
76	0.9368		
78	0.9232		
80	0.8615		
82	0.9121		
84	0.8311		

$R_f^*(m^2K/kW)$	θ_c *(min)*	Unc(BDC)%
0.8244	10.77	11.39

Run 8

Bulk concentration (%)	20.0
Mixture Re	10615.
Water Re	8706.
Water average Temp.(°C)	12.51
M. average Temp. (°C)	31.30
Q_w at θ=0	= 0.444 kW

Time (min)	Fouling Res. (m^2 K/kW)	Time (min)	Fouling Res. (m^2 K/kW)
0	0.0000	86	0.7276
2	0.3622	88	0.7053
4	0.3402	90	0.7644
6	0.4229	92	0.7974
8	0.4533	94	0.7656
10	0.4669	96	0.7538
12	0.4660	98	0.7409
14	0.5202	100	0.6855
16	0.5122	102	0.8194
18	0.5441	104	0.6910
20	0.5389	106	0.7536
22	0.5847	108	0.7737
24	0.5713	110	0.7427
26	0.6170	112	0.7779
28	0.6622	114	0.7826
30	0.6939	116	0.8416
32	0.6761	118	0.7699
34	0.6962	120	0.8853
36	0.7142	122	0.8177
38	0.7306	124	0.8813
40	0.7396	126	0.8489
42	0.7772	128	0.7773
44	0.7681	130	0.7905
46	0.7638	132	0.6784
48	0.7780	134	0.8399
50	0.7570	136	0.8374
52	0.8583	138	0.8671
54	0.7938	140	0.7980
56	0.7371	142	0.8168
58	0.7844	144	0.8661
60	0.8673	146	0.8107
62	0.7821	148	0.7857
64	0.8639	150	0.8621
66	0.8574		
68	0.8135		
70	0.7955		
72	0.8086		
74	0.7935		
76	0.7982		
78	0.8489		
80	0.7953		
82	0.7579		
84	0.8065		

$R_f^*(m^2K/kW)$	θ_c (min)	Unc(BDC)%
0.7926	13.21	8.89

Run 9

Bulk concentration (%)	20.0
Mixture Re	12184.
Water Re	8103.
Water average Temp.(°C)	9.96
M. average Temp. (°C)	31.16
Q_w at θ=0	=0.452 kW

Time (min)	Fouling Res. (m^2 K/kW)	Time (min)	Fouling Res. (m^2 K/kW)
0	0.0000	86	0.7645
2	0.2961	88	0.6151
4	0.3281	90	0.7091
6	0.3394	92	0.7571
8	0.3789	94	0.7543
10	0.4138	96	0.6615
12	0.4301	98	0.7036
14	0.3866	100	0.7130
16	0.4198	102	0.8062
18	0.4952	104	0.6967
20	0.4904	106	0.7254
22	0.4573	108	0.6530
24	0.4944	110	0.7117
26	0.5156	112	0.7282
28	0.5462	114	0.6691
30	0.5387	116	0.6092
32	0.5473	118	0.6729
34	0.5322	120	0.6777
36	0.6014	122	0.8016
38	0.5208	124	0.8154
40	0.5463	126	0.7269
42	0.6192	128	0.7825
44	0.6017	130	0.6676
46	0.5673	132	0.8419
48	0.5809	134	0.8974
50	0.6561	136	0.8715
52	0.7042	138	0.8241
54	0.7044	140	0.7821
56	0.6295	142	0.6475
58	0.8028	144	0.6871
60	0.7300	146	0.6108
62	0.7062	148	0.6477
64	0.7040	150	0.6675
66	0.7196		
68	0.7406		
70	0.7245		
72	0.7072		
74	0.7084		
76	0.8759		
78	0.7100		
80	0.7372		
82	0.7063		
84	0.8423		

$R_f^*(m^2K/kW)$	θ_c (min)	Unc(BDC)%
0.7244	18.09	9.21

Run 10

Bulk concentration (%)	20.0
Mixture Re	14430.
Water Re	7685.
Water average Temp.(°C)	8.13
M. average Temp. (°C)	31.33
Q_w at θ=0	= 0.522 kW

Time (min)	Fouling Res. (m^2 K/kW)	Time (min)	Fouling Res. (m^2 K/kW)
0	0.0000	86	0.6502
2	0.2904	88	0.6458
4	0.3469	90	0.7001
6	0.3856	92	0.6940
8	0.4020	94	0.6075
10	0.4830	96	0.7266
12	0.4874	98	0.7221
14	0.5071	100	0.6833
16	0.4671	102	0.7064
18	0.4984	104	0.7650
20	0.5450	106	0.7171
22	0.5138	108	0.5147
24	0.5417	110	0.7602
26	0.5061	112	0.6587
28	0.5575	114	0.6025
30	0.5260	116	0.6262
32	0.5842	118	0.6907
34	0.5421	120	0.6608
36	0.5895	122	0.6662
38	0.6010	124	0.5923
40	0.5933	126	0.6947
42	0.6780	128	0.6763
44	0.6367	130	0.5609
46	0.7312	132	0.6550
48	0.6619	134	0.7447
50	0.7166	136	0.6772
52	0.6726	138	0.5808
54	0.6908	140	0.7250
56	0.6541	142	0.6024
58	0.7259	144	0.4911
60	0.6696	146	0.6404
62	0.6582	148	0.7185
64	0.6485	150	0.7072
66	0.6888		
68	0.6457		
70	0.7713		
72	0.7068		
74	0.6666		
76	0.7547		
78	0.6655		
80	0.7676		
82	0.8343		
84	0.6846		

$R_f^*(m^2K/kW)$	θ_c (min)	Unc(BDC)%
0.6668	10.34	7.99

Run 11

Bulk concentration (%)	20.0
Mixture Re	6586.
Water Re	7474.
Water average Temp.(°C)	7.20
M. average Temp. (°C)	31.32

Q_w at θ=0 = 0.289 kW

Time (min)	Fouling Res. (m^2 K/kW)	Time (min)	Fouling Res. (m^2 K/kW)
0	0.0000	86	0.6666
2	0.5410	88	0.5462
4	0.7250	90	0.6401
6	0.7019	92	0.8349
8	0.7522	94	0.7242
10	0.7626	96	0.6603
12	0.8757	98	0.6826
14	0.8910	100	0.5674
16	0.8524	102	0.7945
18	0.9283	104	0.6493
20	0.8100	106	0.7654
22	0.9110	108	0.7626
24	0.8191	110	0.6971
26	0.9388	112	0.8677
28	0.8597	114	0.7664
30	0.9759	116	0.6399
32	0.7736	118	0.6799
34	1.2896	120	0.7637
36	1.0417	122	0.7706
38	1.0816	124	0.7877
40	1.0629	126	0.8238
42	0.9107	128	0.7476
44	1.0762	130	0.7984
46	0.9751	132	0.6544
48	1.0087	134	0.9873
50	0.7359	136	0.7909
52	0.8249	138	0.8075
54	0.8263	140	0.8315
56	0.8642	142	0.8869
58	0.8966	144	0.7237
60	0.7726	146	0.9006
62	0.8906	148	0.7026
64	0.7511	150	0.8685
66	0.8640		
68	0.8780		
70	0.8612		
72	0.7999		
74	0.8208		
76	0.9067		
78	0.9050		
80	0.8747		
82	0.7554		
84	0.7042		

$R_f^*(m^2K/kW)$	θ_c (min)	Unc(BDC)%
0.8238	2.07	17.80

Run 12

Bulk concentration (%)	20.0
Mixture Re	9224.
Water Re	7511.
Water average Temp.(°C)	7.36
M. average Temp. (°C)	31.34
Q_w at θ=0	= 0.338 kW

Time (min)	Fouling Res. (m^2 K/kW)	Time (min)	Fouling Res. (m^2 K/kW)
0	0.0000	86	0.5615
2	0.4187	88	0.6161
4	0.5065	90	0.5854
6	0.4510	92	0.4546
8	0.6059	94	0.6359
10	0.6654	96	0.5154
12	0.626	98	0.6135
14	0.6019	100	0.6116
16	0.6172	102	0.2521
18	0.6124	104	0.5746
20	0.7411	106	0.5373
22	0.6628	108	0.7396
24	0.7318	110	0.5611
26	0.6682	112	0.7292
28	0.7473	114	0.4921
30	0.7076	116	0.5552
32	0.7562	118	0.6752
34	0.6447	120	0.6174
36	0.6787	122	0.554
38	0.7263	124	0.6421
40	0.6761	126	0.5323
42	0.6775	128	0.375
44	0.567	130	0.5585
46	0.717	132	0.4836
48	0.6105	134	0.4985
50	0.6263	136	0.555
52	0.6126	138	0.609
54	0.5844	140	0.541
56	0.6503	142	0.6394
58	0.5699	144	0.6152
60	0.5778	146	0.656
62	0.4968	148	0.5153
64	0.7304	150	0.6409
66	0.5732		
68	0.603		
70	0.588		
72	0.6293		
74	0.593		
76	0.5247		
78	0.4529		
80	0.6818		
82	0.542		
84	0.6733		

$R_f^*(m^2K/kW)$	θ_c (min)	Unc(BDC)%
0.6031	2.08	15.14

Run 13

Bulk concentration (%)	20.0
Mixture Re	9208.
Water Re	7494.
Water average Temp.(°C)	7.29
M. average Temp. (°C)	31.24

Q_w at θ=0 = 0.374 kW

Time (min)	Fouling Res. (m^2 K/kW)	Time (min)	Fouling Res. (m^2 K/kW)
0	0.0000	86	0.5837
2	0.3749	88	0.6151
4	0.4131	90	0.5309
6	0.5793	92	0.5945
8	0.5843	94	0.6114
10	0.6339	96	0.5698
12	0.6817	98	0.6064
14	0.7225	100	0.5282
16	0.5321	102	0.6010
18	0.5747	104	0.6335
20	0.5302	106	0.5921
22	0.5697	108	0.6368
24	0.5760	110	0.5529
26	0.5855	112	0.4512
28	0.6781	114	0.5692
30	0.5665	116	0.5977
32	0.5674	118	0.6182
34	0.6315	120	0.5516
36	0.7590	122	0.5392
38	0.5830	124	0.6182
40	0.6367	126	0.6030
42	0.5829	128	0.5362
44	0.6127	130	0.5429
46	0.5546	132	0.5897
48	0.6185	134	0.5975
50	0.6706	136	0.5527
52	0.6307	138	0.5737
54	0.5816	140	0.5624
56	0.6495	142	0.6163
58	0.4924	144	0.5891
60	0.6267	146	0.4776
62	0.6174	148	0.5409
64	0.6039	150	0.5798
66	0.6357		
68	0.3178		
70	0.5383		
72	0.5348		
74	0.5981		
76	0.4994		
78	0.5318		
80	0.4934		
82	0.5998		
84	0.4869		

$R_f^*(m^2K/kW)$	θ_c (min)	Unc(BDC)%
0.5814	2.16	15.55

Run 14

Bulk concentration (%)	20.0
Mixture Re	11015.
Water Re	7597.
Water average Temp.(°C)	7.75
M. average Temp. (°C)	31.29
Q_w at θ=0	= 0.408 KW

Time (min)	Fouling Res. (m^2 K/kW)	Time (min)	Fouling Res. (m^2 K/kW)
0	0.0000	86	0.5774
2	0.4471	88	0.6229
4	0.6013	90	0.6407
6	0.5177	92	0.5105
8	0.4849	94	0.4801
10	0.5546	96	0.6043
12	0.5935	98	0.6308
14	0.5710	102	0.5923
18	0.5879	104	0.5966
20	0.5688	106	0.5956
22	0.6027	108	0.5803
24	0.5674	110	0.5952
26	0.6972	112	0.5337
28	0.5253	114	0.6103
30	0.5863	116	0.6258
32	0.6373	118	0.6138
34	0.6078	120	0.6229
36	0.6341	122	0.5866
38	0.6015	124	0.6180
40	0.5583	126	0.5701
42	0.6162	128	0.5425
44	0.5351	130	0.5816
46	0.6144	132	0.5613
48	0.6335	134	0.5863
50	0.6388	136	0.6186
52	0.6033	138	0.6215
54	0.5911	140	0.5921
56	0.5709	142	0.6362
58	0.6201	144	0.5965
60	0.5980	146	0.7184
62	0.6306	148	0.5892
64	0.5935	150	0.5741
66	0.6144		
68	0.5792		
70	0.6221		
72	0.6424		
74	0.6280		
76	0.5864		
78	0.5953		
80	0.6074		
82	0.5900		
84	0.5210		

$R_f^*(m^2K/kW)$	θ_c (min)	Unc(BDC)%
0.5941	1.42	11.59

Run 15

Bulk concentration (%)	20.0
Mixture Re	13156.
Water Re	7604.
Water average Temp.(°C)	7.78
M. average Temp. (°C)	31.25

Q_w at θ=0 = 0.482 kW

Time (min)	Fouling Res. (m^2 K/kW)	Time (min)	Fouling Res. (m^2 K/kW)
0	0.0000	86	0.5628
2	0.4232	88	0.4769
4	0.4887	90	0.5180
6	0.4618	92	0.5022
8	0.4186	94	0.5577
10	0.5109	96	0.5611
12	0.4778	98	0.5824
14	0.5208	100	0.5643
16	0.4983	102	0.5359
18	0.5635	104	0.5881
20	0.5223	106	0.4950
22	0.5258	108	0.5644
24	0.3444	110	0.5487
26	0.5101	112	0.4830
28	0.5133	114	0.5322
30	0.5039	116	0.5775
32	0.5487	118	0.4866
34	0.5187	120	0.5415
36	0.5389	122	0.5357
38	0.3859	124	0.5348
40	0.5103	126	0.4840
42	0.4830	128	0.5614
44	0.5070	130	0.5020
46	0.4984	132	0.5532
48	0.5314	134	0.5141
50	0.5600	136	0.5659
52	0.5597	138	0.8016
54	0.4613	140	0.5908
56	0.5275	142	0.5197
58	0.5393	144	0.5004
60	0.4729	146	0.4877
62	0.5418	148	0.5000
64	0.5629	150	0.5000
66	0.4839		
68	0.5554		
70	0.5146		
72	0.5189		
74	0.5128		
76	0.5367		
78	0.5254		
80	0.5317		
82	0.5308		
84	0.5808		

$R_f^*(m^2K/kW)$	θ_c (min)	Unc(BDC)%
0.5240	1.34	9.80

Run 16

Bulk concentration (%)	20.0
Mixture Re	14428.
Water Re	7700.
Water average Temp.(°C)	8.20
M. average Temp. (°C)	31.32
Q_w at θ=0	= 0.545 kW

Time (min)	Fouling Res. (m^2 K/kW)	Time (min)	Fouling Res. (m^2 K/kW)
0	0.0000	86	0.4492
2	0.3175	88	0.4448
4	0.2162	90	0.5544
6	0.2603	92	0.4117
8	0.3090	94	0.5079
10	0.3691	96	0.5171
12	0.3410	98	0.4658
14	0.4723	100	0.4923
16	0.4813	102	0.4581
18	0.3504	104	0.4694
20	0.5087	106	0.4457
22	0.4509	108	0.6174
24	0.4370	110	0.5133
26	0.4795	112	0.5298
28	0.4725	114	0.5039
30	0.4483	116	0.2992
32	0.5029	118	0.4705
34	0.5026	120	0.5081
36	0.5190	122	0.4957
38	0.4649	124	0.4627
40	0.4882	126	0.4444
42	0.5187	128	0.4896
44	0.5075	130	0.4997
46	0.5192	132	0.5230
48	0.5110	134	0.5117
50	0.4655	136	0.4373
52	0.4161	138	0.6130
54	0.4533	140	0.4738
56	0.5491	142	0.4470
58	0.4987	144	0.4983
60	0.5640	146	0.5126
62	0.4699	148	0.4559
64	0.4217	150	0.5634
66	0.4737		
68	0.5695		
70	0.4992		
72	0.4871		
74	0.3995		
76	0.4052		
78	0.4979		
80	0.4217		
82	0.4527		
84	0.3335		

$R_f^*(m^2K/kW)$	θ_c (min)	Unc(BDC)%
0.4817	6.43	9.65

Run 17

Bulk concentration (%)	20.0
Mixture Re	6418.
Water Re	8417.
Water average Temp.(°C)	11.30
M. average Temp. (°C)	30.99
Q_w at θ=0	= 0.276 kW

Time (min)	Fouling Res. (m^2 K/kW)	Time (min)	Fouling Res (m^2 K/kW)
0	0.0000	86	1.2402
2	0.7368	88	1.3519
4	0.7330	90	1.3141
6	0.8910	92	1.1302
8	0.8752	94	1.3962
10	0.8510	96	1.2329
12	1.0074	98	1.1463
14	1.0384	100	1.2379
16	0.9941	102	1.0870
18	0.9146	104	1.3661
20	1.1254	106	1.1579
22	1.1056	108	1.2232
24	1.0644	110	1.2276
26	1.0661	112	1.1293
28	1.1344	114	1.2733
30	1.0454	116	1.3402
32	1.2791	118	1.3344
34	1.2305	120	1.3738
36	1.3763	122	1.3768
38	1.3749	124	1.3925
40	1.2981	126	1.3430
42	1.2393	128	1.4537
44	1.2419	130	1.3039
46	0.9473	132	1.4411
48	1.1412	134	1.2064
50	1.1599	136	1.1258
52	1.0287	138	1.2462
54	1.2030	140	1.4278
56	0.9810	142	1.2682
58	1.1594	144	1.3149
60	1.1379	146	1.1974
62	1.1208	148	1.2940
64	1.1643	150	1.3310
66	1.0404		
68	1.0216		
70	1.1013		
72	1.2017		
74	1.2250		
76	1.3102		
78	1.2291		
80	1.1832		
82	1.2366		
84	1.2001		
86	1.2402		

$R_f^*(m^2K/kW)$	θ_c (min)	Unc(BDC)%
1.2187	5.88	10.14

Run 18

Bulk concentration (%)	20.0
Mixture Re	8734.
Water Re	8233.
Water average Temp.(°C)	10.51
M. average Temp. (°C)	31.30
Q_w at θ=0	= 0.361 kW

Time (min)	Fouling Res. (m^2 K/kW)	Time (min)	Fouling Res. (m^2 K/kW)
0	0.0000	86	0.8754
2	0.3787	88	0.8168
4	0.4663	90	0.7215
6	0.5853	92	0.8259
8	0.6480	94	0.7910
10	0.5519	96	0.8161
12	0.1141	98	0.7642
14	0.1540	100	0.7946
16	0.7583	102	0.7725
18	0.7310	104	0.8036
20	0.6911	106	0.6893
22	0.8869	108	0.9088
24	0.7078	110	0.7963
26	0.7691	112	0.8420
28	0.8021	114	0.7689
30	0.8599	116	0.8214
32	0.7385	118	0.8150
34	0.8156	120	0.7601
36	0.8093	122	0.8495
38	0.8024	124	0.7747
40	0.7604	126	0.8464
42	0.7634	128	0.7769
44	0.7914	130	0.7618
46	0.7986	132	0.8208
48	0.9238	134	0.7945
50	0.7672	136	0.8197
52	0.8512	138	0.8431
54	0.7816	140	0.8644
56	0.7844	142	0.7647
58	0.8123	144	0.8330
60	0.7570	146	0.8170
62	0.8492	148	0.9015
64	0.6426	150	0.8146
66	0.9419		
68	0.8492		
70	0.7762		
72	0.8103		
74	0.8023		
76	0.7619		
78	0.7674		
80	0.7397		
82	0.7390		
84	0.7510		

$R_f^*(m^2K/kW)$	θ_c (min)	Unc(BDC)%
0.8027	9.30	11.66

Run 19

Bulk concentration (%)	20.0
Mixture Re	11340.
Water Re	8463.
Water average Temp.(°C)	11.49
M. average Temp. (°C)	31.37
Q_w at θ=0	= 0.460 kW

Time (min)	Fouling Res. (m^2 K/kW)	Time (min)	Fouling Res. (m^2 K/kW)
0	0.0000	86	0.7974
2	0.4138	88	0.7292
4	0.4247	90	0.7428
6	0.4603	92	0.8092
8	0.5597	94	0.6901
10	0.5687	96	1.3474
12	0.5327	98	0.7553
14	0.1459	100	0.7389
16	0.6147	102	0.8125
18	0.6568	104	0.7639
20	0.7093	106	0.7057
22	0.6795	108	0.7615
24	0.6662	110	0.7554
26	0.6920	112	0.7765
28	0.7538	114	0.7667
30	0.7659	116	0.7256
32	0.7419	118	0.7423
34	0.7604	120	0.7271
36	0.7188	122	0.7736
38	0.7654	124	0.7689
40	0.7286	126	0.8019
42	0.7363	128	0.8033
44	0.7129	130	0.7701
46	0.7530	132	0.6996
48	0.7347	134	0.7849
50	0.7397	136	0.8425
52	0.7106	138	0.7676
54	0.6776	140	0.7623
56	0.7054	142	0.8045
58	0.7442	144	0.8237
60	0.6191	146	0.8181
62	0.7101	148	0.7903
64	0.7367	150	0.7671
66	0.7466		
68	0.7615		
70	0.7799		
72	0.7699		
74	0.7203		
76	0.7386		
78	0.7292		
80	0.7674		
82	0.7391		
84	0.7650		

$R_f^*(m^2K/kW)$	θ_c (min)	Unc(BDC)%
0.7614	8.89	7.62

Run 20

Bulk concentration (%)	20.0
Mixture Re	12732.
Water Re	8461.
Water average Temp.(°C)	11.48
M. average Temp. (°C)	31.13
Q_w at θ=0	= 0.468 kW

Time (min)	Fouling Res. (m^2 K/kW)	Time (min)	Fouling Res. (m^2 K/kW)
0	0.0000	86	0.6607
2	0.3060	88	0.6788
4	0.3350	90	0.7044
6	0.4359	92	0.6717
8	0.4320	94	0.6544
10	0.5048	96	0.6621
12	0.5429	98	0.6821
14	0.5226	100	0.6602
16	0.5211	102	0.7283
18	0.5960	104	0.7050
20	0.5242	106	0.7214
22	0.5560	108	0.7106
24	0.5911	110	0.7261
26	0.5788	112	0.7013
28	0.5486	114	0.7418
30	0.5905	116	0.7292
32	0.5880	118	0.7295
34	0.6159	120	0.7072
36	0.6108	122	0.7076
38	0.6572	124	0.7130
40	0.6093	126	0.7294
42	0.6210	128	0.6908
44	0.6085	130	0.7082
46	0.6161		
48	0.6009		
50	0.6292		
52	0.6167		
54	0.6410		
56	0.5716		
58	0.6343		
60	0.6128		
62	0.6477		
64	0.6568		
66	0.6727		
68	0.6746		
70	0.6612		
72	0.6711		
74	0.6838		
76	0.6678		
78	0.6327		
80	0.7181		
82	0.6630		
84	0.6379		

$R_f^*(m^2K/kW)$	θ_c (min)	Unc(BDC)%
0.6609	7.61	7.72

Run 21

Bulk concentration (%)	20.0
Mixture Re	14440.
Water Re	8579.
Water average Temp.(°C)	11.98
M. average Temp. (°C)	31.37
Q_w at θ=0	= 0.480 kW

Time (min)	Fouling Res. (m^2 K/kW)	Time (min)	Fouling Res. (m^2 K/kW)
0	0.0000	86	0.6279
2	0.2516	88	0.6302
4	0.3352	90	0.6304
6	0.3122	92	0.5727
8	0.4343	94	0.6231
10	0.4739	96	0.6121
12	0.5145	98	0.6188
14	0.5060	100	0.5815
16	0.4963	102	0.5792
18	0.4205	104	0.6043
20	0.5125	106	0.6196
22	0.5629	108	0.6050
24	0.5389	110	0.6176
26	0.5185	112	0.6053
28	0.5544	114	0.6267
30	0.5590	116	0.6512
32	0.5756	118	0.5680
34	0.5626	120	0.6291
36	0.5852	122	0.6381
38	0.5809	124	0.6352
40	0.5638	126	0.6120
42	0.5334	128	0.6247
44	0.5942	130	0.6354
46	0.6179	132	0.6151
48	0.5605	134	0.5984
50	0.5986	136	0.6362
52	0.6209	138	0.6181
54	0.5998	140	0.6432
56	0.6222	142	0.6248
58	0.5929	144	0.6253
60	0.5689	146	0.6165
62	0.5909	148	0.6421
64	0.6047	150	0.4387
66	0.6143		
68	0.6024		
70	0.6255		
72	0.6325		
74	0.6131		
76	0.6130		
78	0.6116		
80	0.6197		
82	0.6149		
84	0.6039		

$R_f^*(m^2K/kW)$	θ_c (min)	Unc(BDC)%
0.6016	7.33	6.70

Run 22

Bulk concentration (%)	20.0
Mixture Re	6629.
Wate Re	9019.
Water average Temp.(°C)	13.81
M. average Temp. (°C)	31.42

Q_w at θ=0 = 0.282 kW

Time (min)	Fouling Res. (m^2 K/kW)	Time (min)	Fouling Res. (m^2 K/kW)
0	0.0000	86	0.8029
2	0.3475	88	0.8473
4	0.4359	90	0.8697
6	0.4613	92	0.8291
8	0.5619	94	0.7654
10	0.4985	96	0.6451
12	0.5420	98	0.7441
14	0.5340	100	0.7655
16	0.6696	102	0.9005
18	0.6134	104	0.8554
20	0.5258	106	0.6940
22	0.6899	108	0.8370
24	0.6498	110	0.5948
26	0.6650	112	0.7193
28	0.7290	114	0.8528
30	0.6137	116	0.7679
32	0.6037	118	0.8709
34	0.6145	120	0.8273
36	0.7101	122	0.4462
38	0.4537	124	0.7520
40	0.7457	126	0.6709
42	0.7144	128	0.8355
44	0.7132	130	0.7767
46	0.7170	132	0.7902
48	0.7436	134	0.7608
50	0.7115	136	0.7526
52	0.7864	138	0.6345
54	0.7999	140	0.9283
56	0.7107	142	0.8609
58	0.7439	144	0.6751
60	0.6635	146	0.8218
62	0.7380	148	0.9892
64	0.7806	150	0.8494
66	0.7191		
68	0.7170		
70	0.7972		
72	0.4289		
74	0.6391		
76	0.7570		
78	0.7506		
80	0.8206		
82	0.5838		
84	0.7768		

$R_f^*(m^2K/kW)$	θ_c (min)	Unc(BDC)%
0.7407	7.92	15.93

Run 23

Bulk concentration (%)	20.0
Mixture Re	8773.
Water Re	8702.
Water average Temp.(°C)	12.50
M. average Temp. (°C)	31.50
Q_w at θ=0	= 0.303 kW

Time (min)	Fouling Res. (m^2 K/kW)	Time (min)	Fouling Res. (m^2 K/kW)
0	0.0000	86	0.5665
2	0.0885	88	0.6014
4	0.1721	90	0.4520
6	-0.0591	92	0.3084
8	0.1744	94	0.2458
10	0.2343	96	0.3591
12	0.2563	98	0.4825
14	0.3249	100	0.6111
16	0.346	102	0.5565
18	0.3496	104	0.5664
20	0.3378	106	0.5606
22	0.3127	108	0.6091
24	0.2665	110	0.4572
26	0.3982	112	0.4509
28	0.3211	114	0.4914
30	0.4268	116	0.4907
32	0.4101	118	0.4367
34	0.3557	120	0.5132
36	0.3891	122	0.5873
38	0.3582	124	0.5410
40	0.3950	126	0.4272
42	0.3565	128	0.5838
44	0.4294	130	0.5334
46	0.2981	132	0.3656
48	0.3850	134	0.4837
50	0.3700	136	0.4990
52	0.4694	138	0.4936
54	0.4469	140	0.5371
56	0.4760	142	0.4832
58	0.4587		
60	0.3946		
62	0.4883		
64	0.4790		
66	0.3721		
68	0.4675		
70	0.4489		
72	0.4065		
74	0.4603		
76	0.4124		
78	0.4672		
80	0.4788		
82	0.5168		
84	0.5301		

$R_f^*(m^2K/kW)$	θ_c (min)	Unc(BDC)%
0.4854	20.86	19.35

Run 24

Bulk concentration (%)	20.0
Mixture Re	11314.
Water Re	8977.
Water average Temp.(°C)	13.64
M. average Temp. (°C)	31.35
Q_w at θ=0	= 0.399 kW

Time (min)	Fouling Res. (m^2 K/kW)	Time (min)	Fouling Res. (m^2 K/kW)
0	0.0000	86	0.5180
2	0.2395	88	0.5359
4	0.2759	90	0.4130
6	0.3030	92	0.4436
8	0.4661	94	0.4452
10	0.4087	96	0.4685
12	0.4034	98	0.5383
14	0.4062	100	0.3881
16	0.4090	102	0.5179
18	0.4370	104	0.4572
20	0.4194	106	0.4719
22	0.3993	108	0.4902
24	0.4055	110	0.5823
26	0.4781	112	0.3661
28	0.5589	114	0.5608
30	0.4325	116	0.5146
32	0.4744	118	0.4405
34	0.4220	120	0.4618
36	0.4304	122	0.4663
38	0.4499	124	0.4182
40	0.5307	126	0.4085
42	0.5546	128	0.4678
44	0.4563	130	0.3637
46	0.4258	132	0.4812
48	0.5152	134	0.4402
50	0.4264	136	0.4199
52	0.4339	138	0.3997
54	0.4542	140	0.5000
56	0.4963	142	0.4945
58	0.4915	144	0.4410
60	0.4565	146	0.4710
62	0.4015	148	0.4751
64	0.4556	150	0.4817
66	0.3870		
68	0.2969		
70	0.4124		
72	0.5105		
74	0.4991		
76	0.4358		
78	0.5222		
80	0.4549		
82	0.5597		
84	0.4852		

$R_f^*(m^2K/kW)$	θ_c (min)	Unc(BDC)%
0.4605	4.15	11.53

Run 25

Bulk concentration (%)	20.0
Mixture Re	12888.
Water Re	9002.
Water average Temp.(°C)	13.74
M. average Temp. (°C)	31.26
Q_w at θ=0	= 0.416 kW

Time (min)	Fouling Res. (m^2 K/kW)	Time (min)	Fouling Res. (m^2 K/kW)
0	0.0000	86	0.4681
2	0.1549	88	0.3878
4	0.2589	90	0.4120
6	0.2994	92	0.4384
8	0.2940	94	0.4294
10	0.3517	96	0.3457
12	0.3774	98	0.5222
14	0.4316	100	0.4540
16	0.4250	102	0.4972
18	0.4083	104	0.4912
20	0.3889	106	0.4312
22	0.4550	108	0.4634
24	0.4195	110	0.4573
26	0.4930	112	0.4854
28	0.4602	114	0.4000
30	0.4213	116	0.4633
32	0.4011	118	0.5296
34	0.3859	120	0.4628
36	0.4377	122	0.5393
38	0.3596	124	0.4480
40	0.4759	126	0.4414
42	0.4697	128	0.5350
44	0.5196	130	0.4326
46	0.4235	132	0.4878
48	0.5875	134	0.4567
50	0.4055	136	0.5205
52	0.4323	138	0.4562
54	0.5151		
56	0.4692		
58	0.4261		
60	0.4875		
62	0.4693		
64	0.4531		
66	0.4509		
68	0.4809		
70	0.4484		
72	0.4558		
74	0.4294		
76	0.4528		
78	0.4458		
80	0.5065		
82	0.3811		
84	0.5052		

$R_f^*(m^2K/kW)$	θ_c (min)	Unc(BDC)%
0.4572	6.26	9.55

Run 26

Bulk concentration (%)	20.0
Mixture Re	14642.
Water Re	9110.
Water average Temp.(°C)	14.18
M. average Temp. (°C)	31.16
Q_w at θ=0 = 0.503 kW	

Time (min)	Fouling Res. (m^2 K/kW)	Time (min)	Fouling Res. (m^2 K/kW)
0	0.0000	86	0.4064
2	0.1749	88	0.4871
4	0.2096	90	0.4891
6	0.3161	92	0.4446
8	0.2949	94	0.4134
10	0.2939	96	0.4209
12	0.3332	98	0.4675
14	0.2969	100	0.4525
16	0.3141	102	0.4268
18	0.2755	104	0.4674
20	0.3764	106	0.4833
22	0.3843	108	0.4865
24	0.3470	110	0.4206
26	0.3352	112	0.4372
28	0.3486	114	0.3785
30	0.3475	116	0.4024
32	0.4023	118	0.4268
34	0.4034	120	0.5013
36	0.3453	122	0.4463
38	0.3354	124	0.4810
40	0.4880	126	0.5354
42	0.4001	128	0.5561
44	0.4169	130	0.5730
46	0.4564	132	0.4552
48	0.4010	134	0.4757
50	0.3958	136	0.4772
52	0.4505	138	0.4829
54	0.4290	140	0.5105
56	0.3577	142	0.5042
58	0.3714	144	0.4790
60	0.4295	146	0.4636
62	0.4532	148	0.5042
64	0.4431	150	0.4620
66	0.4784		
68	0.4621		
70	0.4573		
72	0.4158		
74	0.4498		
76	0.5476		
78	0.4339		
80	0.4361		
82	0.5133		
84	0.444		

$R_f^*(m^2K/kW)$	θ_c (min)	Unc(BDC)%
0.4527	12.06	8.13

Run 27

Bulk concentration (%)	20.0
Mixture Re	6567.
Water Re	9663.
Water average Temp.(°C)	13.43
M. average Temp. (°C)	31.60
Q_w at θ=0	= 0.285 kW

Time (min)	Fouling Res. (m^2 K/kW)	Time (min)	Fouling Res. (m^2 K/kW)
0	0.0000	86	0.5688
2	0.3162	88	0.4979
4	0.2911	90	0.5015
6	0.2763	92	0.4079
8	0.4337	94	0.4826
10	0.3532	96	0.5726
12	0.4294	98	0.4991
14	0.4582	100	0.5525
16	0.4719	102	0.5998
18	0.4852	104	0.5592
20	0.4930	106	0.5905
22	0.5416	108	0.2157
24	0.5067	110	0.6144
26	0.3515	112	0.5718
28	0.3272	114	0.7986
30	0.2352	116	0.6555
32	0.2214	118	0.6347
34	0.2746	120	0.4880
36	0.4771	122	0.6327
38	0.4645	124	0.6318
40	0.3953	126	0.6271
42	0.4040	128	0.4584
44	0.3430	130	0.5523
46	0.2590	132	0.4555
48	0.2498	134	0.4074
50	0.2051	136	0.4433
52	0.1610	138	0.3259
54	0.0506	140	0.6103
56	0.4549	142	0.4764
58	0.3519	144	0.6489
60	0.4025	146	0.6723
62	0.3400	148	0.5493
64	0.2969	150	0.6392
66	0.2678		
68	0.1081		
70	0.1697		
72	0.3982		
74	0.4013		
76	0.2638		
78	0.4238		
80	0.4591		
82	0.4308		
84	0.3974		

$R_f^*(m^2K/kW)$	θ_c (min)	Unc(BDC)%
0.4406	3.15	20.99

Run 28

Bulk concentration (%)	20.0
Mixture Re	8819.
Water Re	9326.
Water average Temp.(°C)	12.06
M. average Temp. (°C)	31.29
Q_w at θ=0	= 0.355 kW

Time (min)	Fouling Res. (m^2 K/kW)	Time (min)	Fouling Res (m^2 K/kW)
0	0.0000	86	0.2688
2	0.1466	88	0.3187
4	0.2167	90	0.1590
6	0.2610	92	0.1523
8	0.2622	94	0.4185
10	0.3151	96	0.3352
12	0.2628	98	0.3660
14	0.5789	100	0.3952
16	0.3678	102	0.3596
18	0.5704	104	0.1952
20	0.4241	106	0.3602
22	0.4566	108	0.3060
24	0.4512	110	0.3830
26	0.4798	112	0.3301
28	0.3267	114	0.4159
30	0.6292	116	0.3541
32	0.4557	118	0.3380
34	0.4727	120	0.3765
36	0.6264	122	0.3769
38	0.4884	124	0.3929
40	0.3597	126	0.3949
42	0.3412	128	0.4155
44	0.4936	130	0.4759
46	0.3842	132	0.3616
48	0.3407	134	0.3872
50	0.3225	136	0.3715
52	0.4763	138	0.3561
54	0.4678	140	0.4266
56	0.4866		
58	0.5396		
60	0.5069		
62	0.4916		
64	0.4786		
66	0.5044		
68	0.2074		
70	0.4524		
72	0.4342		
74	0.4688		
76	0.5032		
78	0.3991		
80	0.4650		
82	0.3711		
84	0.4859		

$R_f^*(m^2K/kW)$	θ_c (min)	Unc(BDC)%
0.4056	4.98	15.82

Run 29

Bulk concentration (%)	20.0
Mixture Re	11215.
Water Re	9760.
Water average Temp.(°C)	13.82
M. average Temp. (°C)	31.23
Q_w at θ=0	= 0.407 kW

Time (min)	Fouling Res. (m^2 K/kW)	Time (min)	Fouling Res. (m^2 K/kW)
0	0.0000	86	0.1203
2	0.1593	88	0.1288
4	0.1796	90	0.2402
6	0.2071	92	0.2225
8	0.2107	94	0.2699
10	0.1711	96	0.2548
12	0.2661	98	0.2491
14	0.2262	100	0.2370
16	0.1884	102	0.2482
18	0.1825	104	0.2662
20	0.1500	106	0.2207
22	0.2205	108	0.1944
24	0.2086	110	0.2285
26	0.2636	112	0.2293
28	0.1935	114	0.2352
30	0.2060	116	0.2358
32	0.2665	118	0.2343
34	0.2309	120	0.2633
36	0.2118	122	0.2494
38	0.1754	124	0.2574
40	0.1633	126	0.2038
42	0.1293	128	0.2492
44	0.2585	130	0.1915
46	0.2305	132	0.2194
48	0.2710	134	0.2386
50	0.2211		
52	0.2588		
54	0.2387		
56	0.2749		
58	0.2755		
60	0.2347		
62	0.2213		
64	0.2406		
66	0.2510		
68	0.2650		
70	0.2532		
72	0.1973		
74	0.2550		
76	0.3227		
78	0.2518		
80	0.2346		
82	0.2117		
84	0.1571		

$R_f^*(m^2K/kW)$	θ_c (min)	Unc(BDC)%
0.2263	2.09	18.19

Run 30

Bulk concentration (%)	20.0
Mixture Re	12697.
Water Re	9836.
Water average Temp.(°C)	14.12
M. average Temp. (°C)	31.33
Q_w at θ=0	= 0.351 kW

Time (min)	Fouling Res. (m^2 K/kW)	Time (min)	Fouling Res. (m^2 K/kW)
0	0.0000	86	0.1658
2	0.0876	88	0.1886
4	0.1046	90	0.1736
6	0.1279	92	0.0755
8	0.1083	94	0.1841
10	0.1389	96	0.1601
12	0.1678	98	0.1461
14	0.1760	100	0.1244
16	0.1891	102	0.1155
18	0.1566	104	0.1192
20	0.1333	106	0.0908
22	0.1848	108	0.1044
24	0.2283	110	0.1081
26	0.1557	112	0.2080
28	0.1820	114	0.1622
30	0.1690	116	0.1426
32	0.1827	118	0.1676
34	0.0592	120	0.1732
36	0.1758	122	0.1835
38	0.2066	124	0.0656
40	0.1915	126	0.1681
42	0.1673	128	0.1493
44	0.1261	130	0.2147
46	0.1420	132	0.1951
48	0.1196	134	0.1510
50	0.1239	136	0.1895
52	0.1338	138	0.1677
54	0.1189	140	0.1826
56	0.2153	142	0.0525
58	0.1735	144	0.2025
60	0.1315		
62	0.1813		
64	0.0487		
66	0.0677		
68	0.1705		
70	0.1505		
72	0.1911		
74	0.1629		
76	0.1639		
78	0.2097		
80	0.1561		
82	0.2187		
84	0.1685		

$R_f^*(m^2K/kW)$	θ_c (min)	Unc(BDC)%
0.1534	3.32	24.13

Run 31

Bulk concentration (%)	20.0
Mixture Re	14207.
Water Re	9834.
Water average Temp.(°C)	14.11
M. average Temp. (°C)	31.21
Q_w at θ=0	= 0.401 kW

Time (min)	Fouling Res. (m^2 K/kW)	Time (min)	Fouling Res. (m^2 K/kW)
0	0.0000	86	0.0944
2	0.0130	88	0.0996
4	0.0306	90	0.0900
6	0.0502	92	0.0743
8	0.0498	94	0.0815
10	0.0637	96	0.0693
12	0.0702	98	0.0608
14	0.0457	100	0.0579
16	0.0335	102	0.0476
18	0.0597	104	0.0562
20	0.0534	106	0.0354
22	0.0702	108	0.1081
24	0.0592	110	0.0982
26	0.0738	112	0.0823
28	0.0470	114	0.0761
30	0.0568	116	0.0943
32	0.0463	118	0.0873
34	0.0412	120	0.0712
36	0.0396	122	0.0861
38	0.0473		
40	0.0317		
42	0.1014		
44	0.0711		
46	0.0646		
48	0.0727		
50	0.0788		
52	0.0776		
54	0.0597		
56	0.0771		
58	0.0418		
60	0.0651		
62	0.0707		
64	0.0404		
66	0.0495		
68	0.0177		
70	0.0995		
72	0.1084		
74	0.0487		
76	0.0758		
78	0.0835		
80	0.0897		
82	0.0604		
84	0.0835		

$R_f^*(m^2K/kW)$	θ_c (min)	Unc(BDC)%
0.0700	9.37	55.60

Run 32

Bulk concentration (%)	20.0
Mixture Re	6616.
Water Re	9545.
Water average Temp.(°C)	12.95
M. average Temp. (°C)	31.20
Q_w at θ=0	= 0.244 kW

Time (min)	Fouling Res. (m^2 K/kW)	Time (min)	Fouling Res. (m^2 K/kW)
0	0.0000	86	0.6337
2	0.2265	88	0.4634
4	0.3475	90	0.2779
6	0.3996	92	0.2412
8	0.3684	94	0.5125
10	0.4716	96	0.6167
12	0.4100	98	0.4253
14	0.4354	100	0.6543
16	0.5458	102	0.6265
18	0.4220	104	0.5559
20	0.5099	106	0.4212
22	0.4834	108	0.5247
24	0.5289	110	0.6854
26	0.4995	112	0.7058
28	0.5436	114	0.6392
30	0.6256	116	0.5590
32	0.4238	118	0.6846
34	0.3371	120	0.6084
36	0.1973	122	0.3935
38	0.5762	124	0.6086
40	0.4595	126	0.5832
42	0.5600	128	0.6617
44	0.3644	130	0.4696
46	0.4969	132	0.6697
48	0.5836	134	0.4717
50	0.5342	136	0.6218
52	0.5685	138	0.5973
54	0.6504	140	0.5996
56	0.6014	142	0.6811
58	0.6009	144	0.6223
60	0.6592	146	0.6710
62	0.6111	148	0.6257
64	0.7299	150	0.6641
66	0.5976		
68	0.3170		
70	0.3541		
72	0.5841		
74	0.6459		
76	0.5620		
78	0.6466		
80	0.7928		
82	0.5644		
84	0.6195		

$R_f^*(m^2K/kW)$	θ_c (min)	Unc(BDC)%
0.5552	6.37	21.08

Run 33

Bulk concentration (%)	20.0
Mixture Re	8803.
Water Re	9542.
Water average Temp.(°C)	12.94
M. average Temp. (°C)	31.32
Q_w at θ=0	= 0.340 kW

Time (min)	Fouling Res. (m^2 K/kW)	Time (min)	Fouling Res. (m^2 K/kW)
0	0.0000	86	0.2429
2	0.2713	88	0.1884
4	0.2972	90	0.1589
6	0.3908	92	0.1266
8	0.2528	94	0.1221
10	0.3693	96	0.1094
12	0.4107	98	0.2386
14	0.4271	100	0.3763
16	0.3473	102	0.4341
18	0.4548	104	0.4191
20	0.4550	106	0.3598
22	0.3821	108	0.4482
24	0.3469	110	0.5052
26	0.4308	112	0.4549
28	0.3887	114	0.3389
30	0.4575	116	0.2762
32	0.4446	118	0.3772
34	0.4526	120	0.4591
36	0.4230	122	0.4563
38	0.4494	124	0.4277
40	0.2923	126	0.4461
42	0.3522	128	0.3283
44	0.4560	130	0.6556
46	0.3756	132	0.3992
48	0.2933	134	0.3470
50	0.4151	136	0.3953
52	0.4168	138	0.4270
54	0.4379	140	0.3949
56	0.4559	142	0.3980
58	0.3712	144	0.4356
60	0.3183	146	0.3921
62	0.2345	148	0.4339
64	0.4071	150	0.4070
66	0.3652		
68	0.4169		
70	0.4786		
72	0.4930		
74	0.3927		
76	0.4429		
78	0.4264		
80	0.4133		
82	0.3503		
84	0.2764		

$R_f^*(m^2K/kW)$	θ_c (min)	Unc(BDC)%
0.3804	2.04	17.22

Run 34

Bulk concentration (%)	20.0
Mixture Re	8765.
Water Re	9646.
Water average Temp.(°C)	13.36
M. average Temp. (°C)	31.30
Q_w at θ=0	= 0.349 kW

Time (min)	Fouling Res. (m^2 K/kW)	Time (min)	Fouling Res. (m^2 K/kW)
0	0.0000	86	0.5446
2	0.2433	88	0.4971
4	0.2875	90	0.3993
6	0.3586	92	0.4264
8	0.3324	94	0.4121
10	0.2954	96	0.3947
12	0.2648	98	0.3927
14	0.3382	100	0.4636
16	0.3049	102	0.4032
18	0.3456	104	0.3828
20	0.3454	106	0.1586
22	0.3651	108	0.3905
24	0.3842	110	0.3796
26	0.3587	112	0.4202
28	0.4117	114	0.3800
30	0.3685	116	0.2838
32	0.3349	118	0.2902
34	0.3843	120	0.3751
36	0.3766	122	0.3830
38	0.4205	124	0.3876
40	0.4810	126	0.1574
42	0.4803	128	0.4100
44	0.3222	130	0.3659
46	0.2811	132	0.3599
48	0.2513	134	0.3839
50	0.3358	136	0.4223
52	0.3976	138	0.1438
54	0.3945	140	0.3518
56	0.3976	142	0.418
58	0.3703	144	0.4001
60	0.4149	146	0.3547
62	0.3866	148	0.3423
64	0.3711	150	0.4088
66	0.4264		
68	0.3545		
70	0.3995		
72	0.3703		
74	0.3429		
76	0.3261		
78	0.2785		
80	0.3157		
82	0.4702		
84	0.3003		

$R_f^*(m^2K/kW)$	θ_c (min)	Unc(BDC)%
0.3671	2.30	16.34

Run 35

Bulk concentration (%)	20.0
Mixture Re	11042.
Water Re	9534.
Water average Temp.(°C)	12.91
M. average Temp. (°C)	31.00
Q_w at θ=0	= 0.375 kW

Time (min)	Fouling Res. (m^2 K/kW)	Time (min)	Fouling Res. (m^2 K/kW)
0	0.0000	86	0.1537
2	0.1263	88	0.1843
4	0.1329	90	0.2110
6	0.1131	92	0.1738
8	0.1784	94	0.2150
10	0.1740	96	0.1680
12	0.1507	98	0.2013
14	0.1877	100	0.0490
16	0.1588	102	0.2650
18	0.1956	104	0.3012
20	0.1796	106	0.3583
22	0.2000	108	0.3884
24	0.1984	110	0.1596
26	0.2054	112	0.2118
28	0.1432	114	0.1588
30	0.2215	116	0.2227
32	0.2139	118	0.2081
34	0.1904	120	0.1176
36	0.1696	122	0.2161
38	0.2043	124	0.2497
40	0.2432	126	0.2018
42	0.2387	128	0.1641
44	0.1924	130	0.2118
46	0.1897	132	0.2259
48	0.2066	134	0.2246
50	0.2257	136	0.1324
52	0.1851	138	0.1952
54	0.1633	140	0.1602
56	0.1088	142	0.1645
58	0.0972	144	0.2102
60	0.0917	146	0.1615
62	0.0759	148	0.2176
64	0.2060	150	0.1684
66	0.2072		
68	0.0350		
70	0.2106		
72	0.2025		
74	0.1813		
76	0.2037		
78	0.2275		
80	0.2645		
82	0.1952		
84	0.1481		

$R_f^*(m^2K/kW)$	θ_c (min)	Unc(BDC)%
0.1912	3.71	28.18

Run 36

Bulk concentration (%)	20.0
Mixture Re	12674.
Water Re	9683.
Water average Temp.(°C)	13.51
M. average Temp. (°C)	31.21
Q_w at θ=0	= 0.375 kW

Time (min)	Fouling Res. (m^2 K/kW)	Time (min)	Fouling Res. (m^2 K/kW)
0	0.0000	86	0.1316
2	0.0501	88	0.1264
4	0.0616	90	0.0986
6	0.0670	92	0.1303
8	0.1036	94	0.0529
10	0.0532	96	0.1453
12	0.1083	98	0.1472
14	0.0607	100	0.1521
16	0.1361	102	0.1217
18	0.1076	104	0.1616
20	0.1548	106	0.1608
22	0.0492	108	0.1846
24	0.1164	110	0.1992
26	0.2134	112	0.1243
28	0.1662	114	0.1655
30	0.1249	116	0.0547
32	0.0917	118	0.1373
34	0.1393	120	0.1655
36	0.1716	122	0.1395
38	0.1367	124	0.1587
40	0.1024	126	0.1368
42	0.0913	128	0.148
44	0.0758	130	0.1482
46	0.0937	132	0.0977
48	0.0785	134	0.0050
50	0.1462	136	0.1504
52	0.1480	140	0.1229
54	0.1421	142	0.1683
56	0.1318	144	0.1335
58	0.1226		
60	0.1228		
62	0.1390		
64	0.0381		
66	0.1200		
68	0.0987		
70	0.1020		
72	0.1154		
74	0.1495		
76	0.1077		
78	0.1450.		
80	0.1673		
82	0.1409		
84	0.1363		

$R_f^*(m^2K/kW)$	θ_c (min)	Unc(BDC)%
0.1288	7.91	47.23

Run 37

Bulk concentration (%)	20.0
Mixture Re	14432.
Water Re	9741.
Water average Temp.(°C)	13.74
M. average Temp. (°C)	31.37
Q_w at θ=0	= 0.387 kW

Time (min)	Fouling Res. (m^2 K/kW)	Time (min)	Fouling Res (m^2 K/kW)
0	0.0000	86	0.0252
2	0.0388	88	0.0157
4	0.0511	90	0.0379
6	0.0120	92	0.0425
8	0.0176	94	0.0278
10	0.0555	96	0.0535
12	0.0734	98	0.0745
14	0.0113	100	0.0357
16	0.0404	102	0.0145
18	0.0540	104	0.0310
20	0.0747	106	0.1215
22	0.0418	108	0.1151
24	0.0217	110	0.1161
26	0.1048	112	0.0574
28	0.0651	114	0.0741
30	0.0964	116	0.0587
32	0.0107	118	0.0643
34	0.0578	120	0.0163
36	0.0514	122	0.0139
38	0.0647	124	0.0173
40	0.0621	126	0.0402
42	0.0011	128	0.0616
44	0.0257	130	0.0807
46	0.0233	132	0.0361
48	0.0260	134	0.0330
50	0.0629	136	0.0526
52	0.0746	138	0.0615
54	0.0503	140	0.0918
56	0.0354	142	0.0598
58	0.0496	144	0.0938
60	0.0551	146	0.0663
62	0.0737	148	0.0994
64	0.1085	150	0.0619
66	0.0359		
68	0.0718		
70	0.0266		
72	0.0036		
74	0.0356		
76	0.0520		
78	0.0370		
80	0.0145		
82	0.0338		
84	0.0591		

$R_f^*(m^2K/kW)$	θ_c (min)	Unc(BDC)%
0.0520	4.89	155.10

Run 38

Bulk concentration (%)	20.0
Mixture Re	6631.
Water Re	8854.
Water average Temp.(°C)	13.13
M. average Temp. (°C)	31.50
Q_w at θ=0	= 0.352 kW

Time (min)	Fouling Res. (m^2 K/kW)	Time (min)	Fouling Res. (m^2 K/kW)
0	0.0000	86	0.8311
2	0.2317	88	0.7017
4	0.6261	90	0.7820
6	0.6537	92	0.7330
8	0.5720	94	0.8423
10	0.3310	96	0.7666
12	0.6281	98	0.7373
14	0.5892	100	0.3893
16	0.7603	102	0.7353
18	0.4491	104	0.8007
20	0.7182	106	0.6865
22	0.7597	108	0.6482
24	0.6997	110	0.6168
26	0.5711	112	0.6451
28	0.7489	114	0.3167
30	0.4098	116	0.7581
32	0.7279	118	0.8067
34	0.7327	120	0.8038
36	0.7346	122	0.7151
38	0.7198	124	0.7537
40	0.7042	126	0.7835
42	0.6970	128	0.8169
44	0.7932	130	0.8007
46	0.7706	132	0.8407
48	0.5212	134	0.8306
50	0.6601	136	0.8270
52	0.8312	138	0.8217
54	0.8003	140	0.7287
56	0.7637	142	0.8451
58	0.7260		
60	0.6401		
62	0.6316		
64	0.5949		
66	0.6166		
68	0.7889		
70	0.8246		
72	0.7342		
74	0.7214		
76	0.6820		
78	0.6711		
80	0.6790		
82	0.7630		
84	0.6672		

$R_f^*(m^2K/kW)$	θ_c (min)	Unc(BDC)%
0.7016	4.42	14.36

Run 39

Bulk concentration (%)	20.0
Mixture Re	8734.
Water Re	8939.
Water average Temp.(°C)	13.48
M. average Temp. (°C)	31.39
Q_w at θ=0	= 0.376 kW

Time (min)	Fouling Res. (m^2 K/kW)	Time (min)	Fouling Res. (m^2 K/kW)
0	0.0000	86	0.4883
2	0.2007	88	0.4574
4	0.3766	90	0.5231
6	0.3223	92	0.5403
8	0.3315	94	0.4829
10	0.2939	96	0.5747
12	0.3130	98	0.5214
14	0.3146	100	0.5276
16	0.2570	102	0.4647
18	0.3072	104	0.5244
20	0.3393	106	0.5473
22	0.3797	108	0.5220
24	0.5373	110	0.5223
26	0.3377	112	0.4932
28	0.3068	114	0.5014
30	0.3755	116	0.4481
32	0.3258	118	0.5827
34	0.3648	120	0.5447
36	0.3649	122	0.4172
38	0.3778	124	0.5695
40	0.1419	126	0.6982
42	0.3665	128	0.4108
44	0.3952	130	0.4627
46	0.3274	132	0.4998
48	0.3491	134	0.5165
50	0.5104	136	0.5439
52	0.4136	138	0.4606
54	0.3553	140	0.4965
56	0.3949	142	0.4868
58	0.4338		
60	0.3768		
62	0.3064		
64	0.4053		
66	0.4248		
68	0.7120		
70	0.1724		
72	0.4852		
74	0.4343		
76	0.2763		
78	0.5120		
80	0.5312		
82	0.4396		
84	0.3276		

$R_f^*(m^2K/kW)$	θ_c (min)	Unc(BDC)%
0.4639	14.19	15.65

Run 40

Bulk concentration (%)	20.0
Mixture Re	11084.
Water Re	8890.
Water average Temp.(°C)	13.28
M. average Temp. (°C)	31.67
Q_w at θ=0	= 0.407 kW

Time (min)	Fouling Res. (m^2 K/kW)	Time (min)	Fouling Res. (m^2 K/kW)
0	0.0000	86	0.4700
2	0.1677	88	0.3625
4	0.1953	90	0.3879
6	0.3341	92	0.4138
8	0.2534	94	0.3677
10	0.3154	96	0.4442
12	0.3005	98	0.4164
14	0.3579	100	0.4668
16	0.3129	102	0.4715
18	0.3809	104	0.4626
20	0.3572	106	0.4596
22	0.2744	108	0.4211
24	0.4030	110	0.4545
26	0.4040	112	0.4856
28	0.3387	114	0.5136
30	0.4448	116	0.5130
32	0.3804	118	0.3704
34	0.4169	120	0.4197
36	0.1982	122	0.4041
38	0.4698	124	0.4766
40	0.4414	126	0.4714
42	0.4914	128	0.4695
44	0.5315	130	0.4375
46	0.4972	132	0.4155
48	0.4677	134	0.5379
50	0.3601	136	0.4987
52	0.4839	138	0.4051
54	0.3935	140	0.5077
56	0.4441	142	0.5440
58	0.5406	144	0.4115
60	0.5308	146	0.4869
62	0.4737	148	0.4338
64	0.4538	150	0.5441
66	0.4601		
68	0.4674		
70	0.5572		
72	0.4919		
74	0.4246		
76	0.3653		
78	0.3912		
80	0.4164		
82	0.4031		
84	0.5020		

$R_f^*(m^2K/kW)$	θ_c (min)	Unc(BDC)%
0.4496	10.02	11.45

Run 41

Bulk concentration (%)	20.0
Mixture Re	12672.
Water Re	8835.
Water average Temp.(°C)	13.05
M. average Temp. (°C)	31.42
Q_w at θ=0	= 0.507 kW

Time (min)	Fouling Res. (m^2 K/kW)	Time (min)	Fouling Res. (m^2 K/kW)
0	0.0000	86	0.3223
2	0.2221	88	0.2667
4	0.2191	90	0.2442
6	0.2576	92	0.2342
8	0.2915	94	0.2149
10	0.3131	96	0.1849
12	0.3651	98	0.4455
14	0.3722	100	0.6018
16	0.3722	102	0.5686
18	0.3601	104	0.4926
20	0.3886	106	0.4473
22	0.4288	108	0.4020
24	0.4113	110	0.5427
26	0.3733	112	0.5823
28	0.3343	114	0.4086
30	0.2844	116	0.5696
32	0.3058	118	0.5043
34	0.4121	120	0.4152
36	0.3938	122	0.3523
38	0.3670	124	0.3146
40	0.3474	126	0.2593
42	0.1505	128	0.3561
44	0.2605	130	0.4669
46	0.2194	132	0.3936
48	0.2117	134	0.4068
50	0.1765	136	0.4606
52	0.3974	138	0.3967
54	0.4322	140	0.5380
56	0.3355	142	0.4696
58	0.3108	144	0.4838
60	0.2375	146	0.5972
62	0.2124		
64	0.1935		
66	0.2308		
68	0.2474		
70	0.4586		
72	0.4976		
74	0.4433		
76	0.3549		
78	0.3867		
80	0.4900		
82	0.4449		
84	0.3637		

$R_f^*(m^2K/kW)$	θ_c (min)	Unc(BDC)%
0.3753	4.19	11.63

Run 42

Bulk concentration (%)	20.0
Mixture Re	14147.
Water Re	8796.
Water average Temp.(°C)	12.89
M. average Temp. (°C)	31.69
Q_w at θ=0	= 0.506 kW

Time (min)	Fouling Res. (m^2 K/kW)	Time (min)	Fouling Res. (m^2 K/kW)
0	0.0000	86	0.4428
2	0.0396	88	0.4499
4	0.1226	90	0.3169
6	0.2560	92	0.4353
8	0.2606	94	0.5734
10	0.3147	96	0.4729
12	0.3362	98	0.4020
14	0.3117	100	0.3566
16	0.2921	102	0.2900
18	0.2868	104	0.2708
20	0.2652	106	0.3151
22	0.2871	108	0.4336
24	0.4870	110	0.4704
26	0.4381	112	0.3519
28	0.3727	114	0.3039
30	0.3676	116	0.4981
32	0.2921	118	0.3954
34	0.2973	120	0.4030
36	0.1144	122	0.4445
38	0.2296	124	0.3339
40	0.1854	126	0.3839
42	0.2209	128	0.3832
44	0.1820	130	0.3946
46	0.4967	132	0.4865
48	0.5871	134	0.3812
50	0.5083	136	0.3191
52	0.2431	138	0.2625
54	0.4663	140	0.2588
56	0.5356	142	0.2865
58	0.3807	144	0.3160
60	0.3403	146	0.3470
62	0.3213	148	0.4028
64	0.2977	150	0.4824
66	0.2657		
68	0.2251		
70	0.2073		
72	0.2268		
74	0.2085		
76	0.1533		
78	0.5086		
80	0.5370		
82	0.4160		
84	0.1752		

$R_f^*(m^2K/kW)$	θ_c (min)	Unc(BDC)%
0.3574	6.87	8.96

Run 43

Bulk concentration (%)	10.0
Mixture Re	10766.
Water Re	18408.
Water average Temp.(°C)	9.52
M. average Temp. (°C)	28.69
Q_w at θ=0	= 0.308 kW

Time (min)	Fouling Res. (m^2 K/kW)	Time (min)	Fouling Res. (m^2 K/kW)
0	0.0000	90	3.4701
1	0.4666	91	2.4135
2	0.6087	92	2.4378
3	0.9077	93	3.4898
4	0.9697	94	2.3922
5	1.0823	95	3.4505
6	1.8591	96	3.5038
7	1.8838	97	3.4544
8	1.9524	98	3.4701
9	2.0081	99	3.4858
10	2.9451	100	3.5015
11	1.5067	101	1.7538
12	2.8579	102	3.5408
13	2.8815	103	3.4151
14	4.3914	104	3.4190
15	2.9306	105	2.4377
16	4.5517	106	3.4898
17	4.5615	107	3.4898
18	4.6052	108	2.4469
19	3.0640	109	2.4561
20	3.0821	110	2.4683
21	3.0857	111	3.5871
22	3.1454	112	3.6069
23	3.1125	113	2.5020
24	2.1856	114	1.8168
25	3.1693	115	2.4986
26	3.2012	116	3.3410
27	2.2498	117	5.2145
28	2.2125	118	3.4269
29	2.2532	119	2.3922
30	2.3307	120	3.3993
31	2.3523	121	3.3648
32	1.7356	122	5.0867
33	2.2398	123	9.3581
34	2.2691	124	9.4056
35	3.1571	125	5.1758
36	3.1836	126	5.3424
37	3.2480	127	3.3710
38	3.2562	128	2.3142
39	2.3354	129	3.4112
40	2.3998	130	3.4269
41	2.3974	131	3.4544
42	2.4533	132	2.4074
43	1.8053	133	2.4287
44	1.3710	134	2.4198
45	1.8491	135	3.5072
46	1.4009	136	1.7909

47	3.3047	137	1.7851
48	3.3124	138	1.8023
49	3.3394	139	1.8355
50	3.2589	140	1.8504
51	3.2815	141	1.3767
52	5.0172	142	1.0370
53	5.0119	143	1.8663
54	5.0065	144	1.4195
55	5.0065	145	1.0745
56	3.2321	146	2.2659
57	3.2359	147	3.3482
58	3.2473	148	2.2824
59	3.2550	149	2.3436
60	5.0546	150	2.3040
61	5.0653	151	5.2581
62	3.2704	152	3.2616
63	3.2741	153	3.2139
64	2.2808	154	5.1145
65	3.2971	155	9.1783
66	3.3085	156	9.3369
67	3.3162	157	4.9543
68	3.3200	158	9.4837
69	3.3277	159	9.4442
70	1.6666	160	9.3646
71	2.3254	161	9.0751
72	3.3973	163	4.8364
73	2.3603	164	9.3677
74	2.3633	165	5.1367
75	3.3620	166	5.2382
76	2.3433	167	5.0000
78	2.2914	169	8.9073
79	3.2198	170	9.2865
80	4.9530	171	5.3146
81	3.1761	172	5.6296
82	3.2101	173	5.4721
83	1.1705	174	2.3709
84	3.2397	175	2.3983
85	2.2704	176	3.4998
86	3.2359	177	3.4799
87	3.3047	178	3.4151
88	5.2547	179	3.4482
89	2.3739	180	3.3954

$R_f^*(m^2K/kW)$	θ_c (min)	Unc(BDC)%
3.6474	12.01	21.00

Run 45

Bulk concentration (%)	10.0
Mixture Re	12150.
Water Re	18687.
Water average Temp.(°C)	10.04
M. average Temp. (°C)	36.44
Q_w at θ=0	= 0.610 kW

Time (min)	Fouling Res. (m^2 K/kW)	Time (min)	Fouling Res. (m^2 K/kW)
0	0.0000	90	0.5554
1	0.0269	91	0.4641
2	0.2306	92	0.5467
3	0.1569	93	0.5467
4	0.2685	94	0.5484
5	0.3401	95	0.5501
6	0.2788	96	0.4697
7	0.2277	97	0.6500
8	0.2274	98	0.6518
9	0.4267	99	0.4777
10	0.3625	100	0.4793
11	0.3669	101	0.4793
12	0.3726	102	0.5667
13	0.4367	103	0.5675
14	0.4359	104	0.4849
15	0.4374	105	0.4849
16	0.4381	106	0.5717
17	0.3735	107	0.6695
18	0.3714	108	0.4138
19	0.3749	109	0.4864
20	0.3096	110	0.5760
21	0.3751	111	0.4920
22	0.4522	112	0.3490
23	0.5349	113	0.4896
24	0.3824	114	0.4904
25	0.3853	115	0.5737
26	0.5390	116	0.4176
27	0.5398	117	0.4184
28	0.3884	118	0.4943
29	0.3270	119	0.4943
30	0.4663	120	0.4266
31	0.4719	121	0.2889
32	0.3345	122	0.4070
33	0.4545	123	0.4763
34	0.4443	124	0.4025
35	0.5401	125	0.2746
36	0.5493	126	0.3346
37	0.5537	127	0.4033
38	0.5573	128	0.4048
39	0.6357	129	0.2796
40	0.6331	130	0.2803
41	0.5386	131	0.4071
42	0.4616	132	0.3446
43	0.6397	133	0.2844
44	0.5489	134	0.2857
45	0.4664	135	0.4123
46	0.5443	136	0.4168
47	0.4672	137	0.3522

48	0.4711	138	0.2904
49	0.3984	139	0.3531
50	0.4727	140	0.4213
51	0.5581	141	0.4251
52	0.4791	142	0.2931
53	0.5606	143	0.2927
54	0.4029	144	0.3574
55	0.5587	145	0.4258
56	0.4790	146	0.2972
57	0.4806	147	0.2954
58	0.3390	148	0.4251
59	0.4059	149	0.4289
60	0.5648	150	0.3006
61	0.4854	151	0.3006
62	0.1791	152	0.3623
63	0.4791	153	0.4319
64	0.5482	154	0.3037
65	0.5476	155	0.3044
66	0.4641	156	0.4334
67	0.3915	157	0.4371
68	0.6392	158	0.3033
69	0.5501	159	0.1999
70	0.4688	160	0.5757
71	0.2185	161	0.4819
72	0.5560	162	0.4836
73	0.6532	163	0.4869
74	0.5639	164	0.4852
75	0.4027	165	0.5743
76	0.4759	166	0.6729
77	0.6613	167	0.4183
78	0.5698	168	0.4175
79	0.4080	169	0.5811
80	0.4872	170	0.5845
81	0.5704	171	0.4963
82	0.5611	172	0.4971
83	0.5510	173	0.5020
84	0.4705	174	0.5020
85	0.6442	175	0.3593
86	0.5537	176	0.3600
87	0.5526	177	0.5068
88	0.5543	178	0.5043
89	0.6487	179	0.3628
		180	0.4319

$R_f^*(m^2K/kW)$	θ_c (min)	Unc(BDC)%
0.4632	6.55	27.27

Run 46

Bulk concentration (%)	10.0
Mixture Re	12814.
Water Re	18685.
Water average Temp.(°C)	10.04
M. average Temp. (°C)	39.98
Q_w at θ=0	= 0.725 kW

Time (min)	Fouling Res. (m^2 K/kW)	Time (min)	Fouling Res. (m^2 K/kW)
0	0.0000	90	0.3725
1	0.0972	91	0.4250
2	0.1040	92	0.3725
3	0.1291	93	0.3725
4	0.1656	94	0.3702
5	0.2070	95	0.3225
6	0.2523	96	0.3199
7	0.2998	97	0.3682
8	0.3044	98	0.3676
9	0.2746	99	0.3676
10	0.1650	100	0.2751
11	0.2859	101	0.3191
12	0.3836	102	0.3166
13	0.3900	103	0.3166
14	0.3980	104	0.3643
15	0.4604	105	0.3643
16	0.4091	106	0.3171
17	0.4138	107	0.3177
18	0.4178	108	0.3177
19	0.4209	109	0.3177
20	0.3236	110	0.3177
21	0.4943	111	0.3682
22	0.3242	112	0.3197
23	0.3311	113	0.3658
24	0.3454	114	0.3163
25	0.3536	115	0.1267
26	0.3582	116	0.2714
27	0.3144	117	0.3141
28	0.3166	118	0.3617
29	0.2764	119	0.3129
30	0.2767	120	0.3129
31	0.3118	121	0.3129
32	0.3446	122	0.3104
33	0.3887	123	0.2692
34	0.3962	124	0.3579
35	0.3498	125	0.3579
36	0.3051	126	0.3124
37	0.3495	127	0.3590
38	0.4000	128	0.3633
39	0.4000	129	0.3639
40	0.3994	130	0.4155
41	0.3988	131	0.4161
42	0.3487	132	0.3639
43	0.3992	133	0.3623
44	0.2577	134	0.3639
45	0.3996	135	0.3629
46	0.3478	136	0.3623

47	0.3467	137	0.4144
48	0.2998	138	0.3623
49	0.1146	139	0.3629
50	0.3434	140	0.3152
51	0.3455	141	0.3152
52	0.3470	142	0.3623
53	0.3464	143	0.3152
54	0.2965	144	0.3158
55	0.3964	145	0.3158
56	0.3982	146	0.3608
57	0.3497	147	0.3138
58	0.3043	148	0.3132
59	0.4019	149	0.2701
60	0.3544	150	0.3118
61	0.3555	151	0.3118
62	0.3576	152	0.2688
63	0.3588	153	0.3118
64	0.3606	154	0.3593
65	0.4109	155	0.3129
66	0.3639	156	0.3604
67	0.3629	157	0.3135
68	0.4729	158	0.3135
69	0.3668	159	0.3155
70	0.4169	160	0.3160
71	0.3180	161	0.3166
72	0.4204	162	0.2727
73	0.3692	163	0.3191
74	0.3670	164	0.2757
75	0.3676	165	0.3191
76	0.3202	166	0.3191
77	0.3661	167	0.3191
78	0.3682	168	0.2346
79	0.3838	169	0.2334
80	0.3862	170	0.3177
81	0.3962	171	0.3183
82	0.3596	172	0.3639
83	0.4177	173	0.3188
84	0.3222	174	0.3163
85	0.3707	175	0.3188
86	0.3713	176	0.3188
87	0.3698	177	0.3666
88	0.3725	178	0.3188
		179	0.2754
		180	0.2749

$R_f^*(m^2K/kW)$	θ_c *(min)*	Unc(BDC)%
0.3435	4.41	18.56

Run 47

Bulk concentration (%) 10.0
Mixture Re 13629.
Water Re 18838.
Water average Temp.(°C) 10.32
M. average Temp. (°C) 44.18
Q_w at θ=0 = 0.715 kW

Time (min)	Fouling Res. (m^2 K/kW)	Time (min)	Fouling Res. (m^2 K/kW)
0	0.0000	110	0.2824
1	0.0757	111	0.2537
2	0.0985	112	0.2238
3	0.1716	113	0.2238
4	0.1993	114	0.3468
5	0.2107	115	0.2820
6	0.1704	116	0.3135
7	0.1328	117	0.2541
8	0.2139	118	0.2541
9	0.2178	119	0.2549
10	0.3474	120	0.3150
11	0.1966	121	0.3158
12	0.2251	122	0.3163
13	0.1762	123	0.2558
14	0.1807	124	0.3186
15	0.2075	125	0.2872
16	0.2369	126	0.2578
17	0.2402	127	0.3181
18	0.1916	128	0.2881
19	0.2158	129	0.3200
20	0.2154	130	0.2885
21	0.2154	131	0.2604
22	0.2428	132	0.2894
23	0.2719	133	0.2616
24	0.2710	134	0.2599
25	0.2728	135	0.2907
26	0.2186	136	0.2327
27	0.2736	137	0.3229
28	0.2753	138	0.2650
29	0.2757	139	0.2359
30	0.2473	140	0.2937
31	0.2481	141	0.2645
32	0.2448	142	0.2654
33	0.2736	143	0.2616
34	0.2444	144	0.2899
35	0.2444	145	0.2891
36	0.2453	146	0.3177
37	0.2465	147	0.2868
38	0.2461	148	0.3560
39	0.2481	149	0.3560
40	0.2775	150	0.2953
41	0.2784	151	0.2660
42	0.2498	152	0.3299
43	0.2797	153	0.2966
44	0.2511	154	0.2992
45	0.2523	155	0.2970
46	0.2531	156	0.3249
47	0.2540	157	0.3574

48	0.2557	158	0.3240
49	0.2565	159	0.3573
50	0.2866	160	0.3230
72	0.2810	161	0.3593
73	0.3466	162	0.3571
74	0.2549	163	0.3596
75	0.2540	164	0.4366
76	0.3135	165	0.3605
77	0.3121	166	0.3605
78	0.3126	167	0.4371
79	0.3150	168	0.4381
80	0.2842	169	0.4005
81	0.2846	170	0.4010
82	0.2841	171	0.3998
83	0.3162	172	0.4383
84	0.3171	173	0.4022
85	0.2885	174	0.4022
86	0.3153	175	0.4031
87	0.2806	176	0.3996
88	0.2802	177	0.4381
89	0.2798	178	0.3625
90	0.2528	179	0.3620
91	0.3118	180	0.2953
92	0.2802	181	0.3979
93	0.2806	182	0.3967
94	0.2810	183	0.3603
95	0.2810	184	0.4381
96	0.2828	185	0.3612
97	0.2540	186	0.3993
98	0.3162	187	0.3612
99	0.2845	188	0.3637
100	0.2544	189	0.3653
101	0.3152	190	0.3296
102	0.3162	191	0.3671
103	0.2858	192	0.3665
104	0.2849		
105	0.2582		
106	0.2318		
107	0.2318		
108	0.2561		
109	0.2536		

$R_f^*(m^2K/kW)$	θ_c (min)	Unc(BDC)%
0.3070	11.07	14.17

Run 48

Bulk concentration (%)	20.0
Mixture Re	8391.
Water Re	7448.
Water average Temp.(°C)	7.09
M. average Temp. (°C)	28.90
Q_w at θ=0	= 0.280 kW

Time (min)	Fouling Res. (m^2 K/kW)	Time (min)	Fouling Res. (m^2 K/kW)
0	0.0000	86	1.4243
2	0.5910	88	1.7618
4	0.7963	90	1.7698
6	0.9453	92	1.1881
8	0.7367	94	1.3581
10	1.0500	96	1.4355
12	1.0107	98	1.5660
14	0.9813	100	1.5026
16	0.8728	102	1.7027
18	1.0527	104	1.5624
20	1.0900	106	1.6876
22	0.9658	108	1.4712
24	1.1653	110	1.4997
26	1.2739	112	1.5568
28	1.1227	114	1.5717
30	1.0688	116	1.5851
32	1.2877	118	1.5969
34	1.1686	120	1.5644
36	1.1030	122	1.6815
38	1.1932	124	1.3907
40	1.4985	126	1.5730
42	1.1867	128	1.8154
44	1.2988	130	1.6576
46	1.2177	132	1.6981
48	1.2790	134	1.6835
50	1.1491	136	1.7773
52	1.2791	138	1.5672
54	1.4070	140	1.5389
56	1.2910	142	1.4224
58	1.3549	144	1.6571
60	1.6184	146	1.6043
62	1.4312	148	1.6159
64	1.6457	150	1.6002
66	1.5942		
68	1.4517		
70	1.3269		
72	1.3587		
74	1.4895		
76	1.4238		
78	1.5168		
80	1.5505		
82	1.5135		
84	1.5039		

$R_f^*(m^2K/kW)$	θ_c (min)	Unc(BDC)%
1.5241	16.17	11.01

Run 50

Bulk concentration (%)	20.0
Mixture Re	9372.
Water Re	7788.
Water average Temp.(°C)	8.59
M. average Temp. (°C)	34.98
Q_w at θ=0	= 0.539 kW

Time (min)	Fouling Res. (m^2 K/kW)	Time (min)	Fouling Res. (m^2 K/kW)
0	0.0000	86	0.3728
2	0.1761	88	0.3913
4	0.2386	90	0.3922
6	0.2881	92	0.3630
8	0.2791	94	0.2911
10	0.2911	96	0.4132
12	0.2549	98	0.4057
14	0.3063	100	0.3122
16	0.3654	102	0.4389
18	0.3668	104	0.4690
20	0.3781	106	0.4010
22	0.3847	108	0.3571
24	0.3750	110	0.3225
26	0.4073	112	0.3715
28	0.4161	114	0.3207
30	0.4017	116	0.3245
32	0.4498	118	0.3632
34	0.3808	120	0.3601
36	0.3756	122	0.3432
38	0.3598	124	0.3326
40	0.4245	126	0.3094
42	0.4041	128	0.3866
44	0.4161	130	0.3753
46	0.3865	132	0.3862
48	0.4040	134	0.3340
50	0.3979	136	0.2709
52	0.3887	138	0.3427
54	0.4012	140	0.3565
56	0.4386	142	0.3722
58	0.4148	144	0.3533
60	0.3982	146	0.3388
62	0.3959	148	0.3547
64	0.4260	150	0.4124
66	0.3926		
68	0.3869		
70	0.3391		
72	0.3766		
74	0.3453		
76	0.4395		
78	0.3656		
80	0.4436		
82	0.4116		
84	0.4136		

$R_f^*(m^2K/kW)$	θ_c (min)	Unc(BDC)%
0.3788	5.21	13.07

Run 51

Bulk concentration (%)	20.0
Mixture Re	9841.
Water Re	7762.
Water average Temp.(°C)	8.48
M. average Temp. (°C)	38.08
Q_w at θ=0	= 0.703 kW

Time (min)	Fouling Res. (m^2 K/kW)	Time (min)	Fouling Res. (m^2 K/kW)
0	0.0000	86	0.2058
2	0.1303	88	0.2302
4	0.1205	90	0.2205
6	0.2437	92	0.2114
8	0.205	94	0.2166
10	0.2185	96	0.2433
12	0.2165	98	0.2205
14	0.2673	100	0.2370
16	0.2501	102	0.2322
18	0.2549	104	0.2204
20	0.2235	106	0.2246
22	0.2117	108	0.2385
24	0.2382	110	0.2286
26	0.2455	112	0.2245
28	0.2461	114	0.2264
30	0.2371	116	0.2404
32	0.1298	118	0.1696
34	0.2332	120	0.1759
36	0.2258	122	0.1881
40	0.2708	124	0.2112
42	0.2547	126	0.2173
44	0.2522	128	0.2423
46	0.2393	130	0.1714
48	0.2310	132	0.2147
50	0.2415	134	0.2157
52	0.1987	136	0.1901
54	0.2322	138	0.2252
56	0.2027	140	0.2094
58	0.2321	142	0.2134
60	0.1991	144	0.1940
62	0.2472	146	0.2134
64	0.2688	148	0.2102
66	0.2409	150	0.2129
68	0.2396		
70	0.2175		
72	0.2693		
74	0.2431		
76	0.2060		
78	0.2205		
80	0.1954		
82	0.2331		
84	0.2273		

$R_f^*(m^2K/kW)$	θ_c (min)	Unc(BDC)%
0.2205	2.74	16.67

Run 52

Bulk concentration (%)	20.0
Mixture Re	10115.
Water Re	7625.
Water average Temp.(°C)	7.87
M. average Temp. (°C)	40.59
Q_w at θ=0	= 0.768 kW

Time (min)	Fouling Res. (m^2 K/kW)	Time (min)	Fouling Res. (m^2 K/kW)
0	0.0000	86	0.3884
2	0.2160	88	0.3928
4	0.2860	90	0.3981
6	0.4237	92	0.4427
8	0.4031	94	0.3756
10	0.3822	96	0.3699
12	0.4336	98	0.3757
14	0.4068	100	0.3754
16	0.4126	102	0.3511
18	0.4214	104	0.2920
20	0.4228	106	0.4213
22	0.4032	108	0.4078
24	0.4246	110	0.4325
26	0.4396	112	0.4263
28	0.3822	114	0.3690
30	0.4282	116	0.3829
32	0.3907	118	0.3748
34	0.4338	120	0.3565
36	0.4170	122	0.3626
38	0.4370	124	0.4012
40	0.4160	126	0.3892
42	0.3870	128	0.3121
44	0.4103	130	0.3744
46	0.3911	132	0.3638
48	0.4530	134	0.3673
50	0.4388	136	0.3798
52	0.4014	138	0.3702
54	0.4016	140	0.3533
56	0.3996	142	0.3668
58	0.4060	144	0.3580
60	0.3913	146	0.3008
62	0.4031	148	0.3622
64	0.3818	150	0.3328
66	0.4008		
68	0.4393		
70	0.4058		
72	0.3668		
74	0.3743		
76	0.3720		
78	0.3858		
80	0.3761		
82	0.4128		
84	0.3736		

$R_f^*(m^2K/kW)$	θ_c (min)	Unc(BDC)%
0.3916	2.29	7.88

Run 53

Bulk concentration (%)	20.0
Mixture Re	10140.
Water Re	7687.
Water average Temp.(°C)	8.14
M. average Temp. (°C)	40.75
Q_w at θ=0	= 0.811 kW

Time (min)	Fouling Res. (m^2 K/kW)	Time (min)	Fouling Res. (m^2 K/kW)
0	0.0000	86	0.2727
2	0.2040	88	0.2553
4	0.2304	90	0.0913
6	0.2538	92	0.1912
8	0.2422	94	0.2414
10	0.2484	96	0.2527
12	0.2260	98	0.2231
14	0.2349	100	0.2085
16	0.2137	102	0.2251
18	0.2247	104	0.2214
20	0.1908	106	0.2417
22	0.2450	108	0.2349
24	0.2556	110	0.2385
26	0.2389	112	0.2517
28	0.2554	114	0.2861
30	0.2408	116	0.2464
32	0.2523	118	0.2602
34	0.2306	120	0.2292
36	0.2009	122	0.2452
38	0.2711	124	0.2624
40	0.2107	126	0.2245
42	0.2222	128	0.2219
44	0.2458	130	0.2554
46	0.2331	132	0.2183
48	0.2854	134	0.2369
50	0.2478	136	0.2383
52	0.2486	138	0.1824
54	0.2281	140	0.2508
56	0.2136	142	0.2348
58	0.2343	144	0.2333
60	0.2401	146	0.2150
62	0.2423	148	0.2844
64	0.2450	150	0.2817
66	0.2091		
68	0.2343		
70	0.2301		
72	0.2496		
74	0.2606		
76	0.2245		
78	0.2407		
80	0.2302		
82	0.2369		
84	0.2251		

$R_f^*(m^2K/kW)$	θ_c (min)	Unc(BDC)%
0.2359	0.99	14.06

Run 55

Bulk concentration (%)	20.0
Mixture Re	9513.
Water Re	7472.
Water average Temp.(°C)	7.19
M. average Temp. (°C)	35.92
Q_w at θ=0	= 0.519 kW

Time (min)	Fouling Res. (m^2 K/kW)	Time (min)	Fouling Res. (m^2 K/kW)
0	0.0000	86	0.2738
2	0.1038	88	0.2382
4	0.2043	90	0.2481
6	0.2049	92	0.2210
8	0.2242	94	0.1734
10	0.2012	96	0.2415
12	0.1586	98	0.2416
14	0.2165	100	0.2798
16	0.2415	102	0.2542
18	0.2204	104	0.2342
20	0.2102	106	0.2527
22	0.2366	108	0.2595
24	0.2064	110	0.2502
26	0.0930	112	0.2789
28	0.2337	114	0.2604
30	0.2061	116	0.2936
32	0.2055	118	0.3010
34	0.1909	120	0.2939
36	0.1867	122	0.2747
38	0.2428	124	0.2411
40	0.2591	126	0.2321
42	0.2455	128	0.2140
44	0.2068	130	0.2352
46	0.2572	132	0.2342
48	0.0798	134	0.2410
50	0.2606	136	0.2483
52	0.3210	138	0.2967
54	0.2651	140	0.2921
56	0.3297	142	0.2343
58	0.2354	144	0.2192
60	0.2304	146	0.2193
62	0.1820	148	0.2323
64	0.2442	150	0.2796
66	0.2690		
68	0.2444		
70	0.2234		
72	0.2474		
74	0.2317		
76	0.2388		
78	0.2501		
80	0.2375		
82	0.3393		
84	0.3006		

$R_f^*(m^2K/kW)$	θ_c (min)	Unc(BDC)%
0.2409	3.38	23.03

Run 56

Bulk concentration (%)	20.0
Mixture Re	9616.
Water Re	8542.
Water average Temp.(C)	11.82
M. average Temp. (C)	37.32
Q_w at θ=0	= 0.647 kW

Time (min)	Fouling Res. (m^2 K/kW)	Time (min)	Fouling Res. (m^2 K/kW)
0	0.0000	86	0.1355
2	0.1566	88	0.1516
4	0.2040	90	0.1673
6	0.2204	92	0.1386
8	0.2402	94	0.2503
10	0.2010	96	0.2893
12	0.2340	98	0.2413
14	0.2666	100	0.2109
16	0.2424	102	0.1935
18	0.2197	104	0.1860
20	0.2198	106	0.1994
22	0.0651	108	0.1884
24	0.1588	110	0.1734
26	0.1837	112	0.1573
28	0.2605	114	0.1774
30	0.2603	116	0.1467
32	0.2592	118	0.1493
34	0.2390	120	0.1261
36	0.2389	122	0.0579
38	0.2165	124	0.2739
40	0.2192	126	0.2665
42	0.2028	128	0.2478
44	0.1917	130	0.2176
46	0.1695	132	0.2384
48	0.2800	134	0.2366
50	0.3123	136	0.2361
52	0.2644	138	0.2460
54	0.2579	140	0.2531
56	0.2312	142	0.0007
58	0.2550	144	0.2171
60	0.2260	146	0.2245
62	0.2051		
64	0.1993		
66	0.2277		
68	0.2530		
70	0.2556		
72	0.2167		
74	0.2173		
76	0.1110		
78	0.1610		
80	0.1982		
82	0.1716		
84	0.1609		

$R_f^*(m^2K/kW)$	θ_c (min)	Unc(BDC)%
0.2056	1.27	42.46

Run 57

Bulk concentration (%)	20.0
Mixture Re	10163.
Water Re	8577.
Water average Temp.(C)	11.97
M. average Temp. (C)	40.90
Q_w at θ=0	=0.816 kW

Time (min)	Fouling Res. (m^2 K/kW)	Time (min)	Fouling Res. (m^2 K/kW)
0	0.0000	86	0.1184
2	0.0540	88	0.1262
4	0.0876	90	0.0980
6	0.1477	92	0.1078
8	0.1345	94	0.0949
10	0.0853	96	0.0821
12	0.1385	98	0.1057
14	0.1273	100	0.0779
16	0.1292	102	0.1412
18	0.1444	104	0.1452
20	0.1684	106	0.1536
22	0.1324	108	0.1145
24	0.1365	110	0.1468
26	0.1351	112	0.1401
28	0.1829	114	0.1465
30	0.1993	116	0.1244
32	0.1725	118	0.1252
34	0.2113	120	0.1132
36	0.1792	122	0.1150
38	0.0418	124	0.1321
40	0.1807	126	0.1040
42	0.1826	128	0.1208
44	0.1443	130	0.1217
46	0.1324	132	0.1385
48	0.1286	134	0.1067
50	0.1165	136	0.1414
52	0.1395	138	0.1378
54	0.1426	140	0.1441
56	0.1291	142	0.1207
58	0.1352	144	0.1213
60	0.1220	146	0.1314
62	0.1117	148	0.1580
64	0.1741	150	0.1336
66	0.1758		
68	0.0341		
70	0.1481		
72	0.1117		
74	0.1434		
76	0.1210		
78	0.1188		
80	0.1266		
82	0.1153		
84	0.1071		

$R_f^*(m^2K/kW)$	θ_c (min)	Unc(BDC)%
0.1187	2.31	21.10

Run 59

Bulk concentration (%)	20.0
Mixture Re	9060.
Water Re	8478.
Water average Temp.(C)	11.55
M. average Temp. (C)	33.56

Q_w at θ=0 = 0.489 kW

Time (min)	Fouling Res. (m^2 K/kW)	Time (min)	Fouling Res. (m^2 K/kW)
0	0.0000	86	0.5576
2	0.4047	88	0.4584
4	0.3847	90	0.4641
6	0.4104	92	0.5339
8	0.3811	94	0.5685
10	0.3716	96	0.5212
12	0.4111	98	0.4959
14	0.3182	100	0.4869
16	0.3439	102	0.6139
18	0.3217	104	0.5114
20	0.4286	106	0.5482
22	0.3976	108	0.3622
24	0.4018	110	0.4526
26	0.4505	112	0.4141
28	0.3660	114	0.5955
30	0.3904	116	0.4292
32	0.3702	118	0.5666
34	0.4147	120	0.5492
36	0.4123	122	0.6008
38	0.4420	124	0.5824
40	0.4781	126	0.5439
42	0.2152	128	0.5422
44	0.4189	130	0.0700
46	0.4130	132	0.5372
48	0.3768	134	0.5751
50	0.5064	136	0.6082
52	0.4973	138	0.5514
54	0.4145	140	0.4998
56	0.4899		
58	0.4629		
60	0.5046		
62	0.2791		
64	0.2596		
66	0.4848		
68	0.5618		
70	0.2910		
72	0.5372		
74	0.5512		
76	0.5198		
78	0.5203		
80	0.4621		
82	0.5260		
84	0.4760		

$R_f^*(m^2K/kW)$	θ_c (min)	Unc(BDC)%
0.4572	1.14	20.21

Run 60

Bulk concentration (%)	20.0
Mixture Re	9583.
Water Re	8635.
Water average Temp.(C)	12.21
M. average Temp. (C)	37.11
Q_w at θ=0	= 0.585 kW

Time (min)	Fouling Res. (m^2 K/kW)	Time (min)	Fouling Res. (m^2 K/kW)
0	0.0000	86	0.3654
2	0.1075	88	0.3688
4	0.1442	90	0.3149
6	0.2120	92	0.3675
8	0.1883	94	0.3638
10	0.2382	96	0.3107
12	0.2254	98	0.3726
14	0.2749	100	0.4059
16	0.2632	102	0.3802
18	0.2999	104	0.3454
20	0.2941	106	0.3513
22	0.2215	108	0.3618
24	0.2748	110	0.3735
26	0.3207	112	0.3890
28	0.2928	114	0.4318
30	0.2760	116	0.3663
32	0.2521	118	0.3292
34	0.3373	120	0.3589
36	0.3867	122	0.3649
38	0.3269	124	0.3629
40	0.3314	126	0.3888
42	0.3048	128	0.3710
44	0.3398	130	0.4104
46	0.3031	132	0.4046
48	0.3514	134	0.3467
50	0.3421	136	0.3892
52	0.3083	138	0.3758
54	0.3368	140	0.3798
56	0.3717	142	0.4057
58	0.3385	144	0.4176
60	0.3640	146	0.3910
62	0.3776	148	0.3713
64	0.3373	150	0.4013
66	0.3721		
68	0.3586		
70	0.3366		
72	0.3608		
74	0.4209		
76	0.3265		
78	0.3280		
80	0.3672		
82	0.3909		
84	0.3744		

$R_f^*(m^2K/kW)$	θ_c (min)	Unc(BDC)%
0.3645	12.82	11.65

Run 61

Bulk concentration (%)	20.0
Mixture Re	10049.
Water Re	8697.
Water average Temp.(C)	12.47
M. average Temp. (C)	40.17
Q_w at θ=0	= 0.751 kW

Time (min)	Fouling Res. (m^2 K/kW)	Time (min)	Fouling Res. (m^2 K/kW)
0	0.0000	86	0.2818
2	0.1327	88	0.2887
4	0.1373	90	0.2893
6	0.1883	92	0.2729
8	0.1994	94	0.2999
10	0.1223	96	0.2773
12	0.1883	98	0.2810
14	0.2154	100	0.2761
16	0.2258	102	0.2958
18	0.2217	104	0.2896
20	0.2216	106	0.3104
22	0.2245	108	0.2815
24	0.3464	110	0.2770
26	0.2424	112	0.2911
28	0.2534	114	0.2645
30	0.2497	116	0.3020
32	0.2118	118	0.2985
34	0.2204	120	0.2805
36	0.2175	122	0.2680
38	0.2381	124	0.0580
40	0.2585	126	0.2780
42	0.2189	128	0.2883
44	0.2379	130	0.2732
46	0.2583	132	0.2810
48	0.2605	134	0.2700
50	0.2613	136	0.3267
52	0.2494	138	0.2812
54	0.2726	140	0.2679
56	0.2692	142	0.2961
58	0.2638	144	0.2914
60	0.2723	146	0.2763
62	0.2649	148	0.2458
64	0.2388	150	0.2652
66	0.2613		
68	0.2525		
70	0.2813		
72	0.2804		
74	0.2570		
76	0.2931		
78	0.2953		
80	0.2918		
82	0.2647		
84	0.2769		

$R_f^*(m^2K/kW)$	θ_c (min)	Unc(BDC)%
0.2664	7.79	11.14

Run 63

Bulk concentration (%)	20.0
Mixture Re	9054.
Water Re	9288.
Water average Temp.(C)	12.91
M. average Temp. (C)	33.52

Q_w at θ=0 = 0.422 kW

Time (min)	Fouling Res. (m^2 K/kW)	Time (min)	Fouling Res. (m^2 K/kW)
0	0.0000	86	0.2669
2	0.2092	88	0.2799
4	0.2234	90	0.3267
6	0.2361	92	0.3548
8	0.2262	94	0.3641
10	0.2481	96	0.3249
12	0.2609	98	0.4037
14	0.2851	100	0.3947
16	0.2897	102	0.3092
18	0.2478	104	0.2802
20	0.2730	106	0.4029
22	0.2669	108	0.4361
24	0.3683	110	0.4602
26	0.2973	112	0.3846
28	0.2724	114	0.3927
30	0.2921	116	0.2882
32	0.2668	118	0.2752
34	0.3164	120	0.3046
36	0.2658	122	0.3045
38	0.2387	124	0.2238
40	0.3241	126	0.2983
42	0.2897	128	0.3159
44	0.2900	130	0.3943
46	0.2495	132	0.4272
48	0.3001	134	0.4541
50	0.2721	136	0.4759
52	0.2793	138	0.3094
54	0.2954	140	0.3746
56	0.2742	142	0.3591
58	0.2619	144	0.2949
60	0.3084	146	0.1824
62	0.2652	148	0.3654
64	0.2771	150	0.2595
66	0.2770		
68	0.2547		
70	0.3078		
72	0.2321		
74	0.2792		
76	0.3032		
78	0.3762		
80	0.4356		
82	0.3983		
84	0.4211		

$R_f^*(m^2K/kW)$	θ_c (min)	Unc(BDC)%
0.3180	4.45	16.61

Run 64

Bulk concentration (%)	20.0
Mixture Re	9555.
Water Re	9460.
Water average Temp.(C)	12.61
M. average Temp. (C)	36.92
Q_w at θ=0	= 0.506 kW

Time (min)	Fouling Res. (m^2 K/kW)	Time (min)	Fouling Res. (m^2 K/kW)
0	0.0000	86	0.2612
2	0.0723	88	0.2179
4	0.1383	90	0.2259
6	0.0159	92	0.1910
8	0.2059	94	0.1964
10	0.1919	96	0.2271
12	0.2024	98	0.1814
14	0.2034	100	0.1797
16	0.1875	102	0.1885
18	0.2036	104	0.2452
20	0.1981	106	0.2047
22	0.2276	108	0.1856
24	0.2109	110	0.2459
26	0.2340	112	0.1421
28	0.2144	114	0.2312
30	0.2658	116	0.2537
32	0.2072	118	0.0906
34	0.0918	120	0.1388
36	0.1612	122	0.2275
38	0.1322	124	0.2267
40	0.2221	126	0.1384
42	0.2115	128	0.2301
44	0.2220	130	0.2450
46	0.2359	132	0.2008
48	0.1922		
50	0.1960		
52	0.2141		
54	0.2152		
56	0.2292		
58	0.2170		
60	0.2633		
62	0.2208		
64	0.2436		
66	0.2576		
68	0.2700		
70	0.2617		
72	0.2159		
74	0.2294		
76	0.2031		
78	0.1651		
80	0.1677		
82	0.2273		
84	0.2235		

$R_f^*(m^2K/kW)$	θ_c (min)	Unc(BDC)%
0.2098	5.73	20.62

Run 65

Bulk concentration (%)	20.0
Mixture Re	10183.
Water Re	9872.
Water average Temp.(C)	13.26
M. average Temp. (C)	41.03

Q_w at θ=0 = 0.511 kW

Time (min)	Fouling Res. (m^2 K/kW)	Time (min)	Fouling Res. (m^2 K/kW)
0	0.0000	86	0.0679
2	0.0115	88	0.0468
4	0.0092	90	0.0255
6	0.0138	92	0.0924
8	0.0073	94	0.0857
10	0.0320	96	0.0752
12	0.0134	98	0.0263
14	0.0469	100	0.0454
16	0.0477	102	0.0515
18	0.0444	104	0.0406
20	0.0515	106	0.0349
22	0.0746	108	0.0342
24	0.0648	110	0.0911
26	0.0531	112	0.0526
28	0.0649	114	0.0615
30	0.0453	116	0.0617
32	0.0690	118	0.0451
34	0.0628	120	0.0157
36	0.0657	122	0.1036
38	0.0803	124	0.0921
40	0.0208	126	0.1298
42	0.1161	128	0.0944
44	0.1172	130	0.1045
46	0.0981	132	0.0897
48	0.1247		
50	0.1339		
52	0.0596		
54	0.0523		
56	0.0859		
58	0.0807		
60	0.0655		
62	0.0558		
64	0.0565		
66	0.0405		
68	0.0265		
70	0.0198		
72	0.0467		
74	0.0121		
76	0.0386		
78	0.0597		
80	0.0690		
82	0.0026		
84	0.0875		

$R_f^*(m^2K/kW)$	θ_c (min)	Unc(BDC)%
0.0640	12.51	60.64

Run 66

Bulk concentration (%)	5.0
Mixture Re	11942.
Water Re	17980.
Water average Temp.(C)	8.71
M. average Temp. (C)	32.57

Q_w at θ=0 = 0.415 kW

Time (min)	Fouling Res. (m^2 K/kW)	Time (min)	Fouling Res. (m^2 K/kW)
0	0.0000	90	0.3855
1	0.0537	91	0.3217
2	0.0646	92	0.2680
3	0.0855	93	0.3268
4	0.2220	94	0.3355
5	0.1957	95	0.4738
6	0.2030	96	0.5219
7	0.2125	97	0.5072
8	0.1552	98	0.5158
9	0.2139	99	0.5193
10	0.3424	100	0.5215
11	0.0459	101	0.4458
11	0.1351	102	0.4458
13	0.2437	103	0.4456
14	0.2432	104	0.4532
15	0.3089	105	0.4644
16	0.2034	106	0.3927
17	0.3244	107	0.2156
18	0.3275	108	0.4005
19	0.2177	109	0.4785
20	0.4804	110	0.4042
21	0.3417	111	0.3994
22	0.2734	112	0.4815
23	0.3227	113	0.4823
24	0.2076	114	0.4839
25	0.2063	115	0.4502
26	0.2638	116	0.5044
27	0.2645	117	0.4230
28	0.2689	118	0.5956
29	0.2703	119	0.3569
30	0.2190	120	0.5162
31	0.2766	121	0.5241
32	0.2781	122	0.5294
33	0.2795	123	0.3113
34	0.2824	124	0.4611
35	0.3447	125	0.2729
36	0.2840	126	0.3950
37	0.0686	127	0.3399
38	0.0252	128	0.5659
39	0.3126	129	0.6075
40	0.2535	130	0.5034
41	0.3156	131	0.5900
42	0.3143	132	0.5039
43	0.3211	133	0.5109
44	0.3286	134	0.4424
45	0.4024	135	0.4490
46	0.3355	136	0.4521

47	0.3423	137	0.3866
48	0.3454	138	0.5457
49	0.2315	139	0.3999
50	0.2329	140	0.4705
51	0.3546	141	0.3253
52	0.3569	142	0.3990
53	0.2379	143	0.4716
54	0.2967	144	0.7633
55	0.3638	145	0.6557
56	0.3523	146	0.4123
57	0.2819	147	0.5756
58	0.3415	148	0.4436
59	0.3431	149	0.5846
60	0.3492	150	0.4923
61	0.4230	151	0.5837
62	0.3631	152	0.4165
63	0.3646	153	0.5051
64	0.3653	154	0.4314
65	0.3064	155	0.5171
66	0.3746	156	0.5250
67	0.3123	157	0.1998
68	0.3792	158	0.3834
69	0.3855	159	0.3215
70	0.3239	160	0.3943
71	0.268	161	0.3296
72	0.3304	162	0.4741
73	0.3939	163	0.5808
74	0.4179	164	0.6629
75	0.4737	165	0.6609
76	0.4703	166	0.668
77	0.4709	167	0.6742
78	0.4016	168	0.9511
79	0.4129	169	0.6955
80	0.425	170	0.6016
81	0.1779	171	0.7158
82	0.3757	172	0.6231
83	0.3947	173	0.6182
84	0.4824	174	0.6337
85	0.3438	175	0.6403
86	0.3576	176	0.6459
87	0.3630	177	0.6480
88	0.3754		
89	0.3123		

$R_f^*(m^2K/kW)$	θ_c *(min)*	Unc(BDC)%
0.5368	79.60	35.99

Run 67

Bulk concentration (%)	10.0
Mixture Re	11428.
Water Re	17827.
Water average Temp.(C)	8.42
M. average Temp. (C)	32.46
Q_w at θ=0	= 0.448 kW

Time (min)	Fouling Res. (m^2 K/kW)	Time (min)	Fouling Res. (m^2 K/kW)
0	0.0000	90	0.9493
1	0.1148	91	0.9325
2	0.4597	92	1.3345
3	0.5181	93	1.1199
4	0.9055	94	1.0653
5	1.0652	95	1.2695
6	1.0965	96	0.8923
7	1.1144	97	1.2945
8	1.1506	98	0.9310
9	0.975	99	0.9512
10	1.2037	100	0.9736
11	1.1289	101	0.9926
12	1.5169	102	1.1003
13	2.1637	103	1.7710
14	2.6787	104	2.7675
15	3.7632	105	2.2302
16	3.8769	106	1.5204
17	4.036	107	1.5477
18	3.0749	108	1.3175
19	1.9706	109	0.9359
20	1.1497	110	1.1499
21	1.2134	111	0.9887
22	0.8910	112	0.8433
23	0.9127	113	1.5833
24	1.1085	114	1.3138
25	0.8744	115	1.5732
26	1.1738	116	1.5996
27	1.4238	117	1.1257
28	1.7968	118	1.3718
29	1.2801	119	0.9876
30	0.9366	120	1.6006
31	1.0432	121	1.3158
32	0.8840	122	1.3377
33	1.5301	123	1.1247
34	1.2988	124	1.1394
35	1.3160	125	1.1638
36	0.9340	126	1.6722
37	1.7418	127	1.4041
38	2.7991	128	1.0008
39	1.2304	129	0.8537
40	1.2864	130	1.0224
41	1.1137	131	1.1314
42	0.9298	132	1.8427
43	1.3290	133	1.4973
44	1.0913	134	1.5099
45	1.0900	135	1.8860
46	0.7917	136	1.9106

47	0.6788	137	1.3261
48	0.6244	138	1.3336
49	1.5084	139	1.1465
50	0.9112	140	1.6491
51	1.0963	141	1.1574
52	0.6706	142	1.3997
53	1.0795	143	1.6508
54	0.8946	144	1.1473
55	1.5328	145	0.9624
56	1.0793	146	1.1638
57	1.3082	147	1.3835
58	1.0354	148	0.8234
59	1.8297	149	0.8311
60	1.2590	150	0.9996
61	0.8896	151	1.1399
62	0.9131	152	1.1278
63	0.9225	153	1.1372
64	0.9151	154	1.3615
65	1.2963	155	0.8207
66	1.2825	156	0.9912
67	1.2834	157	1.0033
68	1.2602	158	1.2050
69	1.2668	159	1.0238
70	1.0587	160	1.1691
71	1.2682	161	0.6712
72	1.2762	162	1.3792
73	1.0652	163	1.1617
74	1.0757	164	0.9863
75	1.5264	165	1.1871
76	1.2682	166	0.8324
77	1.0704	167	1.0021
78	1.2820	168	0.9425
79	1.0743	169	1.1007
80	1.0848	170	1.1047
81	1.2935	171	0.9364
82	0.9159	172	1.1355
83	0.9171	173	0.9680
84	1.0911	174	0.9814
85	1.1017	175	1.1865
86	1.1124	176	0.8508
87	1.0955	177	1.3435
88	0.9298		
89	1.1147		

$R_f^*(m^2K/kW)$	θ_c *(min)*	Unc(BDC)%
1.2719	2.89	15.07

Run 68

Bulk concentration (%)	15.0
Mixture Re	10195.
Water Re	18695.
Water average Temp.(C)	10.06
M. average Temp. (C)	32.49
Q_w at θ=0	= 0.300 kW

Time (min)	Fouling Res. (m^2 K/kW)	Time (min)	Fouling Res. (m^2 K/kW)
0	0.0000	90	3.2422
1	0.3328	91	2.3186
2	0.5510	92	1.7064
3	0.5977	93	1.7356
4	0.8991	94	2.4129
5	0.9206	95	2.4102
6	0.9383	96	2.3374
7	0.9608	97	1.6759
8	1.3666	98	3.2732
9	1.3960	99	3.2557
10	1.4395	100	3.2828
11	1.8498	101	1.2649
12	1.8742	102	1.6647
13	1.8996	103	4.6109
14	0.9907	104	7.7140
15	1.9733	105	3.1573
16	2.0319	106	2.2269
17	2.8777	107	3.1750
18	2.1085	108	3.2625
19	2.1443	109	3.3064
20	2.1749	110	1.7199
21	1.6285	111	1.7277
22	2.2606	112	1.7737
23	2.8008	113	2.3294
24	2.743	114	2.3240
25	4.0884	115	1.6974
26	2.7943	116	2.3591
27	2.8360	117	2.3672
28	2.8841	118	3.3208
29	2.9322	119	2.3401
30	2.9834	120	3.3630
31	2.1512	121	2.3645
32	2.1822	122	3.1914
33	1.6115	123	3.2257
34	2.9037	124	3.2566
35	2.8326	125	4.9554
36	4.2239	126	2.3591
37	2.8810	127	2.3646
38	2.9230	128	1.7358
39	2.9682	129	2.3837
40	2.1392	130	2.2006
41	3.0927	131	3.1192
42	2.2290	132	3.1433
43	1.6449	133	2.2070
44	2.2174	134	2.2799
45	2.1846	135	2.3073
46	2.9977	136	2.3129

47	2.9943	137	1.71548
48	3.0175	138	1.7426
49	3.0571	139	1.7896
50	3.0967	140	1.8170
51	3.1264	141	0.9938
52	3.1522	142	1.0091
53	3.1388	143	1.3800
54	3.2018	144	1.0312
55	3.2186	145	1.0481
56	3.2253	146	0.7727
57	2.3001	147	1.0854
58	2.3295	148	2.2163
59	2.3298	149	4.5536
60	2.3565	150	3.0528
61	2.2948	151	4.6321
62	1.6295	152	4.7788
63	3.1180	153	3.2156
64	7.5226	154	2.2878
65	7.4824	155	1.6756
66	7.5361	156	2.3730
67	4.5918	157	2.4143
68	4.6634	158	1.7736
69	4.7260	159	1.7248
70	3.2490	160	2.3620
71	2.2970	161	2.4149
72	2.3051	162	2.4225
73	4.9046	163	1.7782
74	3.2760	164	1.3193
75	3.2625	165	1.8394
76	3.2794	166	3.3067
77	3.3165	167	3.2928
78	3.3651	168	2.3235
79	2.3509	169	3.3264
80	2.3374	170	2.3730
81	3.3379	171	2.4088
82	2.3428	172	2.3785
83	1.6398	173	3.2840
84	0.8562	174	4.9599
85	2.2916	175	5.0108
86	3.2220	176	3.3447
87	3.1848	177	2.3998
88	2.2613	178	2.3974
89	3.1949	179	2.4083

$R_f^*(m^2K/kW)$	θ_c *(min)*	Unc(BDC)%
2.7913	5.51	25.29

Run 69

Bulk concentration (%)	20.0
Mixture Re	9089.
Water Re	18622.
Water average Temp.(C)	9.92
M. average Temp. (C)	32.39
Q_w at θ=0	= 0.502 kW

Time (min)	Fouling Res. (m^2 K/kW)	Time (min)	Fouling Res. (m^2 K/kW)
0	0.0000	55	7.4835
1	0.6930	56	7.4978
2	2.3525	57	7.4835
3	4.9826	58	7.5478
4	2.7740	59	7.4531
5	3.0367	60	19.3502
6	5.8166	61	7.5257
7	6.3371	62	7.6350
8	6.3307	63	18.8928
9	6.3307	64	18.8161
10	6.6772	65	7.6276
11	3.4662	66	19.6836
12	14.6704	67	19.5248
13	15.3872	68	19.5565
14	15.5039	69	19.4930
15	6.5651	70	19.6518
16	16.0695	71	19.6518
17	6.7084	73	18.9234
18	6.7754	74	7.5258
19	16.1230	77	19.6836
20	16.9078	85	7.6663
21	6.9179	94	22.4439
22	16.5213	99	21.0500
23	16.5626	100	20.9510
24	15.9089	101	21.1159
25	16.5626	102	21.3302
26	16.4934	103	20.4560
27	17.2331	106	20.5880
28	16.6318	109	19.8267
29	16.5902	110	18.9386
30	17.2331	111	18.2178
31	15.9892	117	18.4394
32	16.7837	118	18.2771
33	16.7837	119	7.3094
34	7.09290	120	19.0152
35	17.5472	122	19.0152
36	17.7326	127	18.9231
37	7.3763	128	18.9537
42	16.7147	129	19.0304
43	17.2902	130	19.2292
44	17.2902	131	7.5907
45	17.2617	132	18.6784
46	17.8336	138	20.3026
47	17.9665	170	21.6542
48	18.1587	171	21.5685
49	17.5045	172	22.5811
50	17.5045	173	21.6372

51	17.0903	176	21.8778
52	7.2761	178	22.5633
53	7.3476	179	21.7916
54	7.4191		

$R_f^*(m^2K/kW)$	θ_c (min)	Unc(BDC)%
17.1193	15.25	32.99

Run 70

Bulk concentration (%) 5.0
Mixture Re 11185.
Wate Re 9344.
Water average Temp.(C) 15.14
M. average Temp. (C) 29.02
Q_w at θ=0 = 0.439 kW

Time (min)	Fouling Res. (m^2 K/kW)	Time (min)	Fouling Res. (m^2 K/kW)
0	0.0000	86	0.0959
2	0.0594	88	0.0967
4	0.0619	90	0.0857
6	0.0587	92	0.0973
8	0.0681	94	0.0783
10	0.0817	96	0.0771
12	0.0845	98	0.0636
14	0.0834	100	0.0660
16	0.0878	102	0.0842
18	0.0889	104	0.0686
20	0.0750	106	0.0650
22	0.0726	108	0.0652
24	0.0821	110	0.0669
26	0.0705	112	0.0637
28	0.0728	114	0.0586
30	0.0873	116	0.0908
32	0.0813	118	0.0794
34	0.0772	120	0.0747
36	0.0727	122	0.0901
38	0.0396	124	0.0800
40	0.0760	128	0.0779
42	0.0816	130	0.0852
44	0.0818	132	0.0684
46	0.0786	134	0.0743
48	0.0742	136	0.0592
50	0.0742	138	0.0906
52	0.0701	140	0.0794
54	0.0898	142	0.0751
56	0.0840	144	0.0692
58	0.0876	146	0.0862
60	0.0804	148	0.0667
62	0.0911	150	0.0729
64	0.0616		
66	0.1030		
68	0.0802		
70	0.0860		
72	0.0581		
74	0.0587		
76	0.0971		
78	0.0711		
82	0.0797		
84	0.0835		

$R_f^*(m^2K/kW)$	θ_c (min)	Unc(BDC)%
0.0774	1.99	43.56

Run 71

Bulk concentration (%)	10.0
Mixture Re	10714.
Water Re	9262.
Water average Temp.(C)	14.81
M. average Temp. (C)	29.08
Q_w at θ=0	= 0.416 kW

Time (min)	Fouling Res. (m^2 K/kW)	Time (min)	Fouling Res. (m^2 K/kW)
0	0.0000	86	0.0644
2	0.0508	88	0.0855
4	0.0543	90	0.0741
6	0.0517	92	0.0712
8	0.0678	94	0.0674
10	0.0573	96	0.0885
12	0.0396	98	0.0763
14	0.0548	100	0.0845
16	0.0639	102	0.0834
18	0.0578	104	0.0841
20	0.0551	106	0.0794
22	0.0610	108	0.0875
24	0.0703	110	0.1000
26	0.0084	112	0.0763
28	0.0577	114	0.0969
30	0.0692	116	0.0963
32	0.0683	118	0.0893
34	0.0915	120	0.0850
36	0.0204	122	0.0968
38	0.0923	124	0.0843
40	0.0508	126	0.1029
42	0.0729	128	0.0828
44	0.0946	130	0.0867
46	0.0574	132	0.0862
48	0.0486	152	0.0934
50	0.0474	154	0.1037
52	0.0683	156	0.0561
54	0.0695	158	0.0941
56	0.0601	160	0.0847
58	0.0724	162	0.1172
60	0.0816	164	0.0617
62	0.0706	166	0.0743
64	0.0651	168	0.0938
66	0.0914		
68	0.0826		
70	0.0635		
72	0.1114		
74	0.0776		
76	0.0864		
78	0.0663		
80	0.0755		
82	0.0629		
84	0.0449		

$R_f^*(m^2K/kW)$	θ_c (min)	Unc(BDC)%
0.0799	13.62	57.45

Run 72

Bulk concentration (%)	15.0
Mixture Re	9569.
Water Re	9018.
Water average Temp.(C)	13.80
M. average Temp. (C)	29.24
Q_w at θ=0	= 0.364 kW

Time (min)	Fouling Res. (m^2 K/kW)	Time (min)	Fouling Res. (m^2 K/kW)
0	0.0000	86	0.4989
2	0.2776	88	0.4640
4	0.2370	90	0.4692
6	0.2157	92	0.5005
8	0.2997	94	0.5442
10	0.3144	96	0.5721
12	0.3085	98	0.4882
14	0.3084	100	0.4303
16	0.3423	102	0.5028
18	0.3490	104	0.4480
20	0.3665	106	0.5602
22	0.3837	108	0.5066
24	0.4079	110	0.4563
26	0.3780	112	0.4820
28	0.3971	114	0.5424
30	0.4162	116	0.4079
32	0.3990	118	0.5746
34	0.4105	120	0.5187
36	0.4194	122	0.5274
38	0.4217	124	0.6135
40	0.4354	126	0.5233
42	0.4396	128	0.6838
44	0.2138	130	0.4487
46	0.3940	132	0.5107
48	0.4720	134	0.5271
50	0.4293	136	0.5289
52	0.4663	138	0.4795
54	0.4725	140	0.5058
56	0.4650	142	0.5133
58	0.4629	144	0.4803
60	0.4601	146	0.4873
62	0.4359	148	0.3886
64	0.4252	150	0.5446
66	0.4777		
68	0.4507		
70	0.4857		
72	0.4876		
74	0.5164		
76	0.4869		
78	0.5135		
80	0.4835		
82	0.5706		
84	0.5398		

$R_f^*(m^2K/kW)$	θ_c (min)	Unc(BDC)%
0.4899	13.62	13.06

Run 73

Bulk concentration (%)	20.0
Mixture Re	8545.
Water Re	8765.
Water average Temp.(C)	12.76
M. average Temp. (C)	29.28
Q_w at θ=0 = 0.265 kW	

Time (min)	Fouling Res. (m^2 K/kW)	Time (min)	Fouling Res. (m^2 K/kW)
0	0.0000	86	1.0446
2	0.3669	88	1.0454
4	0.4297	90	1.0078
6	0.5662	92	1.0852
8	0.5522	94	1.0644
10	0.5533	96	1.0288
12	0.6390	98	1.0782
14	0.6291	100	1.2041
16	0.6580	102	1.0552
18	0.5780	104	1.0891
20	0.6094	106	1.1399
22	0.6223	108	1.0892
24	0.5917	110	1.1891
26	0.5932	112	1.0822
28	0.6897	114	1.2008
30	0.7214	116	1.2186
32	0.8319	118	1.2354
34	0.7189	120	1.2057
36	0.6966	122	1.1966
38	0.7611	124	1.2036
40	0.7535	126	1.1875
42	0.7407	128	1.1771
44	0.8456	130	1.1202
46	0.7897	132	1.1053
48	0.7604	134	1.0912
50	0.9654	136	1.1378
52	0.9929	138	1.1053
54	0.9518	140	0.9872
56	0.9822	142	1.1022
58	0.9247	144	1.0480
60	0.9574	146	1.1268
62	0.9986	148	1.1855
64	0.8534		
66	0.9208		
68	0.9785		
70	0.8852		
72	0.9736		
74	0.8344		
76	1.0150		
78	1.0170		
80	1.1302		
82	0.9811		
84	0.9837		

$R_f^*(m^2K/kW)$	θ_c (min)	Unc(BDC)%
1.1080	26.92	15.48